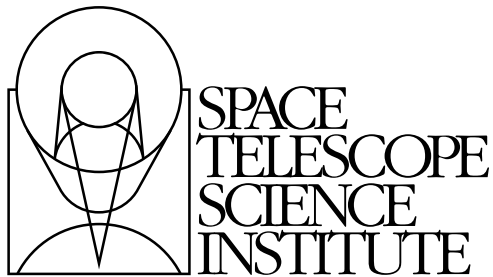


---

Version 4.0  
January, 2002

# WFPC2 Data Handbook



Hubble Division  
3700 San Martin Drive  
Baltimore, Maryland 21218  
[help@stsci.edu](mailto:help@stsci.edu)

## User Support

For prompt answers to any question, please contact the STScI Help Desk.

- **E-mail:** [help@stsci.edu](mailto:help@stsci.edu)
- **Phone:** (410) 338-1082  
(800) 544-8125 (U.S., toll free)

## World Wide Web

Information and other resources are available on the WFPC2 World Wide Web site:

- **URL:** <http://www.stsci.edu/instruments/wfpc2>

## WFPC2 Revision History

| Version      | Date          | Editor  |
|--------------|---------------|---|
| 1.0          | February 1994 | Stefi Baum  |
| 2.0          | December 1995 | Claus Leitherer   |
| 3.0, Vol., I | Oct 1997      | Mark Voit   |
| 3.0, Vol. II | Oct 1997      | Tony Keyes  |
| 4.0          | January 2002  | Sylvia Baggett, Matthew McMaster, Editors,<br>WFPC2 Data Handbook<br>Bahram Mobasher, Chief Editor, HST Data Handbook |

Send comments or corrections to:  
Hubble Division  
Space Telescope Science Institute  
3700 San Martin Drive  
Baltimore, Maryland 21218  
E-mail:[help@stsci.edu](mailto:help@stsci.edu)

# Table of Contents

|   |      |
|---|------|
| <b>Preface</b> .....                                      | vii  |
| <i>How to Use this Handbook</i> .....                     | vii  |
| <b>Chapter 1: WFPC2 Instrument Overview</b> .....         | 1-1  |
| <b>Chapter 2: WFPC2 Data Structures</b> .....             | 2-1  |
| 2.1 Data Files and Suffixes .....                         | 2-1  |
| 2.2 Header Keywords .....                                 | 2-6  |
| 2.3 Correlating Phase II Exposures with Data Files .....  | 2-13 |
| 2.4 WFPC2 Paper Products .....                            | 2-16 |
| 2.4.1 Visit-level Output .....                            | 2-16 |
| 2.4.2 Exposure-level Output .....                         | 2-17 |
| 2.4.3 A note about grayscales .....                       | 2-17 |
| 2.4.4 Obtaining paper products .....                      | 2-18 |
| <b>Chapter 3: WFPC2 Calibration</b> .....                 | 3-1  |
| 3.1 Data Processing Pipelines .....                       | 3-2  |
| 3.2 Data Processing Steps .....                           | 3-4  |
| 3.2.1 Calibration of WFPC2 Images .....                   | 3-6  |
| 3.3 Standard Pipeline Calibration .....                   | 3-8  |
| 3.3.1 Calibration Files .....                             | 3-9  |
| 3.3.2 Calibration Steps .....                             | 3-10 |
| 3.4 Recalibration .....                                   | 3-17 |
| 3.4.1 Why and When to Re-retrieve data through OTFR ..... | 3-17 |
| 3.4.2 Running calwp2 manually .....                       | 3-21 |
| 3.5 Improving the Pipeline Calibration .....              | 3-24 |
| 3.5.1 Warm Pixels .....                                   | 3-24 |
| 3.5.2 Alternate Flatfields .....                          | 3-29 |

|  |      |
|--|------|
| 3.5.3 Removing Cosmic Rays from<br>Co-aligned Images ..... | 3-31 |
| 3.5.4 Charge Traps.....                                    | 3-34 |
| <b>Chapter 4: WFPC2 Error Sources</b> .....                | 4-1  |
| 4.1 Bias Subtraction Errors.....                           | 4-2  |
| 4.2 Flatfield Correction Errors .....                      | 4-2  |
| 4.3 Dark Current Subtraction Errors .....                  | 4-5  |
| 4.3.1 Electronic Dark Current .....                        | 4-5  |
| 4.3.2 Dark Glow .....                                      | 4-6  |
| 4.3.3 Pointing Information in the Image Headers .....      | 4-7  |
| 4.4 Image Anomalies .....                                  | 4-9  |
| 4.4.1 Bias Jumps .....                                     | 4-9  |
| 4.4.2 Residual Images .....                                | 4-10 |
| 4.4.3 PC1 Stray Light.....                                 | 4-14 |
| 4.4.4 Other Anomalies.....                                 | 4-15 |
| <b>Chapter 5: WFPC2 Data Analysis</b> .....                | 5-1  |
| 5.1 Photometric zeropoint .....                            | 5-2  |
| 5.1.1 Photometric Systems Used for WFPC2 Data .....        | 5-2  |
| 5.1.2 Determining the Zeropoint .....                      | 5-4  |
| 5.2 Photometric Corrections .....                          | 5-10 |
| 5.2.1 Time-Dependent Corrections .....                     | 5-10 |
| 5.2.2 Position-Dependent Corrections.....                  | 5-15 |
| 5.2.3 Other Photometric Corrections .....                  | 5-20 |
| 5.2.4 An Example of Photometry with WFPC2 .....            | 5-23 |
| 5.3 Polarimetry .....                                      | 5-24 |
| 5.4 Astrometry .....                                       | 5-26 |
| 5.5 Dithering .....  | 5-29 |
| 5.6 Accuracy of WFPC2 Results .....                        | 5-33 |
| <b>References</b> .....                                    | 1    |
| <i>WWW References</i> .....                                | 3    |
| <b>Index</b> .....   | 1    |



# Preface

---

## How to Use this Handbook

This handbook is designed to help you manipulate, process and analyze data from the Wide Field and Planetary Camera 2 (WFPC2) instrument on-board the Hubble Space Telescope (HST). The book is presented as an independent and self-contained document, extensively based on the contents of an older edition (version 3.0) of the HST Data Handbook. The HST Data Handbook has now been subdivided into separate volumes for each instrument. Users who require more general information about details of acquiring HST data from archive, their file formats, and general purpose software for displaying and processing these data, are referred to a companion volume, the Introduction to Reducing the HST Data.

The current edition of the WFPC2 Data Handbook is being written in late 2001, as we approach Servicing Mission 3b (SM3b). The behavior of this instrument is not likely to change after the servicing mission. Therefore, the material presented in this handbook is expected to remain up-to-date during the next cycles. However, as each servicing mission is followed by a checkout period, to verify that no changes in the camera calibrations have occurred, any such changes are reported in Instrument Science Reports (e.g., see ISRs on WFPC2 observatory verifications after SM3a and SM2 (ISR 00-02 and 97-09)).

The present revision incorporates our detailed knowledge of the behavior and characteristics of the WFPC2 and the data obtained by this instrument. The main changes to the current WFPC2 data handbook over its previous version (revised in 1997) include; discussion of correction flatfields, which can be useful for highly-exposed science images in PC and lower exposure levels in UV filters on WF chips; advice on generating custom dark reference files, which could improve hot pixel corrections; summary of the WFPC2 pipeline processing history (OPUS, OTFC, OTFR) and the introduction of On The Fly Reprocessing (OTFR); and detailed information for converting the photometry from the WFPC2 filters to other systems widely used in literature.

While the present version of the Data Handbook contains the latest information for accurate reduction and analysis of the WFPC2 data, readers are advised to consult the Space Telescope Science Institute web site

([http://hst.stsci.edu/HST\\_overview/instruments](http://hst.stsci.edu/HST_overview/instruments)) for the most recent up-dates regarding WFPC2 performance.

Sylvia Baggett and Matthew McMaster, Editors,  
WFPC2 Data Handbook  
Bahram Mobasher, Chief Editor, HST Data Handbook

# WFPC2 Instrument Overview

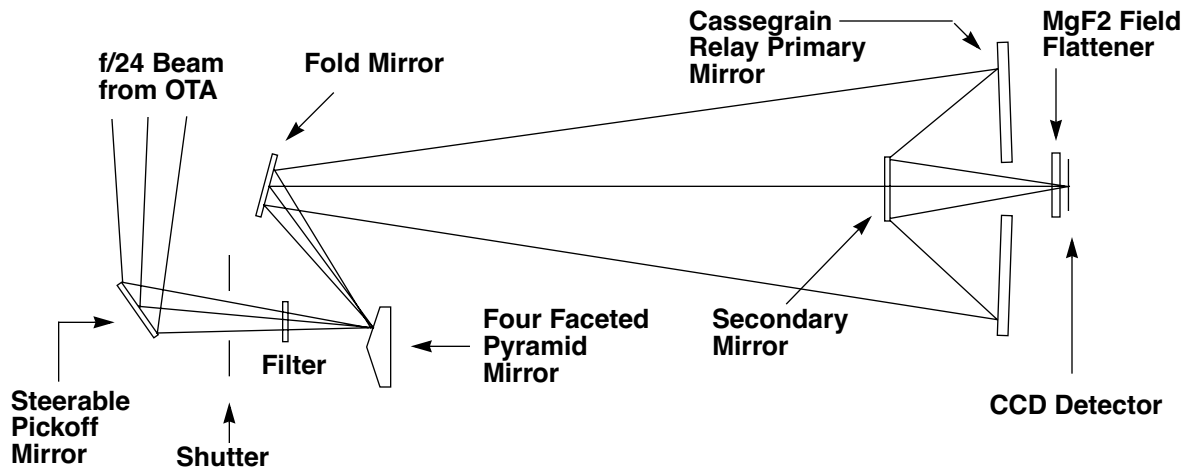
The Wide Field and Planetary Camera 2 (WFPC2) is a two-dimensional imaging device covering a wavelength range from Lyman- $\alpha$  to about 1  $\mu\text{m}$ . Built at the Jet Propulsion Laboratory by an Investigation Definition Team (IDT) headed by John Trauger, WFPC2 was the replacement for the first Wide Field and Planetary Camera (WF/PC-1) and includes built-in corrections for the spherical aberration of the HST Optical Telescope Assembly (OTA). The WFPC2 was installed in HST during the First Servicing Mission in December 1993. An early IDT report of the WFPC2 on-orbit performance can be found in Trauger et al. (1994, *ApJ*, 435, L3), and a more detailed assessment of its capabilities can be found in Holtzman et al. (1995, *PASP*, 107, page 156 and page 1065).

The WFPC2 field of view is located at the center of the HST focal plane; figure 1.1 shows a schematic of its optical arrangement. The central portion of the  $f/24$  beam coming from the OTA is intercepted by a steerable pick-off mirror attached to the WFPC2 and is diverted through an open port entry into the instrument. The beam then passes through a shutter and interposable filters. A total of 48 spectral elements and polarizers are contained in an assembly of 12 filter wheels. The light then falls onto a shallow-angle, four-faceted pyramid, located at the aberrated OTA focus. Each face of the pyramid is a concave spherical surface, dividing the OTA image of the sky into four parts. After leaving the pyramid, each quarter of the full field of view is relayed by an optically flat mirror to a Cassegrain relay that forms a second field image on a charge-coupled device (CCD) of 800 x 800 pixels. Each of these four detectors is housed in a cell sealed by a  $\text{MgF}_2$  window, which is figured to serve as a field flattener.

The aberrated HST wavefront is corrected by introducing an equal but opposite error in each of the four Cassegrain relays. An image of the HST primary mirror is formed on the secondary mirrors in the Cassegrain relays.

The spherical aberration from the telescope's primary mirror is corrected on these secondary mirrors, which are extremely aspheric; the resulting point spread function is quite close to that originally expected for WF/PC-1.

Figure 1.1: WFPC2 Optical Configuration



The optics of three of the four cameras - the Wide Field Cameras (WF2, WF3, WF4) - are essentially identical and produce a final focal ratio of  $f/12.9$ . The fourth camera, known as the Planetary Camera (PC or PC1), has a focal ratio of  $f/28.3$ . figure 1.2 shows the field of view of WFPC2 projected on the sky; the U2,U3 axes are defined by the "nominal" Optical Telescope Assembly (OTA) axis, which is near the center of the WFPC2 FOV. The readout direction is marked with an arrow near the start of the first row in each CCD; note that it rotates 90 degrees between successive chips. The  $x,y$  arrows mark the coordinate axes for any POS TARG commands<sup>1</sup> that may have been specified in the proposal; the [Proposal Instructions](#) elaborate on the use of this requirement.

The position angle of V3 on the sky varies with pointing direction and observation epoch and is recorded in the calibrated science header keyword PA\_V3. Note that for WFPC2, the PA\_V3 is offset 180 degrees from any ORIENT that may have been requested in the HST proposal; as an optional parameter, ORIENT can be found in the proposals but is not recorded in the WFPC2 headers. The orientation of each camera on the sky, i.e., position angle of the y-axis of each detector, is provided by the ORIENTAT group keyword in the image headers. The geometry of the

1. POS TARG, an optional special requirement in HST observing proposals, places the target an offset of POS TARG (in arc sec) from the specified aperture.



cameras and the related group and image keywords are explained in greater detail in chapter 2.

Figure 1.2: WFPC2 Field of View Projected on the Sky

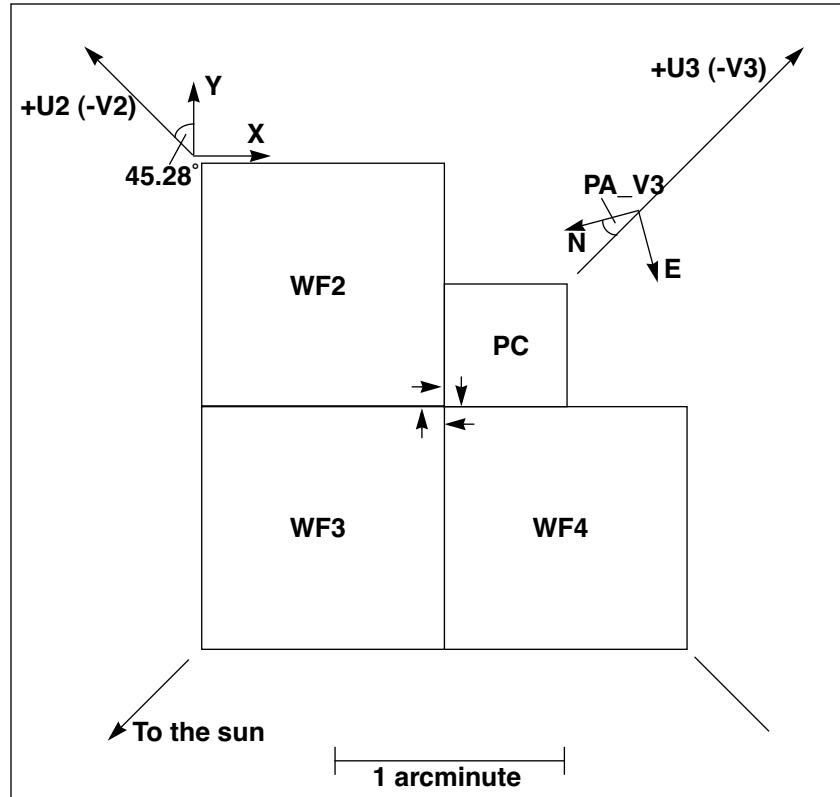


Table 1.1: Camera Configurations

| Camera    | Pixels    | Field of View | Scale             | f/ratio |
|-----------|-----------|---------------|-------------------|---------|
| PC        | 800 x 800 | 36" x 36"     | 0.0455" per pixel | 28.3    |
| WF2, 3, 4 | 800 x 800 | 80" x 80"     | 0.0996" per pixel | 12.9    |

The Planetary Camera (PC) provides a field of view sufficient to obtain full disk images of all planets except for Jupiter, though the pixels undersample the point spread function of the telescope and camera optics by a factor of two at 5800 Å. The WF pixels are over a factor of two larger, and thus undersample the image by a factor of four at visual wavelengths. It is possible to recover some of the sampling lost to these large pixels by image dithering, i.e., taking observations at different sub-pixel offsets. A short discussion of dithering is provided in section 5.5; more detailed information is available in the [HST Dither Handbook](#).

The readout direction of the four CCDs is defined such that in IRAF pixel numbering (origin at lower left corner), the origin of the CCD lies at

the corner of the chip pointing towards the apex of the WFPC2 pyramid (see figure 1.2). As a result of the aberration of the primary beam, the light from sources near the pyramid edges is divided between adjacent chips. Consequently, the lower columns and rows of the PC and WF chips are strongly vignetted, as shown in table 1.2. The CCD  $x,y$  (column, row) numbers given in this table vary at the 1–2 pixel level because of bending and tilting of the field edge in detector coordinates due to geometric distortion in the camera.

Table 1.2: Inner Field Edges of Field Projected Onto CCDs

| Camera | Start Vignetted Field | Contiguous Field  | Start Unvignetted Field |
|--------|-----------------------|-------------------|-------------------------|
| PC1    | $x>0$ and $y>8$       | $x>44$ and $y>52$ | $x>88$ and $y>96$       |
| WF2    | $x>26$ and $y>6$      | $x>46$ and $y>26$ | $x>66$ and $y>46$       |
| WF3    | $x>10$ and $y>27$     | $x>30$ and $y>47$ | $x>50$ and $y>67$       |
| WF4    | $x>23$ and $y>24$     | $x>43$ and $y>44$ | $x>63$ and $y>64$       |

The STSDAS task **wmosaic** provides a convenient way to piece the four groups into a single image comprising the full WFPC2 field of view. This task, in its default mode, will combine the four chips into a large, 1600 x 1600 pixel image at the resolution of the Wide Field cameras, resampling the pixels and correcting for the chip overlap, rotations, and geometric distortion. Consequently, resolution will be lost in the PC, whose pixels are rebinned to the resolution of the Wide Field Cameras (a factor 2.3 coarser).



*While the images produced by wmosaic are usually adequate for presentations and the identification of interesting features, they are not recommended for science uses because of the loss of resolution and photometric accuracy associated with data resampling, especially in the PC.*

Finally, a comment about readout modes. There are two observation modes available on WFPC2, full and area; the mode used for a given observation is recorded in the image header keyword MODE. In full mode, each pixel is read out individually, while in area mode pixels are summed in 2 x 2 boxes before they are read out. The advantage of area mode is that readout noise for the larger pixels is nearly the same as for the unsummed pixels:  $6e^-$  vs.  $5e^-$  per pixel. Thus, area mode can be useful in observations of extended sources when the primary source of noise is readout noise, as is often the case in the far UV.

In practice, observers have made very limited use of the area mode capability; less than 0.1% of all WFPC2 images in the archive are area mode. As a result, area mode calibration is not supported at the same level as full mode. Although reference files such as biases, darks, and flatfields are available for area mode images, they may not provide the best calibration as they are not updated and improved as frequently as the full mode reference files. Researchers using area mode images are advised to consult the list of best available reference files, and consider generating their own area mode calibration files in order to manually recalibrate their data. See section 3.4 for more information on how to manually recalibrate WFPC2 data. For assistance, questions, or problems, e-mail the HST helpdesk at [help@stsci.edu](mailto:help@stsci.edu).





CHAPTER 2:

# WFPC2 Data Structures

In this chapter. . .

|   |
|---|
| 2.1 Data Files and Suffixes / 2-1                         |
| 2.2 Header Keywords / 2-6                                 |
| 2.3 Correlating Phase II Exposures with Data Files / 2-13 |
| 2.4 WFPC2 Paper Products / 2-16                           |

This chapter describes how WFPC2 data are configured and delivered and how these data products relate to the original specifications in the Phase II proposal. We describe the data format used by STScI to distribute WFPC2 observations and the meanings of the header keywords that the user is likely to find most important. Finally, we describe the paper products made available to the Principal Investigator (PI) with the initial data delivery into the Archive and how users can reproduce them.

---

## 2.1 Data Files and Suffixes

HST data files are distributed by the Archive in FITS format, either via tape or electronically (see chapter 1 of the HST Introduction). For historical reasons, *WFPC2 files are provided in "waivered FITS" format, which is not the same as the extension FITS format of the more recent STIS and NICMOS instruments.* (See chapter 2 of the HST Introduction) The waivered FITS format WFPC2 files can be converted into the so-called GEIS format using the STSDAS task **strfits**. Users unfamiliar with GEIS format or the **strfits** task should consult chapter 2 of the HST Introduction;

in addition, the [WFPC2 Data Analysis Tutorial](#) provides cookbook examples of converting and working with WFPC2 images.

### A Note about HST File Formats

Data for WFPC2 and other older instruments (FOC, FOS, FGS, GHRS, HSP, WF/PC1) are generated in the so-called **GEIS**, or Generic Edited Information Set, format. An HST-specific format, a GEIS image consists of a header file and a binary data file; one of the primary reasons it was used for the early generations of HST instruments was that it easily accommodated multiple images, each assigned to its own group, within a single GEIS file. A WFPC2 exposure, consisting of four images, one from each camera, could be stored in a single GEIS file.

However, GEIS format is also machine-dependent and is therefore not ideal for archival storage and distribution. For this reason, a specialized FITS format was developed, referred to as "*waivered*" **FITS**. Since *waivered* FITS format can only be a single file, multiple group data, such as in WFPC2 exposures, must be stored as a 3-dimensional image. For example, a typical WFPC2 observation file contains four 800x800 pixel images (one for each chip); each of the four images is stored in its own group in one GEIS format file, while the *waivered* FITS format consists of the four images in an 800x800x4 (3-d) cube.




---

*Observers who intend to use IRAF and STSDAS tasks for their WFPC2 data analysis should first convert from FITS format images to GEIS format. Many IRAF and STSDAS tasks do not work properly on the waivered FITS format WFPC2 files, particularly for groups 2 through 4.*

---

Several years after the implementation of the *waivered* FITS format, new enhancements were developed for FITS format data, providing significant flexibility. In particular, FITS files can now contain multiple image extensions, each with its own header, size, and datatype. This type of FITS has been dubbed "*extension*" **FITS** and has now been adopted as the standard for current and future HST data (e.g., STIS, NICMOS, ACS).

The example below illustrates the use of the STSDAS **catfits** task, which can be used to ascertain the FITS format of a file; the WFPC2 image u5kl0101r is in *waivered* FITS format (note the dimensions) while the NICMOS image is in the new extension FITS format. Please refer to chapter 2 of the HST Introduction for a more extensive comparison of the various formats.

```

c1> catfits u5kl0101r_c0f.fits
EXT#  FITSNAME      FILENAME          EXTVE DIMENS
BITPI OBJECT
0      u5kl0101r_c0f  u5kl0101r_cvt.c0h      800x800x4
-32F
1      TABLE      u5kl0101r_cvt.c0h.tab  49Fx4R

c1> catfits n3zd0wetq_ima.fits
EXT#  FITSNAME      FILENAME          EXTVE DIMENS
BITPI OBJECT
0      n3zd0wetq_ima  n3zd0wetq_ima.fits      16
1      IMAGE         SCI                 1    256x256   -32
2      IMAGE         ERR                 1    256x256   -32
3      IMAGE         DQ                  1    256x256   16
4      IMAGE         SAMP                1
5      IMAGE         TIME                1    -32
6      IMAGE         SCI                 2    256x256   -32
7      IMAGE         ERR                 2    256x256   -32
8      IMAGE         DQ                  2    256x256   16
... [lines removed to improve readability]
55     IMAGE         TIME                11   -32

```

To avoid confusion for experienced WFPC2 observers, WFPC2 data continues to be delivered from the Archive in waived FITS format. Note, however, that since observers are becoming more familiar with extension FITS format in the new instruments, adding an extension FITS option to WFPC2 Archive retrieval formats is being considered. Work is underway to upgrade IRAF and STSDAS tasks to handle WFPC2 data in both GEIS and extension FITS format (this is needed before the Archive can begin to deliver WFPC2 data in extension FITS format), though the changes will not guarantee that the tasks will work properly on waived FITS data. This work will require the release of some new conversion tasks (`fits2geis` and `geis2fits`) and changes to the Archive to make extension FITS format an option for retrieving WFPC2 data. In any event, the waived FITS format will not disappear, extension FITS format merely would become a new option for data retrieval and analysis. Any such future enhancements will be clearly advertised via the Newsletters and WWW pages.

## GEIS Files

After conversion to GEIS format, a directory listing (type `dir` within IRAF) will show that the files have a nine-character rootname and a three-character suffix (also called the “extension”). By definition, all files for a single exposure will have the same rootname. The image rootnames (e.g., `u2850303p`) are constructed from several pieces: the first character represents the instrument used (always U for WFPC2), followed by a three character program ID (unique to each proposal), a two character observation set ID (often identical to the visit number), a two character observation number, and a single character for the data transfer path. For each instrument, the suffix uniquely identifies the file contents. The WFPC2 suffixes are listed in table 2.1.

Files whose suffix ends with the letter “h” (e.g., `u2850303p.c1h`) are the ASCII *header files*. The header files contain keywords that describe the parameters used to take the observation, the processing of the data, the properties of the image, and a description of the group keywords. Files whose suffix ends in the letter “d” (e.g., `u2850303p.c1d`) are binary *data files*; these files contain the data as well as values of the group keywords. A single GEIS image is composed of a header and data *pair* (e.g., the files `u2850303p.c1h` and `u2850303p.c1d` together represent a single image). Note that in FITS format, useful for network transfers, header and data are combined into a single file; the name of the FITS file becomes: *rootname\_suffix.fits*, with the letter “f” replacing “h” or “d” in the suffix (e.g., `u2850303p_c1f.fits`). GEIS files may be converted back to waivered FITS format by using the STSDAS task **stwfits**, see chapter 3 of the HST Introduction. As noted in chapter 3 of the HST Introduction, you should set your `'tmp'` directory to `"/"`, `imtype` to `".hhh"`, and `imdir` to `"HDR$"` as shown below:

```
cl> set tmp = "/"
cl> set imtype = "hhh"
cl> set imdir = "HDR$"
```

You can also make these settings in your `login.cl` or `loginuser.cl` files. (Note that most STSDAS tasks will not work properly if you have `imtype` set to `"imh"`.)



Table 2.1: WFPC2 Dataset Suffixes and File Sizes

| GEIS Format Suffix           | Waivered Fits <sup>1</sup> Format Suffix | File Contents   | Approximate Size |
|------------------------------|--|---|------------------|
| <i>Raw Data Files</i>        |  |   |                  |
| .d0h/.d0d                    | _d0f.fits                                | Raw science data  | 5 MB             |
| .q0h/.q0d                    | _q0f.fits                                | Data quality for raw science data   | 5 MB             |
| .x0h/.x0d                    | _x0f.fits                                | Extracted engineering data  | 100 kB           |
| .q1h/.q1d                    | _q1f.fits                                | Data quality for extracted engineering data   | 100 kB           |
| .shh/.shd                    | _shf.fits                                | Standard header packet containing observation parameters                            | 30 kB            |
| .pdq <sup>2</sup>            | _pdq.fits                                | Text file containing jitter statistics and other data quality information           | 20 kB            |
| .dgr                         | _dgr.fits                                | Text file listing the values of the group header keywords in the raw image.         | 5-10 kB          |
| <i>Calibrated Data Files</i> |  |   |                  |
| .c0h/.c0d                    | _c0f.fits                                | Calibrated science data   | 10 MB            |
| .c1h/.c1d                    | _c1f.fits                                | Data quality for calibrated science data  | 5 MB             |
| .c2h/.c2d                    | _c2f.fits                                | Histogram of science data pixel values  | 220 kB           |
| .c3t                         | _c3t.fits                                | The output throughput table generated based upon the PHOTMODE group header keyword. | 10-30 kB         |
| .cgr                         | _cgr.fits                                | Text file listing the values of the group header keywords in the calibrated image.  | 5-10 kb          |
| .trl                         | _trl.fits                                | Trailer file  | 10-30 kB         |

1. Observers using IRAF tasks for their WFPC2 data analysis should first convert their images to GEIS format as many tasks do not work properly on the waivered FITS format files from the Archive.

2. PDQ files and Observation Logs (jitter) files, see appendix C, are not automatically distributed as part of the OTFR products but must be specifically requested, see chapter 1 of the HST Introduction. The jitter files are discussed in appendix C.

A single WFPC2 exposure is obtained as four images, one image for each CCD chip. GEIS files use group format to keep all of the data from a given HST exposure together in a single image file, see chapter 2 of the HST Introduction. The data corresponding to each sub-image for the WFPC2 are stored sequentially in the groups of a single GEIS image. The

header file for an image contains the information that applies to the observation as a whole (i.e., to all the groups in the image); this information is viewable by simply paging the header. The group-specific (that is, chip-specific) keyword information is stored in two places. The descriptions for each keyword can be found in the main header, while the keyword values are stored with the group data itself in the binary data file; group keyword values are only accessible via specialized software, such as the STSDAS tasks **hedit**, **hselect**, or **imhead**.

WFPC2 images are normally four-group images. The first group is used for the planetary camera and groups 2, 3, and 4 are used for the wide field cameras. If only a subset of chips are read out, only a subset of groups will be present. The keyword, **DETECTOR**, gives the chip used for a specific group (1 through 4 for PC1, WF2, WF3, and WF4, respectively). For example, if you have a single-group image (not uncommon before the installation of the solid state recorder) and would like to know which chip was used for the observation, check the **DETECTOR** keyword. The total number of groups within the image is stored in the keyword, **GCOUNT**.

---

## 2.2 Header Keywords

Table 2.3 and table 2.4 list some of the more commonly used keywords found in a calibrated WFPC2 image (.c0h). A complete list of header keywords, with brief explanations, can be found in the [WWW Keyword Dictionary](#).

The values of any of the header and group keywords can be determined using STSDAS tasks such as **hedit**, **hselect**, and **imhead**. The examples below illustrate the use of these tasks on a general image keyword (**EXPSTART**) and a group keyword (**DETECTOR**); the "[3]" string specifies the group desired.

Table 2.2: **hedit**, **hselect** and **imhead** examples

```

c1>hedit u5kl0101r.c0h[3] expstart,detector .
u5kl0101r.c0h[3],EXPSTART = 5.159859322738E+04
u5kl0101r.c0h[3],DETECTOR = 3

c1> hsel u5kl0101r.c0h[3] expstart,detector yes
5.159859322738E+04      3

c1> imhead u5kl0101r.c0h[3] long+ | match EXPSTART
EXPSTART= 5.159859322738E+04 / exposure start time
(Modified Julian Date)

c1> imhead u5kl0101r.c0h[3] long+ | match DETECTOR
DETECTOR= 3

```

Most of the tasks provide only the keyword value; **imhead** shows both the value and the description for primary header keywords, but only the value for group keywords. Descriptions for group keywords can be viewed with a standard editor; each group keyword has three entries in the header file (e.g., `c0h`): one line defining the name and description of the group keyword, one specifying the space required for the keyword in the binary data file, and one providing the data type. As mentioned earlier, the group keyword *value* is stored in the binary data file and is only accessible via one of the STSDAS tasks. As an example, the entries for the group keyword `DETECTOR` are given below.

```

c1>page u5kl0101r.c0h
...
PTYPE19 = 'DETECTOR'      /CCD detector: PC 1, WFC 2-4
PDTYPE19= 'INTEGER*4'    /
PSIZE19 = 32 /
...

```

WFPC2 header keywords include items such as observing mode, integration time, filters and reference files used, calibration steps performed, and the properties of the data itself (e.g., number of groups, dimensions in pixels of each group); some additional calibration information is given at the end of the header file in the header `HISTORY` keywords. Group keywords include the reference pixels, coordinates, scale, flux units, and image statistics for each chip.

Observers new to WFPC2 data should peruse the header keyword comments in their images, as some keywords can occasionally be misleading. For example, `DATE` refers to the date the file was written while `DATE-OBS` refers to the date of the observation and `PROCTIME` refers to the date and time an image was processed through the On-The-Fly system, see section 3.1. The `FILTER1` and `FILTER2` keywords record the numerical designations of the filter(s) used while the filter names are stored in `FILTNAM1` and `FILTNAM2`. Also, `PHOTZPT` is *not* the photometric zeropoint (in the ST magnitude system) as normally understood, but rather the zeropoint in the ST magnitude system to be used after conversion to FLAM units (see table 5.1).

Astrometry keywords can also be confusing. The orientation of the image is specified by a global keyword, `PA_V3`, and a group keyword, `ORIENTAT`. The keyword, `PA_V3`, gives the position angle (in degrees) of the telescope's V3 axis on the sky, measured from North through East (see figure 1.2). The V3 axis is roughly 225 degrees from the  $x$  axis of the PC. The V3 axis differs by exactly 180 degrees from the `ORIENT`<sup>1</sup> value, if any, specified in the Phase II submission. The group keyword, `ORIENTAT`, records, for each detector, the position angle of the  $y$  axis in the plane of the sky, measured from North through East. This angle differs from `PA_V3` by roughly  $-135$ ,  $-45$ ,  $+45$ , and  $+135$  degrees, for PC1, WF2, WF3, and WF4, respectively. See figure 1.2 for a graphic representation of the geometric relationship between the four detectors. Accurate values of the positions and rotations between chips can be obtained from the [Science Instrument Aperture File \(SIAF\)](#), which is available on the WWW. In addition, each group has eight coordinate-related keywords (listed under coordinate-related keywords below) that specify the transformation from pixels to world coordinates (right ascension and declination) in the tangent plane approximation at the center of the chip.

Table 2.3: Frequently-used WFPC2 Group Header Keywords

| Keyword                            | Description  |
|------------------------------------|--|
| <b>Image keywords</b>              |  |
| <code>DETECTOR</code>              | CCD detector contained in group (PC1, WF2, WF3, WF4) |
| <b>Coordinate-related keywords</b> |  |
| <code>CRVAL1</code>                | RA of reference pixel (deg)                          |
| <code>CRVAL2</code>                | Dec of reference pixel (deg)                         |
| <code>CRPIX1</code>                | X coordinate of reference pixel                      |

1. `ORIENT` is an optional parameter used in HST proposals to request a particular orientation of the field of view on the sky and refers to the position angle of the U3 axis.

| Keyword  | Description   |
|--|---|
| CRPIX2   | <i>Y</i> coordinate of reference pixel  |
| CD1_1  | Partial derivative of RA with respect to <i>x</i>   |
| CD1_2  | Partial derivative of RA with respect to <i>y</i>   |
| CD2_1  | Partial derivative of Dec with respect to <i>x</i>  |
| CD2_2  | Partial derivative of Dec with respect to <i>y</i>  |
| <b>Orientation</b>   |   |
| MIR_REVR   | Is image mirror reversed?   |
| ORIENTAT   | Orientation of <i>y</i> axis (deg)—different for each group   |
| <b>Bias level information (based on pixels in columns 9-14, rows 10-790 in .x0h/.x0d file)</b> |   |
| DEZERO   | Bias level from engineering data  |
| BIASEVEN   | Bias level based on average of odd columns in .x0h/.x0d file (used for even columns in science image) |
| BIASODD  | Bias level based on average of even columns in .x0h/.x0d file (used for odd columns in science image) |
| <b>Pixel statistics</b>  |   |
| GOODMIN  | Minimum value of “good” pixels (not flagged in DQF)   |
| GOODMAX  | Maximum value of “good” pixels  |
| DATAMEAN   | Mean value of “good” pixels   |
| GPIXELS  | Number of good pixels (out of 640,000 possible)   |
| ATODSAT  | Number of saturated pixels  |
| <b>Photometry keywords (populated if DOPHOTOM=yes)</b>   |   |
| PHOTMODE   | Photometry mode   |
| PHOTFLAM   | Inverse sensitivity (units of erg/sec/cm <sup>2</sup> /Å for 1 DN/sec)                                |
| PHOTZPT  | Zeropoint (currently -21.10)  |
| PHOTPLAM   | Pivot wavelength (in angstroms)   |
| PHOTBW   | rms bandwidth of filter (in angstroms)  |
| <b>Image statistics keywords</b>   |   |
| MEDIAN   | Middle data value when good quality pixels sorted   |
| HISTWIDE   | Width of the histogram  |
| SKEWNESS   | Skewness of the histogram   |
| MEANC10  | Mean of a 10 x 10 region at the center of the chip  |

| Keyword  | Description  |
|----------|--|
| MEANC100 | Mean of a 100 x 100 region at the center of the chip |
| MEANC300 | Mean of a 300 x 300 region at the center of the chip |
| BACKGRND | Estimated background level                           |

Table 2.4: Frequently-used WFPC2 General Header Keywords

| Keyword                                       | Description   |
|---|---|
| <b>Information about the groups</b>           |   |
| GROUPS  | Multi-group image? Indicates whether data has groups.   |
| GCOUNT  | Number of groups per observation (1 to 4)   |
| <b>Image keywords</b>                         |   |
| INSTRUME                                      | Instrument used; always WFPC2   |
| ROOTNAME                                      | Rootname of the observation set   |
| FILETYPE                                      | SHP - standard header packet<br>EXT - extracted engineering file<br>EDQ - EED data quality file<br>SDQ - science data quality file<br>SCI - science data file |
| MODE  | Mode: FULL (full resolution) or AREA (2 x 2 pixel summation)  |
| SERIALS                                       | Serial clocks: ON, OFF  |
| <b>Data type keywords</b>                     |   |
| IMAGETYP                                      | DARK/BIAS/IFLAT/UFLAT/VFLAT/KSPOT/EXT/ECAL  |
| CDBSFILE                                      | GENERIC/BIAS/DARK/FLAT/MASK/NO Is the image a reference file and if so, type is specified   |
| <b>Reference file selection keywords</b>      |   |
| DATE  | File creation date  |
| FILTNAM1                                      | First filter name   |
| FILTNAM2                                      | Second filter name; blank if none   |
| FILTER1                                       | First filter number (0–48) (Used in SOGS - Science Operations Ground System)  |
| FILTER2                                       | Second filter number (0–48)   |
| FILTROT                                       | Partial filter rotation angle (degrees)   |
| <b>More reference file selection keywords</b> |   |
| ATODGAIN                                      | Analog to digital gain (electrons/DN)   |

| <b>Keyword</b>                                      | <b>Description</b>  |
|---|---|
| <b>Calibration switches</b>                         |   |
| MASKCORR  | Do mask correction: PERFORM, OMIT, COMPLETE   |
| ATODCORR  | Do A-to-D correction: PERFORM, OMIT, COMPLETE   |
| BLEVCORR  | Do bias level correction: PERFORM, OMIT, COMPLETE   |
| BIASCORR  | Do bias correction: PERFORM, OMIT, COMPLETE   |
| DARKCORR  | Do dark correction: PERFORM, OMIT, COMPLETE   |
| FLATCORR  | Do flatfield correction: PERFORM, OMIT, COMPLETE  |
| SHADCORR  | Do shaded shutter correction: PERFORM, OMIT, COMPLETE                                     |
| DOSATMAP  | Output saturated pixel map: PERFORM, OMIT, COMPLETE                                       |
| DOPHOTOM  | Fill photometry keywords: PERFORM, OMIT, COMPLETE   |
| DOHISTOS  | Make histograms: PERFORM, OMIT, COMPLETE  |
| OUTDTYPE  | Output image datatype: REAL, LONG, SHORT  |
| <b>Calibration reference files used<sup>1</sup></b> |   |
| MASKFILE  | Name of the input static mask containing known bad pixels and charge traps                |
| ATODFILE  | Name of the A-to-D conversion file  |
| BLEVFILE  | Name of engineering file with extended register data                                      |
| BLEVDFIL  | Name of data quality file (DQF) for the engineering file                                  |
| BIASFILE  | Name of the superbias reference file  |
| BIASDFIL  | Name of the superbias reference DQF   |
| DARKFILE  | Name of the dark reference file   |
| DARKDFIL  | Name of the dark reference DQF  |
| FLATFILE  | Name of the flatfield reference file  |
| FLATDFIL  | Name of the flatfield reference DQF   |
| SHADFILE  | Name of the reference file for shutter shading  |
| PHOTTAB   | Name of the photometry calibration table  |
| SATURATE  | Data value at which saturation occurs<br>(always 4095 for WFPC2, which includes the bias) |
| <b>Ephemeris data</b>                               |   |
| PA_V3   | Position angle of V3 axis of HST  |
| RA_SUN  | Right ascension of the sun (deg)  |

| <b>Keyword</b>              | <b>Description</b>  |
|-----------------------------|---|
| DEC_SUN                     | Declination of the sun (deg)  |
| EQNX_SUN                    | Equinox of the sun  |
| <b>Fill values</b>          |   |
| PODPSFF                     | 0 (no fill), 1 (fill present)   |
| RSDPFILL                    | Bad data fill value set in pipeline for calibrated image  |
| <b>Exposure Information</b> |   |
| DARKTIME                    | Estimate of darktime (in sec)   |
| EQUINOX                     | Equinox of the celestial coordinate system  |
| SUNANGLE                    | Angle between sun and V1 axis (deg)   |
| MOONANGL                    | Angle between moon and V1 axis (deg)  |
| SUN_ALT                     | Altitude of the sun above Earth's limb (deg)  |
| FGSLOCK                     | Commanded FGS lock (FINE, COARSE, GYROS, UNKNOWN)   |
| <b>Timing information</b>   |   |
| DATE-OBS                    | UT date of start of observation   |
| TIME-OBS                    | UT time of start of observation (hh:mm:ss)  |
| EXPSTART                    | Exposure start time (Modified Julian Date)  |
| PROCTIME                    | Date and time of OTFR pipeline processing (Modified Julian Date)  |
| EXPEND                      | Exposure end time (Modified Julian Date)  |
| EXPTIME                     | Exposure duration (seconds)   |
| EXPFLAG                     | How exposure time was calculated. (NORMAL, INTERRUPTED, INCOMPLETE, EXTENDED, UNCERTAIN, INDETERMINATE, or PREDICTED) |
| <b>Proposal information</b> |   |
| TARGNAME                    | Proposer's target name  |
| RA_TARG                     | Right ascension of the target (deg) (J2000)   |
| DEC_TARG                    | Declination of the target (deg) (J2000)   |
| PROPOSID                    | RPS2 proposal identifier  |

1. Calibration reference file keywords are populated even if unused.



## 2.3 Correlating Phase II Exposures with Data Files

Because of the need to schedule observations as efficiently as possible, the order in which exposures are executed may be different from the order in which they appear in the observer's Phase II submission, unless an explicit special requirement dictates otherwise. As a result, the data may be received in an order that differs from that originally proposed by the observer. In this section, we discuss how to correlate the data received with the exposures specified in the Phase II submission, which can often facilitate the process of interpreting the observations and their interconnection. The Phase II proposal specifications submitted by the investigator can be found by entering the proposal ID on the [HST Program Information](#) page or in the Program Status box on the [top HST page](#).

The first step is often identifying the program to which a data file belongs, and can be accomplished via the header keyword PROPOSID. Data files can then be associated with the corresponding exposure line in the Phase II proposal by comparing exposure information in the Phase II proposal with data file header keywords. For WFPC2 data, the most useful comparisons are shown in the table below.

Table 2.5: Comparing Phase II Proposal Keywords to Data Header Keywords

| Phase II          | Data Header        |
|-------------------|--------------------|
| Proposal ID       | PROPOSID           |
| Target_Name       | TARGNAME           |
| Position          | RA_TARG, DEC_TARG  |
| Spectral Element  | FILTNAM1, FILTNAM2 |
| Time_Per_Exposure | EXPTIME            |

A convenient tool for viewing some of the more important data header keywords in an easy-to-read formatted output is the STSDAS task, **iminfo**. An example of the output of this task is shown in figure 2.1. Note that the data header keywords are expanded to standard English words in this output. The header file (.c0h) can also be examined with IRAF tasks **hedit** or **imhead**, with any standard text editor, or simply by listing the contents of the file. Again, please note that a standard text editor will show only the comments for the group keywords, not the values which are stored in the image file.

Figure 2.1: Displaying WFPC2 Header Keywords with iminfo

```

-----
Rootname          Instrument          Target Name
U2P60204T        WFPC2              CAL-GANY-W

Program           = 2P6              Obs Date          = 19/08/95
Observation set  = 02              Proposal ID       = 05837
Observation      = 04              Exposure ID       = 02-023
Source           = Tape Recorded   Right ascension   = 16:16:34.4
File Type        = SCI           Declination       = -20:45:14
                                           Equinox          = J2000

First filtername = F410M              Number of groups = 4
Second filtername =                               Data type        = real

Image type       = EXT              Exposure time (sec) = 5.
Mode             = FULL            Dark time (sec)    = 5.
Serials         = OFF
Shutter         = B
Kelsall spot lamp = OFF           Calibration steps done:
im> █           MASK ATOD BLEV BIAS FLAT SHAD

```

In the specific example shown in figure 2.1 the Proposal ID is given as 05837. Entering the proposal ID into the space provided on either the [HST Program Information web page](#) or [Program Status box on the HST web page](#) (without the leading 0) and clicking on **[Get Program Information]**, will bring up the Program Information page for that proposal. Under Program Contents on that page you can choose either the file typed in during Phase II or a formatted output. The latter may be easier to read; we reproduce a portion of that file in table 2.6.

The Exposure ID listed by **iminfo** is 02-023. This corresponds to visit 02, exposure 23. A different format was used in Cycles 0 through 4; exposures in these proposals have a single, unique numeric identifier. To reach this exposure line, page down through the proposal until visit 02 is reached. Now search for exposure 23 in visit 02. As shown in table 2.6, this exposure requested a single 5 second exposure of target CAL-GANY-W through filter F410M. A quick comparison with the keywords listed by **iminfo** shows that, indeed, this data file contains the observation specified in this exposure line.

Table 2.6: Exposure Log Sheet for WFPC2

Visit: 02  
 Visit Requirements: BEFORE 16-oct-95  
 On Hold Comments: <none>  
 Additional Comments: This visit has limited scheduling opportunities, we prefer as close to Jupiter opposition as possible exp-time calculated from observed Callisto WF images from SL9 campaign

| Exposures       |             |              |            |             |                  |                 |                     |         |      |                      |
|-----------------|-------------|--------------|------------|-------------|------------------|-----------------|---------------------|---------|------|----------------------|
| Exposure Number | Target Name | Instr Config | Oper. Mode | Aper or FOV | Spectral Element | Central Waveln. | Optional Parameters | Num Exp | Time | Special Requirements |
| 21              | Cal-Gany-W  | WFPC2        | IMAGE      | PC1         | F218W            |                 | ATD-GAIN=7          | 2       | 500s | NO SPLIT             |
| 22              | Cal-Gany-W  | WFPC2        | IMAGE      | PC1         | F255W            |                 | ATD-GAIN=7          | 1       | 40s  |                      |
| 23              | Cal-Gany-W  | WFPC2        | IMAGE      | PC1         | F410M            |                 | ATD-GAIN=15         | 1       | 5s   |                      |
| 24              | Cal-Gany-W  | WFPC2        | IMAGE      | PC1         | F953N            |                 | ATD-GAIN=15         | 1       | 30s  |                      |
| 25              | Cal-Gany-W  | WFPC2        | IMAGE      | PC1         | F675W            |                 | ATD-GAIN=15         | 1       | 0.2s |                      |
| 26              | Cal-Gany-W  | WFPC2        | IMAGE      | PC1         | F300W            |                 | ATD-GAIN=15         | 1       | 10s  |                      |

A comparison of these keywords should quickly reveal the data file corresponding to a given exposure line. There are, however, two cases in which such a comparison is somewhat more complicated.

It is recommended that WFPC2 exposures longer than 600 seconds be split into two shorter exposures to facilitate the removal of cosmic rays. If the optional parameters CR-SPLIT and CR-TOLERANCE are omitted in the Phase II submission, and the exposure is *longer* than 600 seconds, it will be split into two exposures for more efficient scheduling. The default CR-TOLERANCE of 0.2 can be used, meaning that the split exposure times could each range from 30–70% of the total exposure, with their sum equal to the original total exposure time.

Exposure times may occasionally be shortened or lengthened by up to 20% without the approval of the PI, provided that the resulting S/N is 90% of that with the original exposure time. Such changes may be required to fit observations into specific orbital time slots. If, after examining your exposure headers, you still have questions regarding the execution of your observing plan, we recommend you speak with your program coordinator or email [help@stsci.edu](mailto:help@stsci.edu).

The output generated by **iminfo** contains information on the target, exposure time, and filters used, but nothing on guide star status. Any of the STSDAS tasks (**hselect**, **hedit**, or **imhead**), see table 2.2, can provide access to that information by printing the FGSLOCK header keyword to the screen.

The FGSLOCK keyword can have the values FINE, COARSE, GYROS, or UNKNOWN. Coarse tracking is no longer allowed, so this FGSLOCK in recent data will most likely read either FINE or GYROS. Gyro tracking allows a drift rate of approximately 1 mas/sec. It would only be used if requested by the proposer. FINE tracking typically holds pointing with an rms error of less than 7 mas. Normally, two guide stars are used in HST observations, but on occasion only one appropriate guide star can be found. Such observations will suffer from small drift rates (a few mas in a 1000 second exposure). To determine the quality of tracking obtained during

your observations, please review appendix C of the HST Introduction which describes how to determine the number and quality of guide stars actually used, as well as how to use the OMS jitter files.

---

## 2.4 WFPC2 Paper Products

In the past, observers received a package of so-called *paper products* as part of the initial data delivery; mailed in paper form, these products provided a quick-look summary of the data. In August 1999, the Archive discontinued printing and mailing of these products; instead, the summaries are now made available in PDF format to observers via the [Archive's Paper Products WWW page](#). Note, however, that the PDF files on the WWW are available only for the most recent 6 months of data; for older data, observers can generate their own paper products using the STSDAS task `pp_dads`.

### 2.4.1 Visit-level Output

The `pp_dads` output consists of two parts, a visit-level overview of the datasets and an exposure-level summary. The visit-level summary is meant to be similar to the observing log in ground-based observations. The information is presented in three separate tables: Target List, Observation List, and Observation Statistics. The Target List gives the targets, including their positions, observed in the visit. The Observation List includes essential information on each dataset, such as rootname, target name, operating mode, aperture, filter, exposure time, and a number of flags intended to alert the user to any procedural problem with the data. The flags are represented graphically by circles, open when the data are okay, filled if any (potential) problem is encountered; see figure 2.2 for a Target List and Observation List example. The Observation Statistics is a table with basic image statistics for each dataset, such as mean counts, background level, and a rough estimate of the limiting magnitude that can be reached with respect to the background level in the image (see figure 2.3). Note that this limiting magnitude is computed with a rather simple, all-purpose algorithm, and is meant only as an approximate indication; it should not be used for any detailed calculations. Image statistics are given separately for each CCD.

## 2.4.2 Exposure-level Output

The second part of the **pp\_dads** output presents the data exposure by exposure. Usually, there are three pages for each exposure: the first two pages are grayscale representations of the image, one containing all four chips together, the other featuring the PC only (see figure 2.4); the third summarizes various exposure characteristics as well as any flags and error conditions that might have arisen (see figure 2.5). The grayscale presentation on the first page of the four chips together is a crude mosaic; each chip is rotated and placed in the correct position with respect to the others, but the overlap and the small differential rotations between chips (see chapter 1) are not corrected. The next page presents the PC by itself, at a larger scale, which enhances smaller details not evident in the mosaic. The third page, containing the dataset information, is divided into several zones, each summarizing information on a specific topic: the HST Spacecraft Performance Summary, with information on pointing and jitter; the Pipeline Processing Summary, with information on whether the file was processed properly by the pipeline (see chapter 3); the Calibration Data Quality Summary, where any inconsistencies in the choices of calibration files are highlighted; the Exposure Summary, which details when and how the exposure was taken; and the Calibration Status Summary, which reports all reference files used in the calibration and their pedigree, if available. Some basic consistency checks are carried out and the user is alerted to any potential problems.

## 2.4.3 A note about grayscales

A few comments are in order regarding the grayscale representation of the data. The images are presented as they appear after the standard pipeline processing (see chapter 3). Bias, standard dark, and flatfield corrections have been applied, but hot pixels and cosmic rays are not removed; hence, many images will appear mottled, especially those with exposure times longer than a few hundred seconds. In order to limit the size of the printouts, images are block-averaged (2 x 2), causing some details to be lost. In general, because of the limited resolution of even good black-and-white printers, finer image details are lost (see figure 2.4); the grayscale images cannot in any way replace even a quick look on the screen.

Paper products shipped before August 1997 differ from the current **pp\_dads** output in two main respects. First, they did not have the visit-level summary of observations; some of the information was available via the tape log, but without any data quality flags or image statistics. Second, the exposure-level information was presented in a different way; the dataset information page consisted simply of a printout of the PDQ file (see “PDQ Files” in appendix B). The grayscale images were produced by a different

task, which gave them a different appearance, but the overall information content in them was very similar to the current output. Sample paper products in the current format are shown in figure 2.2 - 2.5. Users who have received paper products in the old format can regenerate them in the new format using **pp\_dads**.

#### 2.4.4 Obtaining paper products

Observers with data taken within the last 6 months may obtain PDF format versions of the paper products from the [Archive's Paper Products WWW page](#). The query form provides a wide variety of search options such as dataset name, proposal number, observation date, and so on. Any questions or requests for assistance with the search may be directed to [archive@stsci.edu](mailto:archive@stsci.edu).

For data older than 6 months, observers can generate the data products using the STSDAS task **pp\_dads**. At a minimum, the task requires the calibrated science image (**c0h/c0d**) and the standard header information (**shh/shd**) as input files. The jitter files (see section C.3 in appendix C) are optional; if they are missing, the summary of the spacecraft performance information (see figure 2.5), including number of recenterings and jitter measurements in V2 and V3, are left blank by the task.

To generate the paper products, load the **stsdas**, **hst\_calib**, and **paperprod** packages, then execute the task in the directory containing the input files. The *device* parameter specifies the output device. In the example below, *psi\_land* directs the summaries to a postscript file, which is written to the */tmp* directory. The *output\_select* parameter provides control over the information summarized: cover page, visit page, exposure pages, or all output. Please refer to the online STSDAS help for **pp\_dads** for more details on the available parameters and options.

```
cl> stsdas
cl> hst_calib
cl> paperprod
cl>pp_dads u*c0h device=psi_land output_select=all
    === Space Telescope Paper Product, Version 2.33 (April 24, 2001) ===
/tmp/psk6741a
```

Figure 2.2: Paper Products: List of Targets and Observations

Visit: 35 Proposal: 05370 WFPC2

Target List

| Target Name | R.A. (J2000) | Dec. (J2000) | Description      |
|-------------|--------------|--------------|------------------|
| HI-LAT      | 13:27:11.62  | -47:29:54.8  | STARS; GALAXIES; |

Observation List

| Logsheet Line# | Rootname  | Target Name | Operating Mode | Serials/ Gain | Aperture or FOV | Filters | Wavelength | Exposure (sec) | Quality Flags |      |     |
|----------------|-----------|-------------|----------------|---------------|-----------------|---------|------------|----------------|---------------|------|-----|
|                |           |             |                |               |                 |         |            |                | Obs           | Proc | Cal |
| 35.000         | U27R8502T | HI-LAT      | FULL           | OFF/7.00      | WFALL           | F814W   | 8006.80    | 600.0          | ○             |      | ○   |
| 35.000         | U27R8501T | HI-LAT      | FULL           | OFF/7.00      | WFALL           | F814W   | 8006.80    | 600.0          | ○             |      | ○   |
| 39.000         | U27R9U01T | HI-LAT      | FULL           | OFF/7.00      | WFALL           | F814W   | 8006.80    | 700.0          | ○             |      | ○   |
| 39.000         | U27R9U02T | HI-LAT      | FULL           | OFF/7.00      | WFALL           | F814W   | 8006.80    | 700.0          | ○             |      | ○   |

Quality flags: ○ = OK ● = Not OK Blank = Unknown or file missing

Figure 2.3: Paper Products: Observation Statistics (separately for each CCD)

Visit: 35 Proposal: 05370 WFPC2

Observation Statistics

| Logsheet Line# | Rootname  | Target Name | Filter | Exposure Time | POSTARG | Detector | Modal Sky | Sky Sigma | Min DN | Max DN   | Limiting Mag. |       |
|----------------|-----------|-------------|--------|---------------|---------|----------|-----------|-----------|--------|----------|---------------|-------|
| 35.000         | U27R8502T | HI-LAT      | F814W  | 600.00        | N/A     | N/A      | 1         | 6.14      | 2.51   | -359.14  | 18101.54      | 28.82 |
| 35.000         | U27R8502T | HI-LAT      | F814W  | 600.00        | N/A     | N/A      | 2         | 27.68     | 20.75  | -1126.21 | 52096.83      | 26.74 |
| 35.000         | U27R8502T | HI-LAT      | F814W  | 600.00        | N/A     | N/A      | 3         | 40.38     | 72.99  | -410.52  | 92238.00      | 25.47 |
| 35.000         | U27R8502T | HI-LAT      | F814W  | 600.00        | N/A     | N/A      | 4         | 56.39     | 90.57  | -1382.49 | 125202.3      | 25.14 |
| 35.000         | U27R8501T | HI-LAT      | F814W  | 600.00        | N/A     | N/A      | 1         | 9.37      | 2.60   | -300.12  | 35567.71      | 28.78 |
| 35.000         | U27R8501T | HI-LAT      | F814W  | 600.00        | N/A     | N/A      | 2         | 66.88     | 20.56  | -1131.11 | 287711.6      | 26.75 |
| 35.000         | U27R8501T | HI-LAT      | F814W  | 600.00        | N/A     | N/A      | 3         | 43.30     | 68.34  | -576.75  | 108361.5      | 25.54 |
| 35.000         | U27R8501T | HI-LAT      | F814W  | 600.00        | N/A     | N/A      | 4         | 55.46     | 89.38  | -1570.77 | 124874.8      | 25.15 |
| 39.000         | U27R9U01T | HI-LAT      | F814W  | 700.00        | N/A     | N/A      | 1         | 20.07     | 4.14   | -302.07  | 103304.2      | 28.45 |
| 39.000         | U27R9U01T | HI-LAT      | F814W  | 700.00        | N/A     | N/A      | 2         | 38.79     | 30.39  | -1315.45 | 110014.1      | 26.49 |
| 39.000         | U27R9U01T | HI-LAT      | F814W  | 700.00        | N/A     | N/A      | 3         | 43.25     | 90.29  | -649.44  | 76723.60      | 25.41 |
| 39.000         | U27R9U01T | HI-LAT      | F814W  | 700.00        | N/A     | N/A      | 4         | 60.14     | 103.00 | -1845.88 | 123228.6      | 25.16 |
| 39.000         | U27R9U02T | HI-LAT      | F814W  | 700.00        | N/A     | N/A      | 1         | 6.01      | 2.70   | -354.96  | 12388.22      | 28.91 |
| 39.000         | U27R9U02T | HI-LAT      | F814W  | 700.00        | N/A     | N/A      | 2         | 42.91     | 25.78  | -1234.59 | 121265.8      | 26.67 |
| 39.000         | U27R9U02T | HI-LAT      | F814W  | 700.00        | N/A     | N/A      | 3         | 71.66     | 88.56  | -815.84  | 266563.8      | 25.43 |
| 39.000         | U27R9U02T | HI-LAT      | F814W  | 700.00        | N/A     | N/A      | 4         | 66.55     | 104.06 | -1770.08 | 157240.0      | 25.15 |

Figure 2.4: Paper Products: Combined Grayscale Display

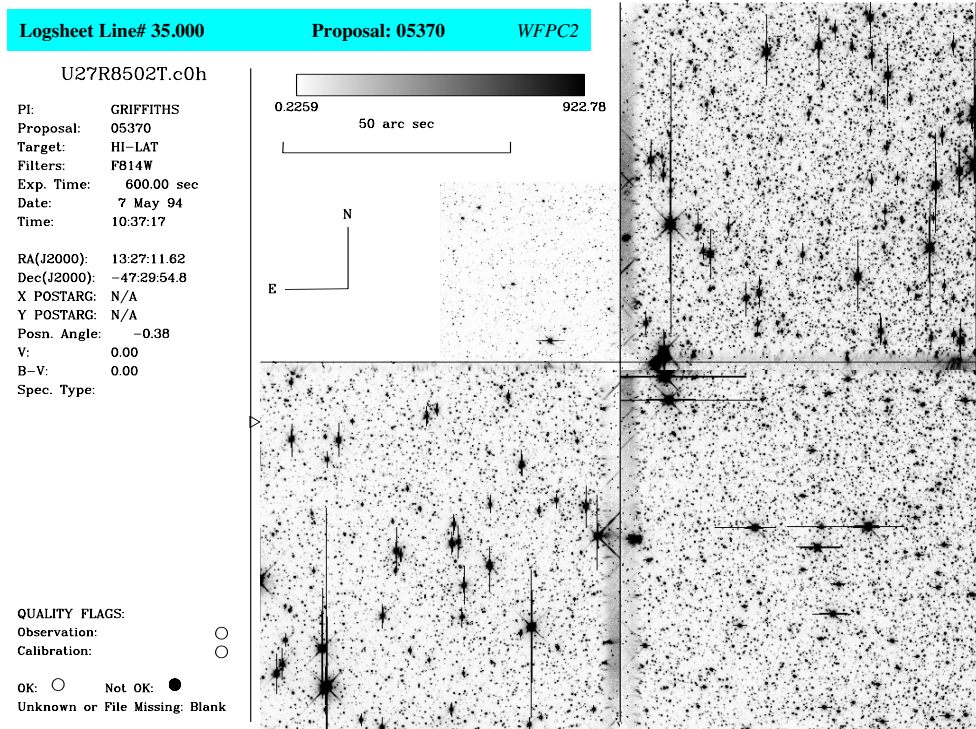


Figure 2.5: Paper Products: Observation Summary

|                              |                               |                        |              |
|------------------------------|-------------------------------|------------------------|--------------|
| <b>Logsheet Line# 35.000</b> | <b>Observation: U27R8502T</b> | <b>Proposal: 05370</b> | <b>WFPC2</b> |
|------------------------------|-------------------------------|------------------------|--------------|

|  |  |
|--|--|
| <p><i>HST Spacecraft Performance Summary</i></p> <p># Recenterings:                      # Losses of Locks:<br/>         V2 Jitter (RMS):                    V2 Jitter (PP):<br/>         V3 Jitter (RMS):                    V3 Jitter (PP):</p> <p>Could not find JITTER file.<br/>         Very highly packed star field.<br/>         Brighter stars saturated and blooming. Filter F814W, exposure 600s</p> | <p><i>Exposure Summary</i></p> <p>Target Name: HI-LAT<br/>         RA (J2000): 13:27:11.62<br/>         Dec (J2000): -47:29:54.8<br/>         X POSTARG: N/A<br/>         Y POSTARG: N/A<br/>         Aperture: WFALL<br/>         Exp Time (sec): 600.0</p> |
| <p><i>Pipeline Processing Summary</i></p> <p>No Error Checks Made.</p>   | <p>Rootname: U27R8502T<br/>         Date: 7 May 94<br/>         Time: 10:37:17<br/>         Proposal: 05370<br/>         PI: GRIFFITHS</p>   |
| <p><i>Calibration Data Quality Summary</i></p> <p>No Anomalies.</p> <p>No Calibration File Pedigree Information available.</p>   | <p>Chip 3 Statistics</p> <p>Sky: 40.38<br/>         Sky Sigma: 72.99<br/>         Minimum: -410.52<br/>         Maximum: 92238.00<br/>         Limiting Mag: 25.47</p>   |

*Calibration Status Summary*

| <u>Switches and Flags</u> |          |                              | <u>Reference Files and Tables</u> |                    |          |
|---------------------------|----------|------------------------------|-----------------------------------|--------------------|----------|
| Keyword                   | Value    | Calibration Step             | Keyword                           | filename           | Pedigree |
| MASKCORR                  | COMPLETE | Mask Correction              | MASKFILE                          | urefSe2112084u.r0h |          |
| ATODCORR                  | COMPLETE | A-to-D Correction            | ATODFILE                          | urefSdbu1405iu.r1h |          |
| BLEVCORR                  | COMPLETE | Bias Level Correction        | BLEVFILE                          | ucalSu27r8502t.x0h |          |
| BIASCORR                  | COMPLETE | Bias Correction              | BIASFILE                          | urefSe4p1629bu.r2h |          |
| DARKCORR                  | COMPLETE | Dark Correction              | DARKFILE                          | urefSe1q1433du.r3h |          |
| FLATCORR                  | COMPLETE | Flat Field Correction        | FLATFILE                          | urefSe391434fu.r4h |          |
| SHADCORR                  | OMIT     | Shaded Shutter Correction    | SHADFILE                          | urefSe371355eu.r5h |          |
| DOPHOTOM                  | COMPLETE | Populate Photometry Keywords | PHOTTAB                           | ucal:u27r8502t.c3t |          |





CHAPTER 3:

# WFPC2 Calibration

**In this chapter. . .**

|   |
|---|
| 3.2 Data Processing Steps / 3-4               |
| 3.3 Standard Pipeline Calibration / 3-8       |
| 3.4 Recalibration / 3-17                      |
| 3.5 Improving the Pipeline Calibration / 3-24 |

This chapter discusses the processing and calibration of WFPC2 data, the routine processing that must be performed before detailed data analysis can commence. We begin by describing the pipeline calibration that occurs before the data are delivered to the observer, then detail possible reasons to refine and enhance the routine calibration and the various options available to do so.

---

## 3.1 Data Processing Pipelines

Up until 1999, HST observers received their data via tape and/or via Archive retrieval requests; the raw and calibrated data were copies of files that had been stored on the archive media and were the result of pipeline processing *at the time the image was taken*. In December 1999, the On-The-Fly Calibration (OTFC) system was released to the public. In response to a user request for data, OTFC retrieved raw files (.d0\*, .q0\*, .x0\*, .q1\*) from the archive, then calibrated and shipped the data to the requestor. The primary advantages of OTFC included the

- automatic application of improved calibration files and switches,
- use of most recent calibration software (allowing for rapid access to improved algorithms, new capabilities, and software fixes), and
- correction of header keywords, if needed.

An additional major benefit to OTFC was that only the uncalibrated data needed to be stored in the archive<sup>1</sup>.

The On-The-Fly Reprocessing (OTFR) system replaced OTFC on May 16, 2001, a change transparent to the majority of HST archive users. Requests for data are submitted either via StarView or the WWW (see chapter 1 of the HST Introduction); freshly-processed raw and calibrated data are delivered<sup>2</sup>. There is no need to explicitly ask for OTFR, *all requests for WFPC2 data are now handled by the OTFR system*.

The primary difference between the two on-the-fly systems is that OTFR begins earlier in the data path. OTFR starts with the original telemetry files ("POD" files) received from Goddard Space Flight Center and performs all pipeline processing steps, including data partitioning, fixing data dropouts, converting the partitioned data packets into raw science files, and calibrating the newly-created raw files. OTFC performed only the last pipeline processing step, calibration, on raw files stored in, and retrieved from, the archive.

An overview of the data flow for both systems is summarized in the table below. The benefits of the new OTFR system encompass the benefits of the OTFC system, plus OTFR data need fewer header corrections since most problems are fixed as part of the pre-calibration pipeline processing. Also, the OTFR system as a whole requires significantly less maintenance effort than OTFC. As of late 2001, both the POD files and raw pre-calibration WFPC2 data are still being archived; the raw files are not used for distribution but kept merely as a backup to the POD files. Future

---

1. As of June 2000, calibrated WFPC2 data are no longer archived.

2. By default, OTFR currently delivers both raw and calibrated data. A future enhancement to the retrieval process will allow requests for subsets of files (e.g., only calibrated).

plans call for the eventual cessation of raw data archiving, after which only the POD files will be archived.

Table 3.1: Comparison of Dataflow in the On-The-Fly Systems

| OTFC (December 1999 - May 2001)  | OTFR (May 2001 - present)  |
|--|--|
| Request for data is submitted to the archive via StarView or WWW interface. Archive responds with acknowledgement email.   | Same as OTFC.  |
| Raw files are retrieved from the HST archive and passed to the OTFC system. For WFPC2, the raw files are the <code>d0</code> , <code>q0</code> , <code>q1</code> , <code>x0</code> , and <code>tr1</code> files. | POD file <sup>1</sup> (original telemetry file) is retrieved from HST archive and passed to OTFR system. Pre-calibration OPUS processing is performed: data partitioning, fixing dropouts, generating raw files ( <code>d0</code> , <code>q0</code> , <code>q1</code> , <code>x0</code> , and <code>tr1</code> files). |
| Any problems in the header keywords are fixed by special lookup table.   | Same as OTFC although the OPUS pre-calibration processing fixes the majority of keyword problems automatically (i.e., significantly fewer header corrections required in OTFR).  |
| The best calibration files & switches are determined by a separate standalone task, and header keywords updated accordingly.   | Not needed. The best calibration files & switches are set by the pre-calibration OPUS code (generic conversion).   |
| Images are calibrated by STSDAS <code>calwp2</code> and sent back to the archive system.   | Same as OTFC.  |
| Archive delivers raw + calibrated data and emails completion notification to the requestor.  | Same as OTFC. Files contain a new keyword, <code>PROCTIME</code> , to record when the OTFR system processed the data.  |

1. For WFPC2, there is 1 image per POD file.

---

## 3.2 Data Processing Steps

After WFPC2 observations have executed, the data pass through the *OPUS pipeline*, where they are processed and calibrated. A substantial fraction of header keyword values are extracted and used to populate the Archive databases; observers access these databases each time they browse the Archive contents and perform searches via the [HST Archive Search WWW form](#) or the Archive's [database browser, StarView](#). The resulting raw and calibrated data files from this first pipeline processing are not seen by the observer. Instead, when an archive data request is submitted, the images are completely reprocessed by the *On-The-Fly Reprocessing (OTFR)* system before they are delivered. The OTFR system processing is identical to the OPUS pipeline processing, except that, as discussed in the previous section, the most up-to-date reference files and software at the time of processing are used. So, for example, if an observer waits several weeks after an observation before requesting the data products, it is very likely that OTFR will have access to an updated dark reference file with which to process the science data - a reference file that was not in place at the time the observation was taken (see [Reference File Memo](#)).

All of the steps performed by OTFR are the same as those performed in the OPUS pipeline; these steps are recorded in the trailer file for each dataset. Figure 3.1 shows an example of a trailer file and identifies the major pipeline steps:

1. The data are partitioned: the POD file is separated into individual files, e.g., the engineering and science data sections.
2. The data are edited to insert dummy values (an arbitrary assigned value given in the header keyword STDCFFP) in place of missing pixel values.
3. The data are evaluated to determine discrepancies between the subset of the planned and executed observational parameters.
4. The data are converted to a generic format and the header keywords populated.
5. The data are calibrated using a standard WFPC2-specific calibration algorithm and the best available reference files.

Figure 3.1: Sample Trailer File

```

2001296190432-I-INFO ----- Data Partitioning Starts ----- (1)
2001296190432-I-INFO POD file name  : /info/opsci/pipe/clark/dat/dct/lz_a2db_161_0000226918_u5kl0101.pod_proc (1)
2001296190432-I-INFO Observation name: u5kl0101r (1)
2001296190438-I-INFO Finished partitioning obs u5kl0101r (1)
2001296190438-I-INFO Expected 3201 packets, Recieved 3201 packets (1)
2001296190438-I-INFO (1 SHP, 0 UDL, 0 BAD, 3200 SCI). (1)
2001296190438-I-INFO ----- Data Partitioning ends ----- (1)
2001296190449-I-INFO ----- Data Quality Editing Started: u5kl0101r ----- (1)
2001296190450-I-INFO ----- Data Quality Editing Completed: u5kl0101r ----- (1)
2001296190502-I-INFO ----- Data Validation Started: u5kl0101r ----- (1)
2001296190502-I-INFO Mismatched weight (0) was lower than threshold (9) (1)
2001296190503-I-INFO ----- Data Validation Completed: u5kl0101r ----- (1)
2001296200730-I-INFO ----- World Coordinate System Beginning: u5kl0101r -----
2001296200734-I-INFO ----- World Coordinate System Started ----- (1)
2001296200736-I-INFO ----- World Coordinate System Ended ----- (1)
2001296200736-I-INFO ----- World Coordinate System Completed: u5kl0101r -----
2001296200747-I-INFO ----- Generic Conversion Started: u5kl0101r ----- (1)
2001296200807-I-INFO ----- Generic Conversion Completed: u5kl0101r ----- (1)
CALBEG ----- Tue Oct 23 20:08:18 GMT 2001-----
--- xWFPC2 Calibration Starting: CALWP2 Version 2.1 (Oct. 13, 2000)
--- Starting CALWP2: Input = u5kl0101r  Output = u5kl0101r
MASKFILE=uref$f8213081u.r0h MASKCORR=COMPLETED
PEDIGREE=INFLIGHT 01/01/1994 - 15/05/1995
DESCRIP=STATIC MASK - INCLUDES CHARGE TRANSFER TRAPS
  uref$dbu1405iu.r1h has no PEDIGREE keyword
BIASFILE=uref$kcd1557lu.r2h BIASCORR=COMPLETED
PEDIGREE=INFLIGHT 26/08/99 - 29/08/00
DESCRIP=not significantly different from j9a1612mu.
DARKFILE=uref$k311100ju.r3h DARKCORR=COMPLETED
PEDIGREE=INFLIGHT 24/02/2000 - 24/02/2000
DESCRIP=Pipeline dark: 120 frame superdark with hotpixels from 24/02/2000
FLATFILE=uref$g640925ru.r4h FLATCORR=COMPLETED
PEDIGREE=INFLIGHT 01/05/1994 - 01/10/1994
DESCRIP=Improved Cyc4 flat, fixed errors at CCD edges - now < 0.5% RMS
--- Starting processing of element 1
PC1: bias jump level ~0.149 DN.
photmode = WFPC2,1,A2D7,F606W,,CAL
--- Starting processing of element 2
WF2: bias jump level ~0.139 DN.
photmode = WFPC2,2,A2D7,F606W,,CAL
--- Starting processing of element 3
WF3: bias jump level ~0.130 DN.
photmode = WFPC2,3,A2D7,F606W,,CAL
--- Starting processing of element 4
photmode = WFPC2,4,A2D7,F606W,,CAL
--- Computing image statistics of element 1
--- Computing image statistics of element 2
--- Computing image statistics of element 3
--- Computing image statistics of element 4
--- WF/PC-2 Calibration Ending for observation
CALEND ----- Tue Oct 23 20:08:29 GMT 2001-----

```

**1 Partitioning****2 Editing****3 Evaluation****4 Conversion****5 Calibration**

### 3.2.1 Calibration of WFPC2 Images

The calibration software used by both the OPUS pipeline and OTFR is the same as that provided within STSDAS (**calwp2** in the **hst\_calib** package). The calibration files and tables used are taken from the Calibration Data Base (CDBS) at STScI and are the most up-to-date calibration files available at the time of processing. All CDBS files are available through the HST Data Archive. (See chapter 1 of the HST Introduction).

The flow of the data through **calwp2** is presented in schematic form in figure 3.2. The software takes as input the raw WFPC2 data file pairs (see table 2.1) and any necessary calibration reference images or tables. The calibration steps performed are determined by the values of the calibration switches (e.g., MASKCORR, BIASCORR, etc.) in the header of the raw data (.d0h) file. Likewise, the reference files to be used in the calibration of the data are set by the values in the reference file keywords (e.g., MASKFILE, BIASFILE, BIASDFILE, etc.). The appropriate settings of the calibration switches and reference file keywords depend on the instrumental configuration used (such as A-to-D gain, MODE, SERIALS, filters), the date of the observation, and any special pre-specified constraints. They are initially set in the headers of the raw data file during the generic conversion step, see figure 3.1; if reprocessing is necessary, they can be redefined by editing the raw header file (.d0h) using the STSDAS tasks **hedit** or **chcalpar** and then running **calwp2** on the raw files.

The values of the calibration switches in the headers of the raw and calibrated data indicate which processing steps the pipeline applied to the data and the reference files used. Calibration switches will have one of the following values:

- PERFORM - calibration step to be applied by **calwp2**
- OMIT - correction is not performed during processing
- COMPLETE - calibration step has been completed
- SKIPPED - step was skipped because the reference file was a dummy or placeholder file (i.e., has no effect on the data, such as a flatfield filled with values of 1).

For convenience, these keywords are reported in several locations:

- In the dataset information page of the paper products, see section 2.4.
- In the trailer files, see figure 3.1.
- In the HISTORY keywords at the end of the calibrated science data image (.c0h) file.

As with other header keywords, the calibration keywords can be viewed using the STSDAS tasks **imhead**, **hselect**, or **hedit**. Alternatively, the **chcalpar** task in the STSDAS **tools** package can be used to view and change the calibration keywords directly.

The flow chart below summarizes the sequence of calibration steps performed by **calwp2**, including the input calibration reference files and tables, and the output data files from each step. The purpose of each calibration step is briefly described in the accompanying table; a more detailed explanation is provided in the following section.

Figure 3.2: Pipeline Processing by calwp2

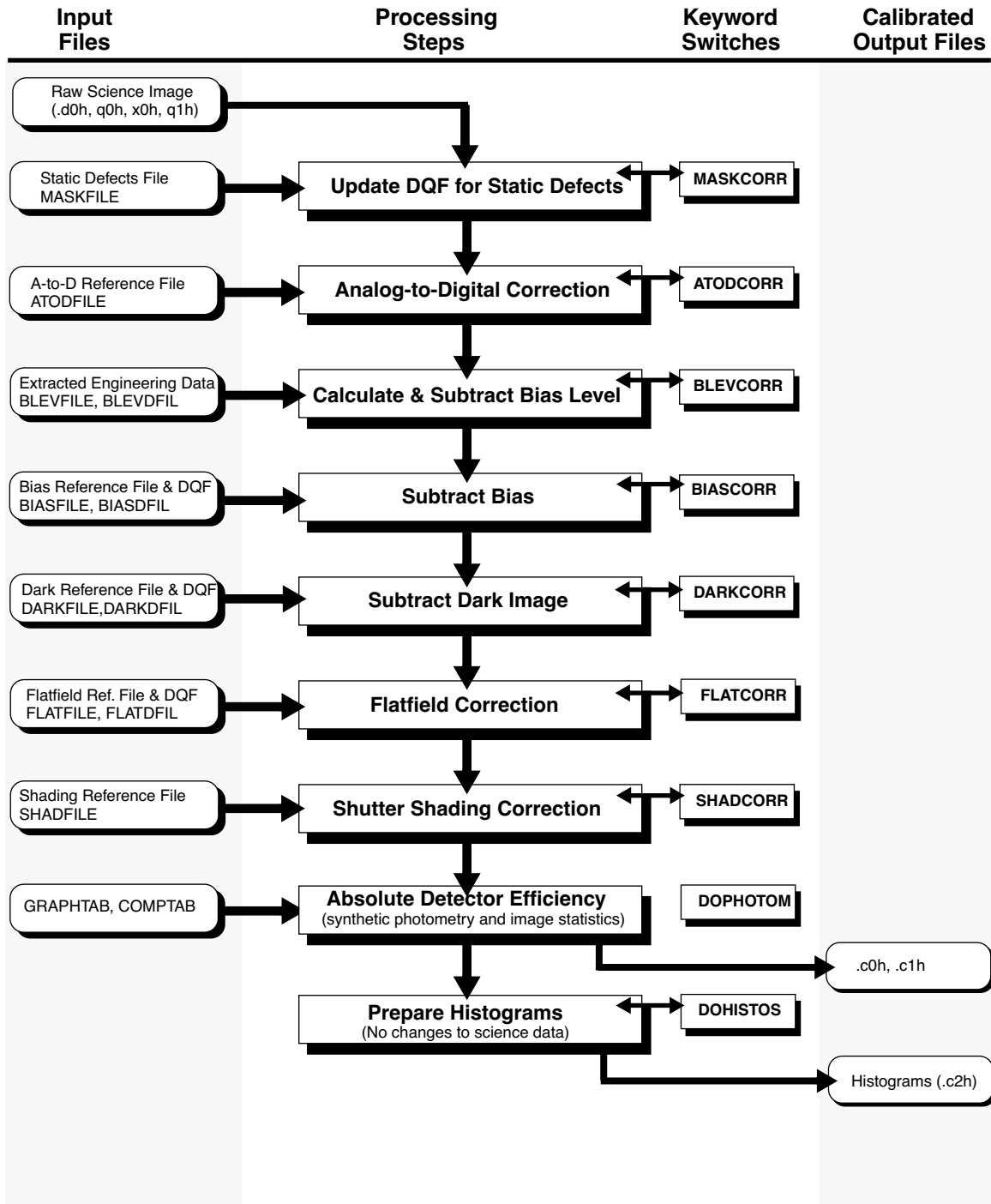


Table 3.2: Calibration Steps and Reference Files Used for WFPC2 Pipeline Processing

| Switch   | Processing Step   | Reference File                       |
|----------|---|--------------------------------------|
| MASKCORR | Update the data quality file using the static bad pixel mask reference file (MASKFILE), which flags defects in the CCD that degrade pixel performance and that are stable over time.  | maskfile<br>(r0h)                    |
| ATODCORR | Correct the value of each pixel for the analog-to-digital conversion error using information in the A/D lookup reference file (ATODFILE).   | atodfile<br>(r1h)                    |
| BLEVCORR | Subtract the mean bias level from each pixel in the science data. Mean values are determined separately for even column pixels (group parameter BIASEVEN) and odd column pixels (BIASODD) because the bias level exhibits a column-wise pattern that changes over time. | blevfile,<br>blevdfil<br>(x0h/ q1h)  |
| BIASCORR | Subtract bias image reference file (BIASFILE) from the input science image and update output data quality file with bias image data quality (BIASDFIL).   | biasfile,<br>biasdfil<br>(r2h/b2h)   |
| DARKCORR | Correct for dark current by scaling the normalized dark image reference file to the exposure time and subtracting it from science data. Dark image is multiplied by total dark accumulation time keyword (DARKTIME).  | darkfile,<br>darkdfil<br>(r3h/b3h)   |
| FLATCORR | Correct for pixel-to-pixel gain variation by multiplying by flat-field image.   | flatfile, flat-<br>dfil<br>(r4h/b4h) |
| SHADCORR | Remove shading due to finite shutter velocity (exposures less than 10 seconds)  | shadfile<br>(r5h)                    |
| DOPHOTOM | Determine absolute sensitivity using throughputs in <b>synphot</b> tables identified in GRAPHTAB and COMPTAB. This step does not change science data values.  |                                      |
| DOHISTOS | Create 3-row image (.c2h) for each group. Row 1 is a histogram of raw science values, row 2 the A/D correction, row 3 the calibrated image. (Optional, default is not to produce them.)   |                                      |

### 3.3 Standard Pipeline Calibration

Each calibration step, and the keyword switches used to turn the step on or off, is described in detail in the following sections. These steps are performed in the following order:

1. Flag static bad pixels.
2. Perform analog-to-digital (A/D) correction.
3. Subtract bias level.



4. Subtract bias image.
5. Scale and subtract dark image for exposures longer than 10 seconds.
6. Multiply by flatfield image.
7. Apply shutter shading correction to exposures of less than 10 seconds.
8. Calculate photometry keywords and update calibrated science image header accordingly (*does not affect pixel values*).
9. Calculate histograms.
10. Generate final science data quality file.

### 3.3.1 Calibration Files

Table 3.3 lists the types and related suffixes of the WFPC2 reference files used in **calwp2**. Most suffixes have the form **rNh/rNd**, where *N* is a number that identifies the step in which the file is used. The associated data quality file, if it exists, has the suffix **bNh/bNd**. The rootname of a reference file is based on the year, date, and time that the file was delivered to the Calibration Data Base System (CDBS).

Table 3.3: WFPC2 Calibration Reference Files

| Suffix             | Reference File                             |
|--------------------|--|
| r0h, r0d           | Static mask                                |
| r1h, r1d           | Analog-to-digital look-up table            |
| r2h, r2d, b2h, b2d | Bias                                       |
| r3h, r3d, b3h, b3d | Dark frame                                 |
| r4h, r4d, b4h, b4d | Flatfield                                  |
| r5h, r5d           | Shutter shading                            |
| c3t                | Photometry table (generated, not required) |

The file names and history of all WFPC2 reference files in CDBS (and retrievable from the HST Archive) are summarized in the [WWW Reference File Memo](#), updated with each new delivery. Any CDBS file is available for retrieval through the HST Data Archive (see chapter 1 of the HST Introduction). Some older, alternative reference files generated by the WFPC2 IDT are listed in the [IDT Reference File Memo](#), also available on the web. All of the installed reference files contain HISTORY keywords at the end of the header that can be viewed using the **imhead** task or a standard editor. These HISTORY keywords provide detailed information

about how the reference file was generated and when it was installed into the database.




---

*There are history records at the bottom of the header file of the calibrated data as well as each of the calibration reference file headers. These history comments sometimes contain important information regarding the reference files used to calibrate the data in the pipeline.*

---

### 3.3.2 Calibration Steps

#### Static Mask Application

Header Switch: MASKCORR

Header Keywords Updated: MASKCORR

Reference File: MASKFILE

The static mask reference file (.r0h/.r0d) contains a map of the known bad pixels and columns; the mask reference filename is recorded in the MASKFILE header keyword in the science header images (.d0h and .c0h). If this correction is requested, (MASKCORR=PERFORM), the mask is included in the calibration output data quality files; the science data themselves are *not* changed in any way. The STSDAS task **wfixup** can be used on the final calibrated science image (.c0h/.c0d) to interpolate across pixels flagged as bad in the final data quality file (.c1h).

#### A/D Correction

Header Switch: ATODCORR

Header Keywords Updated: ATODCORR

Reference File: ATODFILE

The analog-to-digital (A/D) converter takes the observed charge in each pixel in the CCD and converts it to a digital number. Two settings, or gains, of the A/D are used on WFPC2. The first converts a charge of approximately seven electrons to a single count (called a *Data Number* or *DN*), and the second converts a charge of approximately 14 electrons to a DN, also referred to as "*gain 15*" for historical reasons. The precise gain conversion values for each chip are listed in the [WFPC2 Instrument Handbook](#).

A/D converters work by comparing the observed charge with a reference and act mathematically as a "floor" function. However, these devices are not perfect and some values are reported more (or less) frequently than they would be by a perfect device; although the "true" DN values can never be recovered, one can statistically adjust for this systematic bias. Fortunately,

the WFPC2 A/D converters are relatively well-behaved and the correction is small (the largest correction is about 1.8 to 2.0 DN for bit 12, i.e., 2048)

The A/D fix up is applied when the ATODCORR keyword is set to PERFORM; the calibration file (lookup table) used to correct for the A/D errors has the suffix.r1h. The file has four groups, one for each detector; each group has 4096 columns (i.e., all possible DN values for a 12 bit detector) and two rows. The first row contains a -1 in the first pixel, followed by the Bay 3 temperature values in the subsequent pixels; the next row (each row corresponds to one temperature) contains the A-to-D conversion corrections for each DN value<sup>3</sup>. The example below illustrates determining the A-to-D fix up for a DN value of 450, in WF2, for gain 7, assuming the ATODFILE has already been retrieved from the Archive. Note that the correction for a given DN value is found in the DN+1'th pixel (i.e., [DN+1,2]).

```
cl> listpix dbu1405iu.r1h[2][451,2]
1. 450.1722
```

### Bias Level Removal

Header Switch: BLEVCORR

Header Keywords Updated: BLEVCORR

Group Header Keywords Updated: DEZERO, BIASEVEN, BIASODD

Reference File: BLEVFILE, BLEVDFIL

The charges that are in each pixel sit on top of an electronic pedestal, or “bias”, designed to keep the A/D levels consistently above zero. The mean level of the bias must be determined empirically using the extended register (overscan) pixels which do not view the sky. The values of these pixels are placed in the extracted engineering files (.x0h/.x0d). The overscan area used to calculate the mean bias levels is [9:14,10:790], with BIASODD being determined from columns 10, 12, and 14 and a BIASEVEN being determined from columns 9, 11, and 13 (this counter-intuitive nomenclature is due to an offset in the.x0h file; even and odd are correctly oriented with respect to the data file columns). In observations taken before March 8, 1994, the pipeline used a larger part of the overscan region, resulting in occasional oversubtraction of the bias level and possibly large negative pixel values. Separate even and odd bias levels were extracted in data taken and/or processed after May 4, 1994. Note that any data retrieved through the OTFR system will have the correct bias levels determined and removed. The keyword BLEVCORR controls the subtraction of the bias in **calwp2**.

---

3. On-orbit tests have shown that for WFPC2, the conversion values have remained constant; therefore, the A-to-D reference file contains only one temperature and one set (row) of conversion values.

**Bias Image Subtraction**

Header Switch: BIASCORR

Header Keywords Updated: BIASCORR

Reference File: BIASFILE, BIASDFIL

The value of the bias pedestal can vary with position across the chip. Therefore, once the mean bias level correction has been completed, the pipeline looks at the keyword BIASCORR. If it is set to PERFORM, then a bias image (.r2h/.r2d) is subtracted from the data to remove any position-dependent bias pattern. The bias reference file is generated by stacking a large set of A/D and bias-level corrected zero-length exposures. The correction consists of subtracting the bias reference file from the observation; any bad pixels flagged in the data quality file for the bias (.b2h/.b2h) are also flagged in the science image data quality file (.c1h/.c1d).

**Dark Image Subtraction**

Header Switch: DARKCORR

Header Keywords Updated: DARKCORR

Reference File: DARKFILE, DARKDFIL

A dark correction is required to account for the thermally-induced dark current as well as a *glow* (see section 4.3.2) from the field flattening lens. The dark reference file (.r3h/.r3d) is generated from a combination of a superdark image (a stack of typically 120 dark frames<sup>4</sup>) and warm pixels identified from a smaller stack of individual dark frames (five, as of ~1996). Prior to stacking, each dark frame is examined and regions affected by image anomalies, such as CTE residual images (see figure 4.2), are masked out. If a dark correction is requested (DARKCORR=PERFORM), the dark reference file, which was normalized to one second, is scaled by the DARKTIME keyword value and subtracted from the observation. By default, DARKCORR is set to “PERFORM” for all exposures longer than 10 seconds, and set to “OMIT” for shorter exposures.

**Flatfield Multiplication**

Header Switch: FLATCORR

Header Keywords Updated: FLATCORR

Reference File: FLATFILE, FLATDFIL

The number of electrons generated in a given pixel by a star of a given magnitude depends upon the quantum efficiency of that individual pixel as

---

4. A dark frame is a long exposure taken with the shutter closed; each individual dark has the standard calibration corrections applied (ATODCORR, BLEVCORR, and BIASCORR).

well as on any large scale vignetting of the field-of-view caused by the telescope and camera optics. To correct for these variations, the science image is multiplied by an inverse flatfield file. WFPC2 flatfields are currently generated from a combination of on-orbit data (so-called Earthflats, images of the bright Earth) and pre-launch ground data. The on-orbit data allow a determination of the large-scale illumination pattern while the pre-launch data are used to determine the pixel-to-pixel response function. The application of the flatfield file (extension .r4h) is controlled by the keyword FLATCORR.

### Shutter Shading Correction

Header Switch: SHADCORR

Header Keywords Updated: SHADCORR

Reference File: SHADFILE

The finite velocity of the shutter produces uneven illumination across the field of view (thus the term "shutter shading"), resulting in a position-dependent exposure time. *The effect is only significant, however, for exposures of a few seconds or less.* The shutter shading calibration is applied by default to all exposures less than ten seconds. It has the form of an additive correction, scaled to the appropriate exposure time, that varies spatially across the detectors. The keyword switch is SHADCORR, and the shutter shading file name is stored in the keyword, SHADFILE.

### Creation of Photometry Keywords

Header Switch: DOPHOTOM

Header Keywords Updated: DOPHOTOM, PHOTTAB

Group Header Keywords Updated: PHOTMODE, PHOTFLAM, PHOTZPT, PHOTPLAM, PHOTBW

Reference File: GRAPHTAB, COMPTAB

Photometry keywords, which provide the conversion from calibrated counts (DN) to astronomical magnitude, are computed by **calwp2** using the STSDAS package **synphot**. (More information on **synphot** can be found in this document, and in the *Synphot User's Guide*, which is available via the web.) The keyword switch for this step is DOPHOTOM, and the reference file keywords are GRAPHTAB and COMPTAB. *Note that the science data (.c0h/.c0d) pixel values are not changed as a result of performing DOPHOTOM, the data remain in units of DN (data number); calwp2 merely computes the photometric parameters and populates the appropriate header keywords.*

The photometric keywords that are computed are listed in figure 3.3 below; the first two are in the ASCII header (both .d0h and .c0h), while the last five keywords are group parameters (use the IRAF tasks **imheader**, **hselect**, or **hedit** to examine the group keywords—see chapter 2 and chapter 3 of the HST Introduction for more details).

Figure 3.3: Photometry Keyword Descriptions

|                   |   |
|-------------------|---|
| Header parameters | <div style="border: 1px solid black; padding: 5px;"> <pre> DOPHOTOM= 'YES ' / Fill photometry keywords: YES, NO, DONE PHOTTAB = 'ucal\$u27s0301n.c3t' / name of the photometry calibration table 'PHOTMODE' / Photometry mode (for example,WFPC2,1,A2D7,F675W,CAL) 'PHOTFLAM' / Inverse Sensitivity (erg/sec/cm<sup>2</sup>/Å for 1 DN/sec) 'PHOTPLAM' / Pivot wavelength (angstroms) 'PHOTBW ' / RMS bandwidth of the filter (angstroms) 'PHOTZPT' / Photometric zeropoint (magnitude) </pre> </div> |
| Group parameters  |   |

The calwp2 task constructs the PHOTMODE based on the specific image characteristics, which are given in the header keywords (i.e., INSTRUMENT, DETECTOR, ATODGAIN, FILTNAM1, FILTNAM2 and LRFWAVE); the throughput table for that PHOTMODE is then generated based upon the paths and files defined in the GRAPH and COMP tables stored in the HST Calibration Data Base System (CDBS). That path, i.e., the input files used to generate the final throughput table for the image, is recorded in the HISTORY comments of the calibrated science image (.c0h), and may also be viewed by running the STSDAS task **showfiles**.

The example below steps through both options; please refer to the *Synphot Handbook* for more details concerning the synphot tasks and the “Photometric Tables” section for suggestions on how to download the most recent **synphot** tables. Note that in the example below, the individual throughput files that are used to create the final image throughput table are: HST OTA, WFPC2 optics, filter (F606W), detector quantum efficiency table, a-to-d gain, and flatfield. Observers may notice that currently, the flatfield tables wfpc2\_flat\* (invoked by the "cal" in the photmode) are set to 1 though this could of course change with future WFPC2 flatfield and **synphot** table updates.

The final throughput table created for the image is saved in a STSDAS table with extension of ".c3t"; **calwp2** computes the photometric parameters from the .c3t table and updates the group keyword values accordingly.

```

wf> hsel u5kl0101r.c0h[2] $I,instrume,detector,atodgain,filtnam1,filtnam2 yes
u5kl0101r.c0h[2]          WFPC2    2          7.0      F606W
wf> hsel u5kl0101r.c0h[2] photmode,photflam,photplam,photbw,photzpt yes
WFPC2,2,A2D7,F606W,,CAL 1.842431E-18    6004.956      637.824 -21.1
cl> imhead u5kl0101r.c0h long+ | match HISTORY
...[some HISTORY lines removed to save space]
HISTORY The following throughput tables were used:
HISTORY crotacomp$hst_ota_007_syn.fits, crwfpc2comp$wfpc2_optics_006_syn.fits,
HISTORY crwfpc2comp$wfpc2_f606w_006_syn.fits,
HISTORY crwfpc2comp$wfpc2_dqewfc2_005_syn.fits,
HISTORY crwfpc2comp$wfpc2_a2d7wf2_004_syn.fits,
HISTORY crwfpc2comp$wfpc2_flatwf2_003_syn.fits
wf> showfiles "WFPC2,2,A2D7,F606W,,CAL"
#Throughput table names:
crotacomp$hst_ota_007_syn.fits
crwfpc2comp$wfpc2_optics_006_syn.fits
crwfpc2comp$wfpc2_f606w_006_syn.fits
crwfpc2comp$wfpc2_dqewfc2_005_syn.fits
crwfpc2comp$wfpc2_a2d7wf2_004_syn.fits
crwfpc2comp$wfpc2_flatwf2_003_syn.fits
wfl> bandpar "WFPC2,2,A2D7,F606W,,CAL" photlist=all
      # OBSMODE          URESP          PIVWV          BANDW
WFPC2,2,A2D7,F606W,,CAL 1.8424E-18    6004.9          637.82
      # OBSMODE          FWHM          WPEAK          TPEAK
WFPC2,2,A2D7,F606W,,CAL 1502.         6188.8          0.020972
      # OBSMODE          AVGWV          QTLAM          EQUVW
WFPC2,2,A2D7,F606W,,CAL 6038.9        0.0066095       39.467
      # OBSMODE          RECTW          EMFLX          REFWAVE
WFPC2,2,A2D7,F606W,,CAL 1881.8        3.6564E-15     6038.9
      # OBSMODE          TLAMBDA
WFPC2,2,A2D7,F606W,,CAL 0.019887

```




---

**It is not necessary to rerun *calwp2* and/or re-retrieve data via OTFR to merely recompute the photometric parameters; these may be obtained by running the STSDAS Synphot task *bandpar* directly, as shown in the example above.**

---

### **Histogram Creation**

Header Switch: DOHISTOS

Header Keywords Updated: DOHISTOS

Reference File: none

This step will create a multigroup image (*.c2h/ .c2d*) with one group for each group in the calibrated data file. Each group contains a three-line image where the first row is a histogram of the raw data values, the second row is a histogram of the A/D corrected data, and the third row is a histogram of the final calibrated science data. This operation is controlled by the keyword DOHISTOS; the default is to skip this step.

### **Data Quality File Creation**

By performing a bitwise logical OR, the **calwp2** software combines the raw data quality file (*.q0h, .q1h*) with the static pixel mask (*.r0h*) and the data quality files for bias, dark, and flatfield reference files (*.b2h, .b3h, .b4h*) in order to generate the calibrated science data quality file (*.c1h*). This step is always performed; even if no \*CORR keyword is set (i.e., if MASKCORR, BLEVCORR, BIASCORR, etc. were all set to OMIT), a *.c1h* file would still be generated, though it would not contain much useful information. The flag values used are defined below; by convention, DQF pixel values of zero (0) designate *good* pixels. The final calibrated data quality file (*.c1h*) may be examined, for example, using SAOimage, ximtool, or **imexamine**, to identify which pixels may be bad in the science image.



Table 3.4: WFPC2 Data Quality Flag Values

| Flag Value | Description  |
|------------|--|
| 0          | Good pixel   |
| 1          | Reed-Solomon decoding error. This pixel is part of a packet of data in which one or more pixels may have been corrupted during transmission.                 |
| 2          | Calibration file defect—set if pixel flagged in any calibration file. Includes charge transfer traps identified in static pixel mask file (.r0h).            |
| 4          | Permanent camera defect. Static defects are maintained in the CDBS database and flag problems such as blocked columns and dead pixels. (Not currently used.) |
| 8          | A/D converter saturation. The actual signal is unrecoverable but known to exceed the A/D full-scale signal (4095). <sup>1</sup>                              |
| 16         | Missing data. The pixel was lost during readout or transmission. (Not currently used.)   |
| 32         | Bad pixel that does not fall into above categories.  |
| 128        | Permanent charge trap. (Not currently used.)   |
| 256        | Questionable pixel. A pixel lying above a charge trap which may be affected by the trap.   |
| 512        | Unrepaired warm pixel.   |
| 1024       | Repaired warm pixel.   |

1. Calibrated saturated pixels may have values significantly lower than 4095 due to bias subtraction and flatfielding. In general, data values above 3500 DN are likely saturated.

## 3.4 Recalibration

With the advent of the On-The-Fly Reprocessing (OTFR) system in May 2001, all WFPC2 data requested from the Archive are automatically and completely reprocessed from the original telemetry file, using the most up-to-date software and calibration files. As such, the need for observers to manually recalibrate WFPC2 images has been greatly reduced. If recalibration is desired (e.g., due to an improvement in a reference file), the data can be re-retrieved from the Archive.

### 3.4.1 Why and When to Re-retrieve data through OTFR

The primary reason to re-request or reprocess WFPC2 data is the availability of improved or more up-to-date reference files and tables, especially darks, flatfields, **synphot** component tables, and improvements

to the pipeline software, such as the calibration task **calwp2**. In this section, we provide a brief summary of some relevant changes to the pipeline task and related elements as of today (November, 2001). Details on changes to the pipeline software are maintained in the [WFPC2 History Memo](#) (section 5). A quantitative account of the differences between various generations of reference files is given in chapter 4.

### Reference Files

Improved reference files will necessarily lag the science images in time. For example, the best dark reference file for a given WFPC2 observation will generally not be available until a few weeks after the science observation is taken. The time is required to retrieve the dark frames from the Archive, generate a new reference file, deliver the file to CDBS, and install the file for use in OTFR. Generally, there is one dark reference file per week, a combination of the dark frames taken that week and the current super dark.

Other reference files, such as the bias and flatfield, are more stable and thus are updated at less frequent intervals than the weekly darks. Bias reference files are generated roughly on an annual basis from a large set of frames taken over the course of one year. These new bias reference files become retroactive, applicable to any science data taken during the year covered by the individual bias frames used to generate the reference file. Superdarks are also generated about once per year; the input dark frames are processed with the superbias covering that year. The flatfields are typically updated less frequently than biases and darks, usually only once every few years. The mask file, A-to-D lookup table, and shutter shading files were created early in the mission of WFPC2 and have not changed since then. To check the quality of the reference files applied to your science observations, check the PEDIGREE and DESCRIP keywords in the HISTORY comments at the end of the header of the calibrated image (.c0h). For more details, refer to the reference file header itself, particularly the HISTORY records.

### Darks

Prior to the public release of OTFC in 2000, the calibrated data originally delivered to the principle investigator and to the Archive had been processed through the pipeline within a few days of the observation. At that time, the available dark reference file normally did not contain the most up-to-date information about warm pixels, which change on a weekly timescale (see section 3.5.1). Thus, pre-OTFC calibrated data were *always* processed with an out-of-date dark, and the correction of warm pixels could be improved by manually recalibrating with a more appropriate dark file or by using the STSDAS task **warmpix**. In this era of OTFR (see section 3.1) however, reprocessing with updated reference files can be accomplished by simply requesting the data from the Archive at least a few weeks after the science observations were taken.

Since August 1, 1996, the dark reference files used in the pipeline have been generated by combining an appropriate superdark (stack of 120 individual dark frames, taken over the course of about one year) with the information on warm pixels from one week's worth of darks (stack of 5 darks taken over less than two days). Thus, a new pipeline dark reference file exists for every week in which a set of five long dark frames were taken; the primary difference from week to week is the warm pixel population, since the superdark contribution remains the same over a year.

Prior to August 1996, pipeline dark reference files had been generated from a stack of only ten dark frames taken during a two week interval. Thus, very deep observations taken before August 1996 could benefit from recalibration with an improved dark reference file. For observations longer than about 20,000 seconds (10,000 seconds in the UV and in narrow-band filters), the noise in the dark frame is a significant contributor to the total noise in the final calibrated image. For this reason, if the science results are limited by the noise, observers are advised to manually recalibrate their images with a superdark, since this will significantly reduce the noise associated with dark subtraction. Note that it is also advisable to use an appropriate superbias as well as correct for warm pixels independently (e.g., by a post-pipeline processing task such as **warmpix**, discussed in section 3.5.1). Some early superdarks are listed in the [WWW Reference File Memo](#) and are available from the Archive; others are listed in the [IDT Reference File Memo](#). Also, the individual dark frames are always available from the Archive, should observers wish to generate their own custom superdark.

### *Flatfields*

Very early observations, those processed before March 9, 1994, used interim flatfields based on pre-launch data. These flatfields did not have good large-scale properties (peak errors were about 10%) and thus WFPC2 observations processed before that date should be re-retrieved through OTFR (the processing date can be determined from the trailer file). After March 1994, in-flight flatfields were used. Their quality has steadily improved, and those currently in the pipeline are believed to be good to about 0.3% on small scales, and 1% or less on large scales. See section 4.2 for a detailed discussion of the differences between various generations of flatfields.

If you are in doubt about the quality of the flatfielding in your observations, check the PEDIGREE and DESCRIP keywords of the flatfield file, also reported (after December 1994) in the HISTORY comments at the end of the header of the calibrated image. If PEDIGREE is GROUND, the data will need to be recalibrated. If the PEDIGREE is INFLIGHT, the flatfield was obtained from on-orbit data, and the DESCRIP keyword gives some information on its quality. INFLIGHT flatfields are of sufficient quality for most scientific goals, but for especially

demanding applications and data with very high signal-to-noise ratio, it may be advisable to recalibrate with the most recent flatfields.

### Photometric Tables

The photometric component tables are used by **synphot** to determine the photometric calibration header parameters, namely PHOTFLAM and PHOTPLAM (see chapter 5). These component tables have been updated several times, most recently on May 16, 1997, in order to contain the most up-to-date information on the throughput of WFPC2. If the photometric tables have changed, users can either re-retrieve their observations from the Archive or run **synphot** directly to determine the header parameters (see section 3.3.2). Note that to run **synphot** directly, observers must have the most up-to-date **synphot** tables installed at their local site; as a group, these tables are part of the standard STSDAS installation which is described in appendix A. Individual tables may be retrieved via the STScI ftp sites:

```
ftp://ftp.stsci.edu/cdbs/cdbs2/mtab/
```

```
ftp://ftp.stsci.edu/cdbs/cdbs2/comp/ota/
```

```
ftp://ftp.stsci.edu/cdbs/cdbs2/comp/wfpc2/
```

Users can also use the alternate methods given in section 5.1 to photometrically calibrate their observations.

### Pipeline Calibration Task **calwp2**

Another possible reason for recalibration is to use a more recent version of the calibration pipeline task **calwp2**. This task has seen several minor revisions, usually to add information to processed data; the current version, as of this writing, is 1.3.5.2. Only three of the **calwp2** revisions since WFPC2 operations began actually affect the calibrated data. The first two were changes in how the bias level is computed. Starting in March 8, 1994 (version 1.3.0.5), columns 3 through 8 of the overscan data were no longer used because they could be affected by the image background; beginning on May 4, 1994 (version 1.3.0.6), separate bias levels were computed for even and odd columns, resulting in a slightly better image flatness for about 1% of all WFPC2 images (see [WFPC2 ISR 97-04](#)).

The third update (version 1.3.5.2, January 3, 1997) corrects a bug introduced in December 1994 (1.3.0.7) in the calibration of WFPC2 single-chip, two-chip, or three-chip observations that do not include the PC (about 1% of all archived observations). We recommend that observers in possession of observations taken and processed between December 1994 and January 1997, re-request their data from the Archive.

### 3.4.2 Running calwp2 manually

As of May 2001, all WFPC2 data requested from the archive are processed through the On-The-Fly Reprocessing (OTFR) system, using the most up-to-date reference files and software. As such, recalibrating WFPC2 images can be done by simply re-retrieving the data via OTFR. However, occasionally, users may wish to recalibrate manually, for example, to make use of a non-standard dark or flatfield. In these cases, **calwp2** will need to be run from the IRAF/STSDAS command line. To recalibrate, the raw data and all reference files must be retrieved, the headers must be updated with the desired corrections to be performed, and the reference file names must be changed as needed. This section outlines in detail the necessary steps required to manually recalibrate WFPC2 data.

#### Retrieve necessary files

In order to recalibrate a WFPC2 observation, you need to retrieve the dataset as well as *all* of the reference files and tables needed for calibration. Since standard pipeline processing uses those files listed by StarView as the best reference files, see chapter 1 of the HST Introduction for a description of how to obtain the appropriate reference files from the STScI Archive. We suggest copying the raw data files and the required reference files and tables to a subdirectory used for recalibration as this will preserve all original files. Before beginning, any calibrated files (e.g., `.c0h/.c0d`, `.c1h/.c1d`, `.c3t`, `.cgr`) must be removed from the recalibration directory, since **calwp2** will not overwrite pre-existing calibrated products.

#### Edit calibration switches and reference files

The next step in recalibrating WFPC2 data is to set the calibration switches and reference keywords in the header of your raw data file (`.d0h`). These switches determine which calibration steps will be performed and which reference files will be used at each step in the process. The calibration header keywords in a dataset can be changed using the **hedit** or **chcalpar** task in the STSDAS **hst\_calib.ctools** package. The **hedit** task provides more detailed control over individual keywords and is preferred by some users experienced with calibration of WFPC2; though simpler to use, each switch and file must be changed individually.

The **chcalpar** task takes a single input parameter—the name(s) of the image files to be edited. When **chcalpar** starts, it automatically determines the instrument used to produce that image and opens one of several parameter sets (*pset*) which it loads with the current values of the header keywords. The WFPC2 pset is named `ckwwfp2`. Typing **ckwwfp2**, as a task name, at the `c1>` prompt will also edit this pset.

A detailed description of the steps involved in changing header keywords follows:

1. Start the **chcalpar** task, specifying the image(s) for which you want to change keyword values. If you specify more than one image, say

by using wildcards, the task will take initial keyword values only from the first image. For example, you could change keywords for all WFPC2 raw science images in the current directory (with initial values from the first image), using the following command:

```
wf> chcalpar u*.d0h
```

2. When **chcalpar** starts, you will be placed in **epar**—the IRAF parameter editor, and will be able to edit the parameter set of calibration keywords. Change the values of any calibration switches, reference files or tables to the values you wish to use for recalibrating your data. Remember that **no** processing has been done on the raw datasets. Therefore, even if you wish to correct, for instance, only the flatfielding, you will need to redo the bias and dark current subtraction as well; hence, the switches for all these steps must be set to **PERFORM**. Note that only the keywords you actually type in will be substituted.
3. Exit the editor by typing **:q** two times (the first **:q** to exit the pset editor, the second to exit the task). The task will ask if you wish to accept the current settings. If you type “y”, the settings are saved and you will return to the IRAF prompt. If you type “n”, you will be placed back in the editor to re-define the settings. If you type “a”, you will return to the IRAF prompt and any changes will be discarded. For additional examples of updating the calibration keywords, check the on-line help by typing **help chcalpar**.

### Set directory pointers

The calibration reference file names in the header of the raw data (i.e., the .d0h file) are typically preceded by five characters (e.g., **uref\$** for calibration images and **mtab\$** for calibration tables). These are pointers to the subdirectory where the reference and .x0h/.q1h raw data files are located. Before calibrating your data, you will need to set these pointers. For WFPC2 data, you would use something like the following:

```
to> set uref = "/your/hstdata/caldir/"
to> set mtab = "/your/hstdata/caldir/"
to> set ucal = "/your/hstdata/rawdir/"
```

where **caldir** is the subdirectory for the reference files and **rawdir** is the subdirectory for the uncalibrated images.

To set the **uref** in VMS, one would use:

```
to> set uref = "DISK$SHARE:[HSTDATA.CALDIR]"
```

where `HSTDATA.CALDIR` is the directory where you have stored the calibration reference files and tables.

### Execute `calwp2`

Once you have correctly changed the values of the calibration keywords in the header of the raw data file, you are ready to recalibrate your data. The WFPC2 calibration software, `calwp2`, is run by typing the name of the task followed by the *rootname* of the observation dataset. For example, to recalibrate the dataset `u0w10e02t` and write the log of the results to the file `calwp2.log` (rather than to the screen), type:

```
wf> calwp2 u0w10e02t "" > calwp2.log
```




---

*Note that `calwp2` will not overwrite an existing calibrated file. If you run the task in the directory where you already have calibrated data, you will need to specify a different output file name, for example:*

```
wf> calwp2 u00ug201t wfpc_out > wfpc.log
```

---

For more information about how these routines work, use the on-line help by typing `help calwp2`.

### A note about calculating the absolute sensitivity for WFPC2

If you set `DOPHOTOM=OMIT` before running `calwp2`, then the values of inverse sensitivity (`PHOTFLAM`), pivot wavelength (`PHOTPLAM`), RMS bandwidth (`PHOTBW`), zeropoint (`PHOTZPT`), and observation mode (`PHOTMODE`) will not be written to the header of the recalibrated data file. Remember that the `DOPHOTOM` calibration step does not alter the values of the data (which are always counts or data numbers in the calibrated file), but only writes the information necessary to convert counts to flux in the header of the file. Therefore, unless you wish to recalculate the absolute sensitivity for your observation (e.g., because a more recent estimate of the throughput exists for your observing mode), there is no need to recompute these values and you can simply use the keyword values from your original calibrated file and apply them to your recalibrated data. However, new estimates of WFPC2 transmission and absolute sensitivity were obtained in September 1995, May 1996, and May 1997. If your data were processed in the pipeline before May 1997, you may wish to re-create the absolute sensitivity parameters using the latest version of `synphot`, which contains tables based on the most recent photometric calibration of

WFPC2; see “Creation of Photometry Keywords”, for an example of this computation.

If you wish to recalculate the absolute sensitivity, set DOPHOTOM=YES in the .d0h file before running **calwp2**, or alternately, use the tasks in the **synphot** package of STSDAS. The “**synphot**” section in section 3.3.4 of the the HST Introduction has more information about how to use this package. To calculate the absolute sensitivity, **calwp2** and the **synphot** tasks use a series of component lookup and throughput tables. These tables are not part of STSDAS itself, but are part of the **synphot** dataset, which can easily be installed at your home site (see appendix section A.3.2 for information about how to do this). A more detailed discussion of photometric calibration can be found in section 5.2.




---

*The most recent synphot tables must be in place in order to recalculate absolute sensitivity for WFPC2 data using calwp2 or synphot (see chapter 3 of the HST Introduction).*

---

## 3.5 Improving the Pipeline Calibration

The individual calibrated images produced by the standard pipeline processing are, in most respects, as good as our knowledge of the instrument can make them. The usefulness of post-pipeline calibration is, in general, limited to three areas: improving the correction of pixels with elevated dark current (warm pixels), which are known to vary with time; employing a correction flatfield or alternate flatfield; and removing cosmic rays by comparing multiple images of the same field.




---

*The treatment of warm pixels and cosmic rays can be quite different in the case of dithered data. This case is discussed in section 5.5; the present discussion refers to co-aligned data only.*

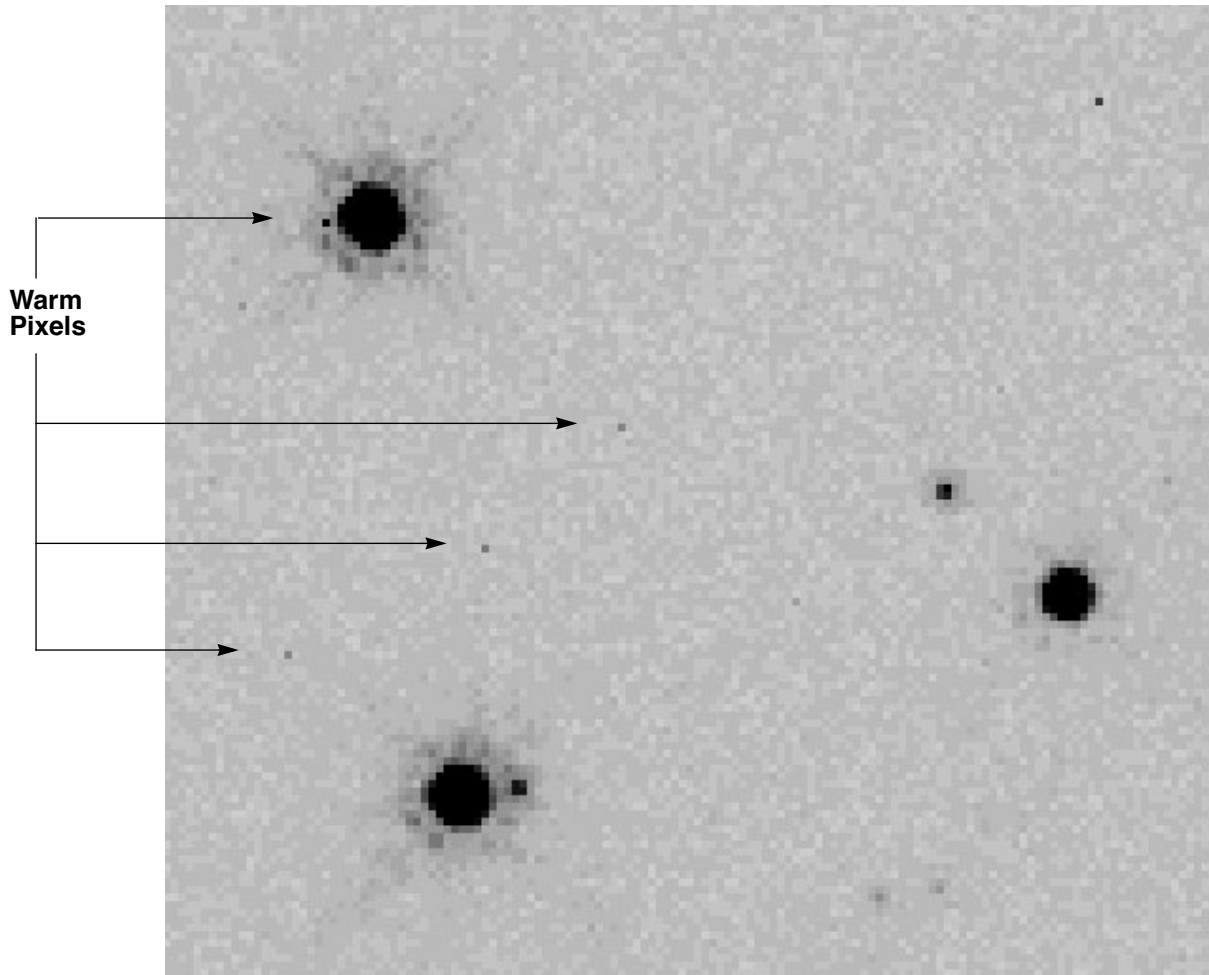
---

### 3.5.1 Warm Pixels

Figure 3.4 shows a section of a PC image of a stellar field where cosmic rays have been removed through comparison of successive images. Nonetheless, individual bright pixels are clearly visible throughout the field.



Figure 3.4: PC Image of Stellar Field Showing Warm Pixels



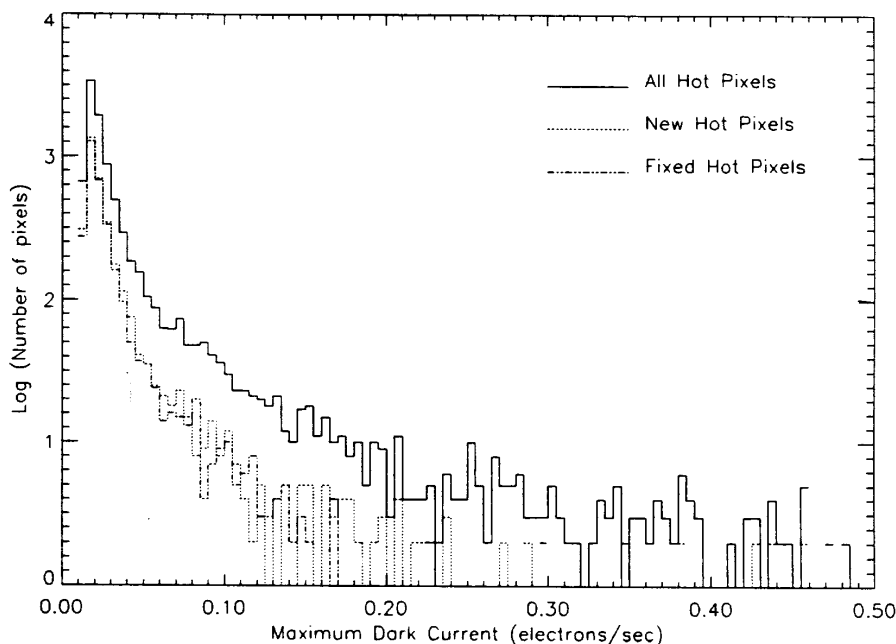
These bright pixels are *warm (or hot)* pixels, i.e., pixels with an elevated dark current. The vast majority of WFPC2 pixels have a total dark current of about  $0.005 \text{ e}^-/\text{s}^{-1}$  (including the *dark glow*, discussed in section 4.3.2). However, at any given time there are a few thousand pixels in each CCD, called warm pixels, with a dark current greater than  $0.02 \text{ e}^-/\text{s}^{-1}$ , up to several  $\text{e}^-/\text{s}^{-1}$  in a few cases (see figure 3.5). Some of these pixels are permanently warm, but most become warm during the course of the month, probably as a consequence of on-orbit bombardment by heavy nuclei. STIS, another instrument currently aboard HST that uses CCDs, exhibits a similar behavior. Most warm pixels return to normal after the CCDs are brought to room temperature for a few hours.

### Will Warm Pixels Hurt my Science?

The impact of warm pixels on the scientific results obtained from WFPC2 images depends on a number of factors: the exposure length, the number of objects, and the science goals. If the principal goal of the program is to acquire morphological information on well-resolved targets,

warm pixels are usually not a serious concern since they are easily recognizable. If the goal is accurate photometry of point sources, the probability that uncorrected warm pixels will influence the measurement at a given level can be computed on the basis of the distribution of warm pixels (see figure 3.5). In general, warm pixels are a concern in two cases: accurate photometry of faint sources in crowded fields, where warm pixels can easily be confused with cores of faint sources; and aperture photometry with very large apertures and/or of extended objects. In the latter case, warm pixels cause a positive tail in the count distribution that is not included in the background determination, but—depending on the software used—could be included in the integrated source flux, which then will be positively biased.

Figure 3.5: Distribution of Dark Current for Warm Pixels



### Repairing warm pixels

Decontaminations, during which the instrument is warmed up to about 22° C for a period of six hours, are performed about once per month. These procedures are required in order to remove the UV-blocking contaminants which gradually build-up on the CCD windows (thereby restoring the UV throughput) as well as fix warm pixels. These pixels, with dark current levels of 0.02 electrons per sec or higher, generally appear at a rate of about 30 pixels per detector per day. A decontamination procedure typically anneals about 80% of the new warm pixels that arise during the month. Of those pixels that are not fixed, about half are fixed after two or three additional decontamination procedures. After that, the rate of correction

decreases; longer decontaminations do not appear to improve the fraction of pixels fixed. For more detailed information, see the *WFPC2 Instrument Handbook*.

Because of the time variability of warm pixels, the standard pipeline dark correction (generally, one dark reference file per week) may not deal with them adequately. Even dark frames taken within a day of the observation will contain some warm pixels that vary significantly from those in the science observation. There are several ways to improve the correction for pixels which are known to be warm or which have varied near the time of the observations: flag the pixels in some way; use the STSDAS task, **warmpix**; or generate a custom dark reference file and recalibrate manually. These methods will be outlined in the following sections.

### *Identifying and flagging warm pixels*

The first method to treat warm pixels is to identify and flag them. Depending on the software used, the flagged pixels can either be ignored (PSF fitting software generally allows this) or be interpolated from nearby pixels (for software that requires a valid value for all pixels, such as most aperture photometry tasks). The identification of warm pixels can be accomplished by taking advantage of the fact that they are the only WFPC2 feature to extend across only one pixel; both cosmic rays and photons, in the form of point sources, involve more than one pixel. The IRAF task **cosmicrays**, written originally to remove single-pixel cosmic rays in ground-based data, has been used with some success to identify warm pixels in WFPC2 data. Identification of warm pixels is also possible using information from dark frames taken before and after the observations were executed, as described below.

### *Subtracting warm pixels via warmpix*

The second option is to attempt subtraction of the warm pixel dark current that existed at the time of the observations. This has the advantage that the information that exists in the measured signal in the pixel is retained, but it does require independent timely information on the dark current. WFPC2 takes about five long dark frames every week, thus information on warm pixels is available with a time resolution of about one week. The STSDAS task **warmpix**, will flag and/or correct warm pixels using an input [table, available on the WWW](#), containing the locations and dark count rates for warm pixels that existed around the time of the science observation. Each table typically spans the time interval between decontamination procedures, with information derived from dark files taken at several epochs (roughly once per week) within that period. This procedure will generally fix 90% to 95% of the warm pixels found in typical user data, though there are some uncertainties in the results due to the intrinsic variability of warm pixels and the time span between darks. The steps necessary to run **warmpix** are summarized below.

1. Obtain the relevant [warm pixel tables from the WWW](#). Each table name reflects its applicability dates; for example, the table named *decon\_951214\_960111.tab.Z* applies to all observations between December 14, 1995 and January 11, 1996.




---

*These tables are in Unix-compressed format. On some systems, the retrieved table will not have the .Z extension, but they still need to be renamed to add the .Z extension and uncompressed by the Unix task **uncompress**. Please contact the Help Desk at [help@stsci.edu](mailto:help@stsci.edu) if you have a non-Unix system or if you encounter difficulties in retrieving the tables.*

---

2. Retrieve the calibration reference files used for dark subtraction and flatfielding from the Archive, see section 1.1 of the HST Introduction. The filenames are recorded in the science header keywords DARK-FILE and FLATFILE, respectively.
3. Redefine the IRAF variable `uref$` to point to the directory where the dark and flatfield files are stored. This step is required for **warmpix** to undo the dark current subtraction performed in the pipeline and substitute its own. *If **warmpix** cannot find these reference files, it will not be able to correct the dark current subtraction and will flag all pixels as being uncorrectable.*
4. Run **warmpix** to correct and/or flag warm pixels. There are a number of user-adjustable parameters to decide which pixels should be fixed and which should be flagged as uncorrectable. Please see the online **warmpix** STSDAS help file for more details (type "help warmpix" at the iraf prompt).

At the end of this process, pixels that exceed the user-defined thresholds either will be corrected for the dark current measured in the darks, linearly interpolated to the date of the observation, or flagged as uncorrectable. Specifically, if the pixel has a high or extremely variable dark count rate, **warmpix** will not change the pixel value in the science image but the data quality file will have its 10th least significant bit set to indicate that it is a "bad" or irreparable pixel (i.e. value of 512, logically OR'ed with the other calibration reference data quality file flags for that pixel). If the pixel has a moderate dark count rate, **warmpix** will fix the pixel in the image and insert a value determined from an extrapolation of the warm pixel's value between two epochs that cover the time of observation for the image. In addition, the data quality file will have the value 1024 logically OR'ed with the other data quality files. Pixels with low dark count rates are not modified by **warmpix**.




---

*Non-STSDAS tasks generally ignore the data quality files, and thus may not properly use the information indicating which pixels need to be rejected. Users should propagate this information by the appropriate method, which will depend on the specifics of the task.*

---

#### *Generating a custom dark reference file using "daily darks"*

In July 1997, a calibration program was begun to obtain up to three dark frames every day, to allow for better warm pixel corrections. These darks, also referred to as "daily darks", are relatively short (1000 seconds) so that the observations can fit into almost any occultation period, making automatic scheduling feasible. In addition, the priority of the daily darks is low; they are taken only when there is no other requirement for that specific occultation period, so daily coverage is not guaranteed. Observers should be aware that only the standard (1800 second) darks, taken at the rate of five per week, are used in generating the pipeline darks, superdarks, and warm pixel tables. The daily darks are available without a proprietary period to the GO community via the Archive.

These daily darks should be used if very accurate identification of warm pixels is needed. Many observers develop their own software to make use of daily darks to improve the warm pixel correction. An alternative, however, is to use canned IRAF scripts available from STScI to generate a custom dark reference file for use in manually recalibrating their science images (see [ISR 01-01](#) and [Addendum 01-08](#)). These reports provide detailed instructions on how to use the scripts to generate a custom dark; section 3.4.2 provides details on how to manually rerun `calwp2`.

### **3.5.2 Alternate Flatfields**

#### *Correction Flatfields*

As of December 2001, the noise characteristics of the WF chips in the standard WFPC2 pipeline flatfield reference files are such that the signal-to-noise achievable in the final calibrated science images is *not* limited by the flatfield. However, all PC1 flatfields (and some WF flatfields in the UV) have less than ideal noise properties; improving these flatfields can improve the resulting signal-to-noise in the calibrated images.

A set of "correction" flatfields, designed to be applied after normal pipeline processing (i.e., OTFR), have been developed in order to help reduce the flatfield noise. In particular, highly-exposed science images (>20,000 e<sup>-</sup>/pixel, or 2860 and 1335 DN/pixel for gains 7 and 15,

respectively) will show significant noise reduction, especially in the PC, if the new correction flatfields are used. Science images in some of the UV filters will show significant improvement as well, even at lower exposure levels. The correction flats are available from the Archive and have been generated so that they merely need to be multiplied into the calibrated (including flatfielded) science images. Please see [ISR 01-07](#) for the details and names of these correction flats, as well as some caveats regarding their application to science images. *Note that these correction flatfields are not, as of November 2001, in the OTFR pipeline, though they may be incorporated for selected filters in the future.*

### *Flatfielding Linear Ramp Filter Images*

Images observed with the linear ramp filters (LRFs) are, by design, currently *not* flatfielded in the OTFR pipeline. The calibrated science headers and trailers will indicate that the flatfield used was a "dummy" (i.e., 1 everywhere) and that the correction was effectively skipped. This is the case in the LRF image example below. The raw file (.d0h) has the FLATCORR set to PERFORM; however, based upon the flatfield reference file PEDIGREE, **calwp2** flags the correction step as SKIPPED in the calibrated image (.c0h).

```

c1> hedit u*d0h flat* .
u51y020cr.d0h,FLATCORR = PERFORM
u51y020cr.d0h,FLATFILE = uref$f4i1559cu.r4h
u51y020cr.d0h,FLATDFIL = uref$f4i1559cu.b4h

c1> hedit uref$f4i1559cu.r4h pedigree,descrip .
uref$f4i1559cu.r4h,PEDIGREE = "DUMMY 18/04/1995"
uref$f4i1559cu.r4h,DESCRIP = "All pixels set to value of 1."

c1> hedit u*c0h flat* .
u51y020cr.c0h,FLATCORR = SKIPPED
u51y020cr.c0h,FLATFILE = uref$f4i1559cu.r4h
u51y020cr.c0h,FLATDFIL = uref$f4i1559cu.b4h

c1> page *trl | grep FLAT
FLATFILE=uref$f4i1559cu.r4h  FLATCORR=SKIPPED

```

A single pipeline flatfield is difficult to generate for the LRFs, primarily due to the lack of an accurate spectrum for the external and internal flatfield light sources (i.e., observations of the bright Earth or images taken with the

internal WFPC2 VISFLAT lamp). The color of the Earth can vary considerably, depending upon the feature observed (land, sea, or clouds). The color of the internal VISFLAT lamp is known to vary as a function of the position in the field of view, the total lamp “on” time, and the total number of times the lamp has been cycled on and off. Furthermore, since the linear ramp filters are far from the focal plane (the OTA beam has a diameter of approximately 33 arcseconds at the filter), any dust spots and other small imperfections in the filter have essentially no effect on the data. Any large-scale variations in the filter are contained in the filter transmission curves and are corrected during photometric calibration. Moreover, some of the ramps have pinholes and if LRF flats were to be made, they would unnecessarily degrade the science data.

Observers with LRF data are advised to check what flatfield has been applied to their data and if necessary, select an existing narrow band flatfield reference file close in wavelength to their LRF science observation (the header parameter `LRFWAVE` records the wavelength of the image) and manually recalibrate using `calwp2`. Since there are no narrow band filters near 8000 Å, the best alternative at these wavelengths is to use the F791W flatfield reference file. The [WWW Reference File memo](#) or the Archive’s [StarView](#) can be used to peruse the flatfields available in neighboring wavelength regimes.

### 3.5.3 Removing Cosmic Rays from Co-aligned Images

WFPC2 images typically contain a large number of *cosmic ray* events, which are caused by the interaction of galactic cosmic rays and protons from the Earth’s radiation belt with the CCD. Hits occur at an average rate of about 1.8 events s<sup>-1</sup> per CCD (1.2 s<sup>-1</sup> cm<sup>-2</sup>), with an overall variation in rate of 60% (peak-to-peak) depending upon geomagnetic latitude and position with respect to the South Atlantic Anomaly (also see the [WFPC2 Instrument Handbook](#), v. 6.0, pages 51-52).

Unlike events seen on the ground, most WFPC2 cosmic ray events deposit a significant amount of charge in several pixels; the average number of pixels affected is 6, with a peak signal of 1500 e<sup>-</sup> per pixel and a few tens of electrons per pixel at the edges. About 3% of the pixels, or 20,000 pixels per CCD, will be affected by cosmic rays in a long exposure (1800 seconds). Figure 3.6, shows the impact of cosmic rays in an 800 second exposure with WFPC2. The area shown is about 1/16th of one chip (a 200 x 200 region); pixels affected by cosmic rays are shown in black and unaffected pixels are shown in white. A typical long WFPC2 exposure (2000 seconds) would have about 2.5 times as many pixels corrupted by cosmic rays.

Cosmic rays are noticeable even for very short exposures. The WFPC2 electronics allow activities to be started only at one-minute intervals; thus, a minimum-length exposure will collect at least one minute’s (the interval

between camera reset and readout) worth of cosmic rays, and will be affected by about a hundred of them per CCD.

As a result of the undersampling of the WFPC2 PSF by the WF and PC pixels, it is very difficult to differentiate stars from cosmic rays using a single exposure. If multiple co-aligned images are available, cosmic rays can be removed simply and reliably by comparing the flux in the same pixel in different images, assuming that any differences well above the noise are positive deviations due to cosmic rays. STSDAS tasks such as **crrej** and **gcombine** can identify and correct pixels affected by cosmic rays in such images. (The task **crrej** has been significantly improved since the previous edition of the *HST Data Handbook* and is now the recommended choice.) If the images are shifted by an integral number of pixels, they can be realigned using a task such as **imshift**. Because each CCD is oriented differently on the sky, this operation will need to be done on one group at a time, using the pixel shift appropriate for each CCD in turn.

Another consequence of the undersampling of WFPC2 pixels is that small pointing shifts will cause measurable differences between images at the same nominal pointing. These differences are especially noticeable in PC data, where offsets of only 10 mas can cause a difference between successive images of 10% or more near the edges of stellar PSFs. We recommend that users allow for such differences by using the multiplicative noise term included in the noise model of the cosmic ray rejection task (**scalenoise** for **crrej** and **snoise** for **gcombine**). For typical pointing uncertainties, a multiplicative noise of 10% is adequate (note, this is specified as 10 for **scalenoise** and 0.1 for **snoise**). It is also strongly recommended that an image mask be generated for each image, in order to determine if an undue concentration of cosmic rays are identified near point sources—usually an indication that the cores of point sources are mistaken for cosmic rays. Detailed explanations of **crrej** and **gcombine** can be found in the on-line help.



Figure 3.6: WF Exposure Showing Pixels Affected by Cosmic Rays



Because sub-pixel dithering strategies are now very common, the image combination tasks in the **drizzle** package (see section 5.5) include a script that can remove cosmic rays from images taken at multiple pointings.

### **How many Images for Proper CR Rejection?**

Cosmic rays are so numerous in WFPC2 data that double hits are not uncommon. For example, the combination of two 2000 second images will typically contain about 500 pixels per CCD that are affected by cosmic rays in both images; in most of these cases, the hit will be marginal in one of the two images. If the science goals require a high level of cosmic ray rejection, it will be desirable to conduct a more stringent test in pixels adjacent to detected cosmic rays (see the parameter **radius** in **crrej**). A better solution would be to break the observation into more than two exposures during the planning stage; the WFPC2 Exposure Time Calculator gives specific recommendations on the number of exposures necessary as a function of the number of pixels lost. In general, three

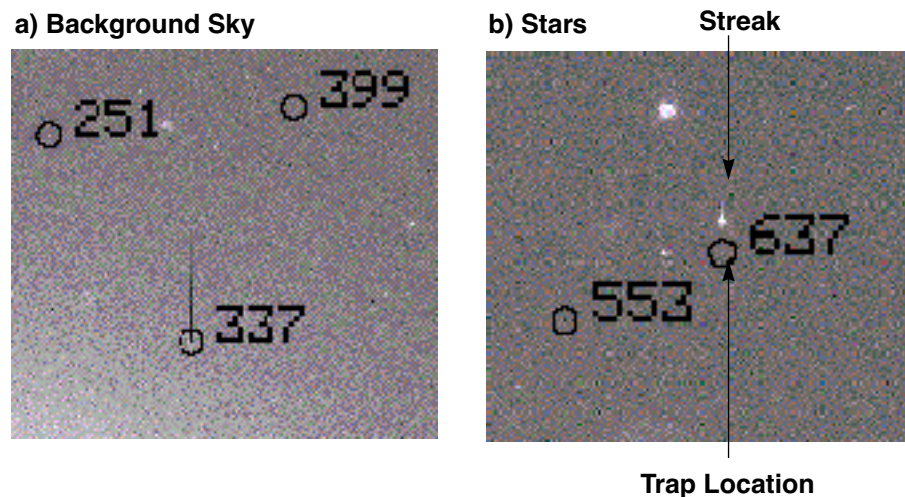
exposures are sufficient for non-stringent programs, and four exposures for any program. [The Exposure Time Calculator](#) is available via the WWW.

### 3.5.4 Charge Traps

There are about 30 pixels in WFPC2 which do not transfer charge efficiently during readout, producing artifacts that are often quite noticeable. Typically, charge is delayed into successive pixels, producing a streak above the defective pixel. In the worst cases, the entire column above the pixel can be rendered useless. On blank sky, these traps will tend to produce a *dark* streak. However, when a bright object or cosmic ray is read through them, a bright streak will be produced. Figure 3.7 shows examples of both of these effects. (Note that these “macroscopic” charge traps are different from the much smaller traps believed to be responsible for the charge transfer effect discussed under “Charge Transfer Efficiency” in section 5.2.2.)

The images in figure 3.7 show streaks (a) in the background sky and, (b) stellar images produced by charge traps in the WFPC2. Individual traps have been cataloged and their identifying numbers are shown.

Figure 3.7: Streaks in a) Background Sky, and b) Stars



Bright tails have been measured on images taken both before and after the April 23, 1994 cool down and indicate that the behavior of the traps has been quite constant with time; fortunately, there is no evidence for the formation of new traps since the ground system testing in May 1993. The charge delay in each of the traps is well characterized by a simple exponential decay which varies in strength and spatial scale from trap to trap.

The positions of the traps, as well as those of pixels immediately above the traps, are marked in the .c1h data quality files with the value of 2,

indicating a chip defect. Obviously, these pixels will be defective even in images of sources of uniform surface brightness. However, after August 1995, the entire column above traps has been flagged with the value of 256, which indicates a “Questionable Pixel.” An object with sharp features (such as a star) will leave a trail should it fall on any of these pixels.

In cases where a bright streak is produced by a cosmic ray, standard cosmic ray removal techniques will usually remove both the streak and the cosmic ray. However, in cases where an object of interest has been affected, the user must be more careful. While standard techniques such as **wfixup** will interpolate across affected pixels and produce an acceptable cosmetic result, interpolation can bias both photometry and astrometry. In cases where accurate reconstruction of the true image is important, modelling of the charge transfer is required. For further information on charge traps, including the measured parameters of the larger traps, users should consult [WFPC2 ISR 95-03](#), available on the WFPC2 web pages.



# WFPC2 Error Sources

## In this chapter. . .

- 4.1 Bias Subtraction Errors / 4-2
- 4.2 Flatfield Correction Errors / 4-2
- 4.3 Dark Current Subtraction Errors / 4-5
- 4.4 Image Anomalies / 4-9

This chapter discusses some of the error sources associated with WFPC2 data. Most of the chapter focuses on specific calibration errors, complementing and partially overlapping the discussion given in "Improving the Pipeline Calibration in section 3.5. Other subtle errors and problems which appear in WFPC2 data, but which are not directly related to data calibration, are discussed at the end of this chapter and in chapter 5.

Note that many of the error sources affecting calibrated WFPC2 data can be reduced by either recalibration with newer reference files or post-pipeline improvements, such as correction flatfields (see section 3.5.2). Recalibration can easily be accomplished by simply re-requesting the data from the Archive through OTFR (On-The-Fly Reprocessing, see section 3.4. An alternative is to use StarView to compare the recommended best reference files with the reference file names recorded in the calibrated science headers; if the names differ, it may be worthwhile to re-retrieve the data. However, finding that a reference file has changed since the data were last calibrated doesn't always mean that recalibration is necessary. The decision to recalibrate depends very much on which reference file or table has changed, and whether that kind of correction may affect the analysis. Section 3.4 gives more details on the required procedures.

---

## 4.1 Bias Subtraction Errors

**All WFPC2 data retrieved from the HST Archive since May 16, 2001 have been through On-The-Fly Reprocessing and are *not* affected by the bias subtraction errors discussed in this section.**

Very early in the WFPC2 mission (January 1994), it was discovered that the first few columns of the overscan region of the WFPC2 CCDs can be positively offset if a strong signal is present in the image itself. These columns were used for the bias level correction (BLEVCORR); the result was an oversubtraction of the bias level, which caused the sky background level in calibrated images to be incorrect. In a few cases, a significant part of the image had negative pixel values. The improvement was implemented in **calwp2** version 1.3.0.5 (March 1994) and is automatically performed on any image processed through OTFR.

Somewhat later in 1994, it was also realized that an improved bias level (BLEVCORR) subtraction could be obtained by using separate bias values for odd and even columns. WFPC2 data processed through the pipeline before May 4, 1994 used only a single average value for the bias level subtraction and as a result, a striated pattern with a typical amplitude of a few electrons (a fraction of a DN) remained. Observers working with versions of these images that were calibrated prior to May 1994 (e.g., from data tapes) should therefore consider re-requesting these data from the Archive. Alternatively, the images could be reprocessed manually using **calwp2**, version 1.3.0.6 or later, unless the signal of the observation is so large that the noise statistics are dominated by Poisson noise. A detailed study of the on-orbit characteristics of bias frames, the overscan region, and superbias used in the pipeline can be found in [WFPC2 ISR 97-04](#).

---

## 4.2 Flatfield Correction Errors

This section summarizes the quality of the various flatfield versions that have been used in the pipeline and, where possible, provides suggestions for improvements. Note that images taken at different times will typically use different flats (i.e., the latest flatfields are *not* the best flatfields for data taken at all times). However, the flats tend to be stable and changes over time are 2% at most, excluding small-scale features such as dust spots. As always, observers can obtain the most up-to-date calibration by re-requesting their science images from the Archive. An alternative is to check whether the flatfield files used by **calwp2** fall into one of the specific cases outlined below before submitting an Archive request.

Cursory information on the flatfielding performed can be found in the calibrated science image header keywords and HISTORY records.

“Flatfielding Linear Ramp Filter Images” provides an example of a linear ramp filter image header: the flatfield correction switch was set to `PERFORM` in the raw header, but since a dummy flatfield was used in the pipeline during processing, the correction was effectively skipped and is noted as such in the calibrated header and `HISTORY` comments. More detailed information concerning the generation of the flatfields can be found in the flatfield reference file image header `HISTORY` comments.

### **Pre-1995 flatfields**

WFPC2 data processed during the first few months of the mission were calibrated using flatfields created from pre-launch ground test data, which did not take into account the large-scale structure of the flatfield. These flats have rootnames<sup>1</sup> that begin with "d" or "e1" and if they have the keyword, `PEDIGREE` (many predated the existence of this keyword), it has been set to `GROUND`. Flatfields installed in CDBS prior to launch were obtained purely from data taken during the pre-launch Thermal Vacuum test, and thus do not reflect properly the illumination function typical of the HST OTA; in this case, zonal errors of several percent can be encountered.

In March 1994, the WFPC2 IDT (Instrument Definition Team) delivered an updated set of flatfields. These flats have rootnames beginning with "e3" and are a combination of pre-launch calibration data and early on-orbit `EARTH-CAL` images (observations of the bright Earth). These on-orbit images were flatfielded with the pre-launch data, then stacked and smoothed so that a map of the OTA illumination pattern could be developed. This map, which included the chip-to-chip normalization, was then applied to the ground flatfields and the resulting flats installed in CDBS. Though they are a combination of ground and on-orbit data, the `PEDIGREE` of these early flatfields is also set to `GROUND`. The `HISTORY` comments at the bottom of the flatfield reference files (`.r4h`) provide more details on their generation.

Reprocessing by OTFR will provide improved flatfielding for any images calibrated with the pre-1995 flats.

### **Flatfields from late 1995 / early 1996**

A completely new set of flatfields were delivered between late 1995 (for the filters used in Hubble Deep Field observations) and early 1996. These flatfields are more accurate than the previous ones, although users may not necessarily need to recalibrate or re-retrieve data through OTFR as a result of this change. The new flats, with rootnames beginning with "g" and having a `PEDIGREE` of `INFLIGHT`, are effectively the preflight ground data flatfields that include an improved on-orbit illumination pattern

---

1. The rootname of a reference file is based on the year, date, and time that the file was delivered to the Calibration Data Base System (CDBS). The first character in the rootname denotes the year, in base 36, since 1980 (i.e., files installed in CDBS in 1993 start with "d", those from 1994 start with "e") while the second and third characters are the month and day, respectively, in base 36.

correction applied to scales larger than 7 pixels. In the optical (400nm to 700nm), the new flats differ from the old by 1% or less over the vast majority of the chip, with differences growing to about 8% at all wavelengths in the outer 50 pixels of the chip. Longward of 850 nm, differences of up to 1.5% are seen across the main body of the chips; and shortward of 300 nm, the differences between the old and new flatfields are less than 3%. As always, the HISTORY comments at the bottom of the flatfield reference files (.r4h) provide more details on their creation.

### **Flatfields after 1996**

The flatfields for WFPC2 are in the process of being updated (November 2001); these improvements are the result of on-going programs of WFPC2 “EARTH-CAL” observations (images of the bright Earth) that have made it possible for flatfields to be created for several different epochs. Depending upon the date of their final installation into CDBS, the new flatfields will have names beginning with the letters ‘l’ or ‘m’ (e.g., "l12" or "m1"). The availability of these new flatfields will be announced in the [WFPC2 Space Telescope Analysis Newsletter \(STAN\)](#), on the [WFPC2 Advisory page](#), and via an Instrument Science Report.

The 1995 epoch flatfields, discussed in the previous section, will still be appropriate for data taken before or during 1995; however, the new flatfields will be appropriate for two new epochs. The first will cover September 1995 to November 1996, during which several strong dust spots appeared. The second covers November 1996 to May 2001, which was a relatively stable period. The new flats generally differ by less than 1-2% from the previous generation in terms of large-scale structure variations across the chips; however, the time-dependence is more pronounced for small-scale features and will allow these to be removed more effectively than with the old flats. In addition, the new flatfields offer improved pixel-to-pixel rms fluctuations of around 0.3% or less. Few users would need to recalibrate their data as a result of these changes; however, any images dating from September 1995 to May 2001 that are retrieved from the Archive after the installation of the new flatfields will automatically be calibrated with the new files.

### **Flatfields for special purpose filters**

Flatfields for infrequently-used filters, such as the polarizers, have generally been available since late 1996 and have rootnames beginning with "g". Other filters, such as the Woods filter (F160BW) and some of the other UV filters, have flatfields with significant noise and other errors; in these cases, the application of a post-pipeline correction flat can provide significant improvement (see section 3.5.2). An alternative would be to use a new pipeline flatfield (it is possible that new flatfield reference files may be available for these filters in early 2002), as discussed in the previous section. Finally, note that by design, linear ramp filters *do not* have a flatfield applied during pipeline calibration; observers with linear ramp



filter data should perform some post-pipeline processing, as recommended in “Flatfielding Linear Ramp Filter Images”.

As always, the [WWW Reference File memo](#) or the Archive’s [StarView](#) can be used to peruse the available flatfields.

### **The effect of WFPC2 flatfields on point source photometry**

WFPC2 flatfields are defined so that a source of uniform brightness produces the same count rate per pixel across the image. However, due to geometric distortion of the image by the optics, the area of WFPC2 pixels on the sky depends on the location on the chip; the total variation across the chip is a few percent, with the largest changes occurring deep in the CCD corners. Therefore, the photometry of *point sources* is slightly corrupted by the standard flattening procedure. This effect, and its correction, are discussed in “Geometric Distortion”. The photometry and astrometry of point sources are also adversely affected by the 34th row effect, see “The 34-th Row Defect” for more details.

## **4.3 Dark Current Subtraction Errors**

### **4.3.1 Electronic Dark Current**

At the operating temperature of -88 C, maintained after April 23, 1994, the WFPC2 CCDs have a low dark background, ranging between 0.002 and 0.01 e<sup>-</sup>/s/pixel. A relatively small number of pixels have dark currents many times this value. These *warm pixels*, and their correction, are discussed in great detail in section 3.5.1. To remove the dark current, the standard pipeline procedure takes a dark reference file (which contains the average dark background in DN/s), multiplies it by the dark time (determined by the header keyword DARKTIME), and subtracts this from the bias subtracted image. Prior to April 23, 1994, the CCDs were operated at -76 C. The correction procedure is the same for these early data, but the average dark current was about an order of magnitude larger due to the higher temperature. Hence, the dark current correction is both more important and less accurate for these images than for later data.

The dark time is usually close to the exposure time, but it can exceed the latter substantially if the exposure was interrupted and the shutter closed temporarily, as in the case of a loss of lock. Such instances are rare and should be identified in the header keyword, EXPFLAG, and in the data quality comments for each observation; it will also be indicated by a difference between the predicted exposure start (PSTRTIME) and end times (PSTPTIME), which is greater than the total exposure time (EXPTIME); that is, PSTPTIME - PSTRTIME will be larger than EXPTIME. The true dark time differs slightly from pixel to pixel because of

the time elapsed between reset and readout (even after the first pixel is read out, the last pixel is still accumulating dark counts). To the extent that dark current is constant with time, this small differential is present both in the bias image and in the observation itself, and therefore is automatically corrected by the bias subtraction.

New dark reference files are delivered on a weekly basis. However, due to the time necessary for processing, they usually aren't available until two to four weeks after the date of their observation. The primary difference between successive darks is in the location and value of warm pixels. This difference will be most noticeable if a decontamination occurred between the images used to create the dark and the observation itself. However, because direct treatment of the warm pixels themselves can be performed via **warmpix**, many users will find that they do not need to reprocess with the most up-to-date dark file. For more details, see section 3.5.1: Warm Pixels. An alternative is to create a custom dark reference file; this procedure is described in more detail in: "Generating a custom dark reference file using "daily darks"".

In order to track variable warm pixels, the weekly standard darks, prior to August 1996, were based on a relatively small number (10) of exposures and taken over a period of two weeks. However, these darks can be a significant component of the total noise in deep images. Observers whose (pre-August 1996) images are formed from exposures totalling more than five orbits may therefore wish to recalibrate their data using one of the *superdarks*, which have been generated by combining over 100 individual exposures (see the [WWW Reference File memo](#) on the WFPC2 Web pages), or generate their own custom superdark.

Since August 1996, the weekly standard darks have been produced by combining the relevant superdark with the warm pixel information in the dark frames taken that week. The combined file is obtained by using the superdark value for all pixels that appear normal in the weekly dark, namely, for which the dark current value in the weekly dark does not differ from the superdark value by more than  $3\sigma$ ; for pixels that do deviate more than  $3\sigma$ , the weekly dark value is used. This compromise allows a timely tracking of warm pixels while maintaining the low noise properties of the superdark for stable pixels. Recalibration may still be appropriate since the weekly standard dark is not yet available when the image is processed and archived.

### 4.3.2 Dark Glow

While the electronic dark current is relatively stable between observations, a variable component has also been seen. The intensity of this *dark glow* is correlated with the observed cosmic ray rate, and is believed to be due to luminescence in the MgF<sub>2</sub> CCD windows from cosmic ray bombardment. As a result of the geometry of the windows, the dark glow is

not constant across the chip, but rather shows a characteristic edge drop of about 50%. The dark glow is significantly stronger in the PC, where it dominates the total dark background, and weakest in WF2. The average *total* signal at the center of each camera is 0.006 e<sup>-</sup>/s in the PC, 0.004 e<sup>-</sup>/s in WF3 and WF4, and 0.0025 e<sup>-</sup>/s in WF2; of this, the true dark current is approximately 0.0015 e<sup>-</sup>/s. For more details, see the *WFPC2 Instrument Handbook*, Version 6.0, pages 87-92.

Because of the variability in the dark glow contribution, the standard dark correction may leave a slight curvature in the background. For the vast majority of observations, this is not a significant problem since the level of the error is very low (worst-case center-to-edge difference of 2 e<sup>-</sup>/pixel) and because it varies slowly across the chips. Some programs, however, may require a careful determination of the absolute background level; observers may wish to consider employing techniques developed by other groups (e.g., Bernstein et al., 2001) or contact the Help Desk ([help@stsci.edu](mailto:help@stsci.edu)).

### 4.3.3 Pointing Information in the Image Headers

#### Updating the pointing information

Improved knowledge of the detector plate scales and chip rotations, as well as changes in reference pixel locations, have resulted in periodic changes to the pointing parameters, especially early in the instrument's lifetime. These header parameters, which define the mapping between the pixel and world coordinate systems, can be updated using the STSDAS task **uchcoord**. The keywords affected include the reference pixel locations (CRPIX\*), the values of the world coordinate system at the reference location (CRVAL\*), the partial derivatives of the world coordinate system with respect to the pixel coordinates (CD\*), and the orientation of the chip (ORIENTAT).

Prior to OTFR (released to the public May 16, 2001), observers requiring the most up-to-date pointing information in their science image headers ran **uchcoord** on their calibrated images. The new OTFR system, however, automatically calculates the best values for these parameters at the time the data are requested so there is no need to run **uchcoord** on freshly-processed OTFR data. OTFR data that have not been recently retrieved (i.e. have been sitting on disk or tape for some time) or pre-OTFR data may benefit from an update; any version of **uchcoord** may be used to update pre-OTFR data, but note that only the June 2001 or later version of **uchcoord** should be run on data processed through OTFR.



---

*Only the June 2001 (or later) version of uchcoord should be used on OTFR data, as older versions of the task may over-correct the images. The version of STSDAS can be verified by typing =stsdas.version at the IRAF prompt.*

---

### **Possible small errors in orientation header information in some images taken prior to Sept. 1997.**

All HST data, including WFPC2 images, taken prior to Sept. 15, 1997, may have slightly incorrect orientation information in the headers (keywords PA\_V3 and ORIENTAT). These very small errors are *not* correctable in OTFR.

For most images the errors are very small (<0.1 degrees), but for images taken during long visits, the errors can accumulate and reach many tenths of a degree. These errors affect only the rotation of the field around the proposed aperture location and otherwise have no impact on the target position in the image. The problem manifests itself in data taken during a long, multi-orbit visit containing one or more POS TARGs, slews, or other small telescope motions; the position angle information reported in the header changes slightly after each motion when in fact there was no change in orientation during the visit. The first image in a long visit contains correct header information; however, with each slew the orientation keywords in subsequent observations begin to deviate from the correct value at a rate of, at most, 1 degree per day ( $\sim 7e-04$  deg/min). The error also depends upon the target's position in the sky (sine of the declination); thus, keywords in images of targets near the equator will have almost no error while images taken near the poles will show larger errors. Note that moving target images appear unaffected by the problem, though further investigation is required to confirm this.

More details, including lists of possible images and visits affected, can be found in the [WWW Orientation memo](#). Observers using the orientation information from any WFPC2 images on those lists should check the jitter data in addition to the science header. For advice on how to perform the check, please see the online FAQ "[How do I best determine an observation's actual orientation?](#)". If you have any additional questions or require further assistance, email [help@stsci.edu](mailto:help@stsci.edu).

---

## 4.4 Image Anomalies

In this section we present a number of features which occasionally affect WFPC2 data.

### 4.4.1 Bias Jumps

The average bias level for each image is obtained from the engineering data file (`.x0h/.x0f`) separately for even and odd columns. However, WFPC2 is subject to *bias jumps*, changes of the bias level during the readout. Large bias jumps ( $> 0.5$  DN) are relatively rare, but small bias jumps, at the 0.1 DN level, affect about 15% of all images. figure 4.1 shows a very unusual event where the bias has jumped twice in the same image.

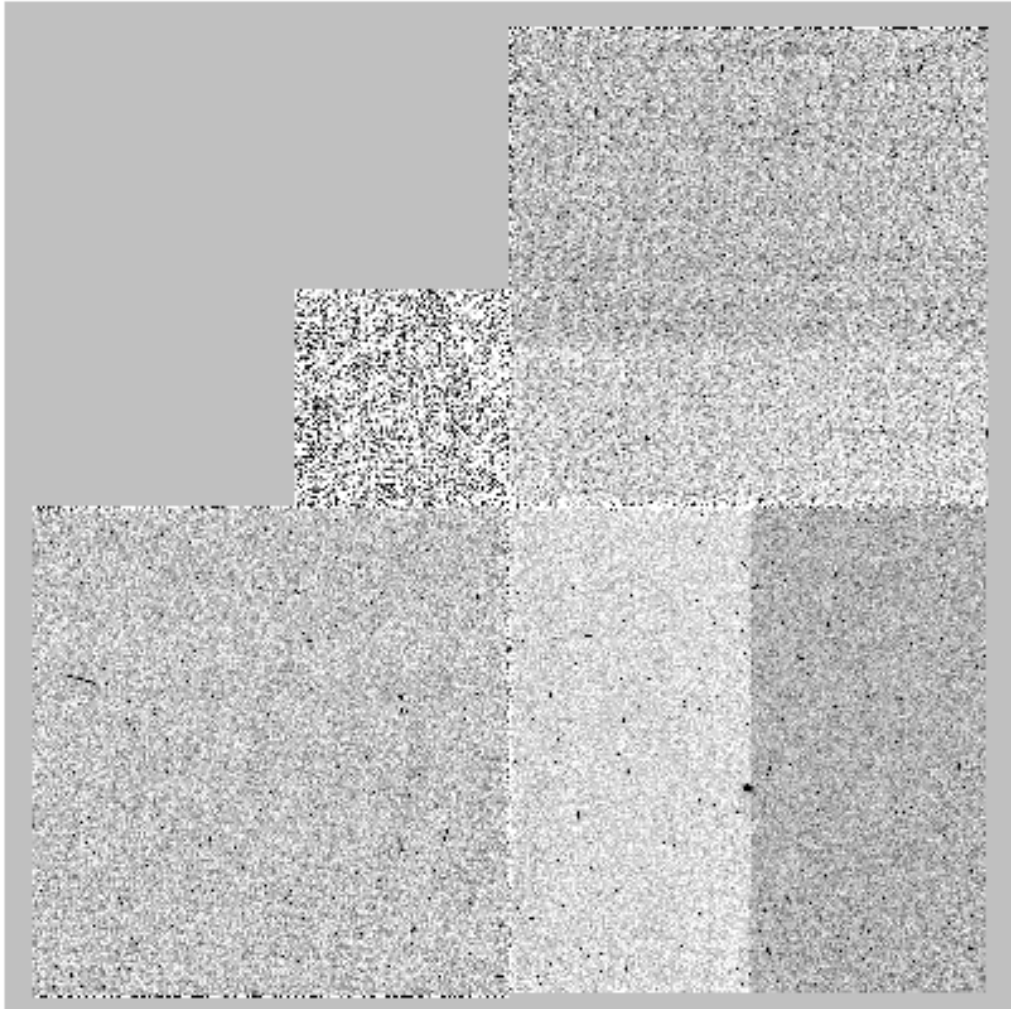
Bias jumps are fairly obvious from a cursory inspection of the image, but users are alerted to their possible presence by a comment in the data quality (`.pdq`) and trailer (`.tr1`) files. Bias jumps are currently identified by an automatic procedure in **calwp2** that searches the overscan data for possible anomalies (for details see *WFPC2 ISR 97-04*) and only jumps larger than 0.09 DN are reported. Prior to August 1996, the identification of bias jumps was done manually. Some of the bias jumps found by **calwp2** and recorded in the data quality and trailer files are false positives, caused by image features such as strongly saturated stars, which affect the overscan data.

There is no standard procedure to remove this defect, but it can be corrected by measuring the jump in the `.x0h` (extracted engineering) file or directly in the image, provided the image is clean enough. Standard IRAF procedures such as **imexamine** or **imstat** are sufficient to obtain a good estimate of the offset. The offset can then be removed, for instance, by subtracting the bias jump and then copying out the affected chip to another image using the command:

```
im> imcalcimage_in image_out "if (y.lt.YJUMP) then im1 \  
>>> else (im1 - BJUMP)"
```

where *YJUMP* is the line at which the jump occurs, and *BJUMP* is its amplitude. The image `image_out` can then be copied back into the appropriate WFPC image group using the **imcopy** task.

Figure 4.1: Bias Jump in Two Chips



#### 4.4.2 Residual Images

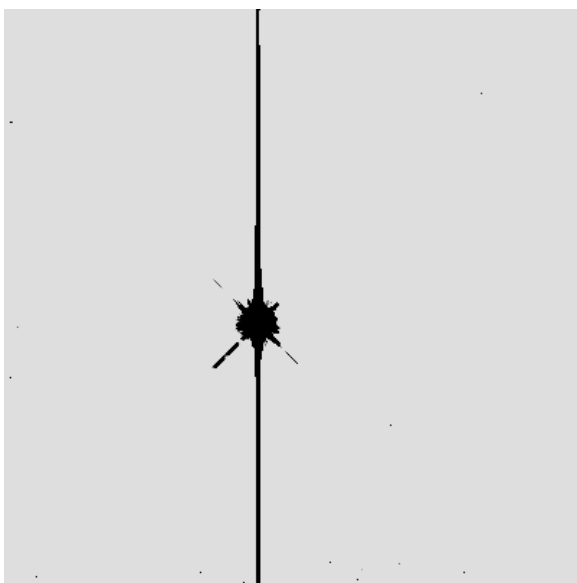
Observations of relatively bright sources can leave behind a residual image. This residual is caused by two distinct effects. In the first, charge in heavily saturated pixels is forced into deeper layers of the CCD, which are not normally cleared by readout. Over time, the charge slowly leaks back into the imaging layers and appears in subsequent images. The time scale for leakage back into the imaging region depends on the amount of over-exposure. Strongly saturated images can require several hours to clear completely. The second effect is caused by charge transfer inefficiencies. At all exposure levels, some charge becomes bound temporarily to impurities in the silicon of the CCD. The effect is most noticeable in images with high exposure levels, probably because electrons become exposed to more impurities as the wells are filled. This effect leaves behind

charge both in bright regions of the image and in the part of the chip through which the bright objects were read out.

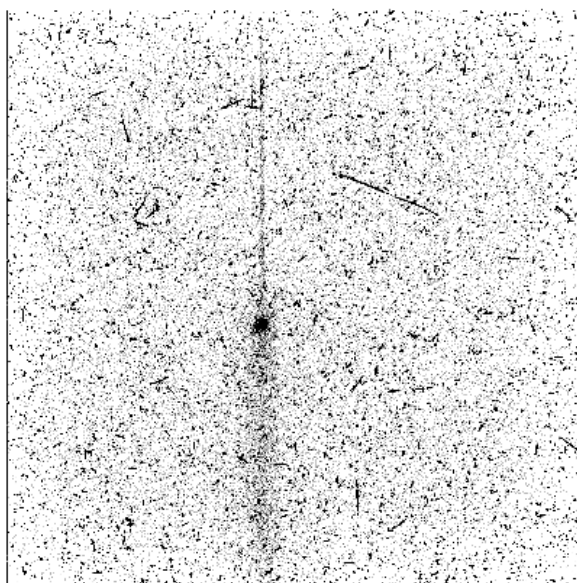
Figure 4.2 shows a saturated star on PC1 (4.2a) and the residual image seen in an 1800 second dark calibration frame started six minutes later (4.2b). Note that the residual image is bright not only where the PC image was overexposed (effect 1), but also in a wide swath below the star due to the second effect and a narrower swath above the star due to bleeding during the exposure.

Figure 4.2: Saturated Star and Residual Image

a) Saturated Star on PC1



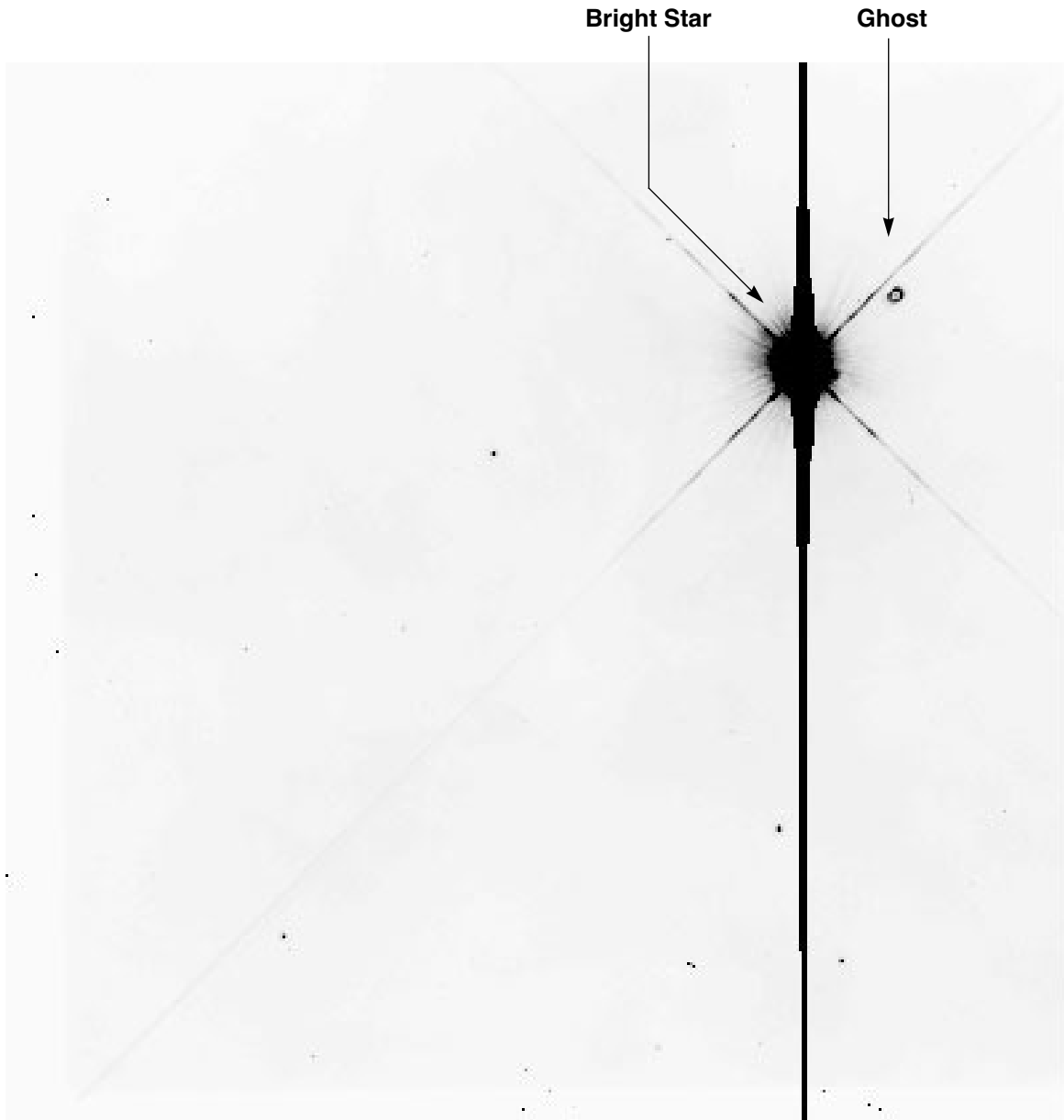
b) Residual Image on Dark Frame 6 Minutes Later



### Ghosts

Ghost images may occur on images of bright objects due to internal reflections in the WFPC2 camera. The most common ghosts are caused by internal reflections in the  $MgF_2$  field flatteners. In these ghosts, the line connecting the ghost and the primary image passes through the optical center of the chip. The ghost always lies further away from the center than the primary image. Figure 4.3 gives an example of one of these ghosts.

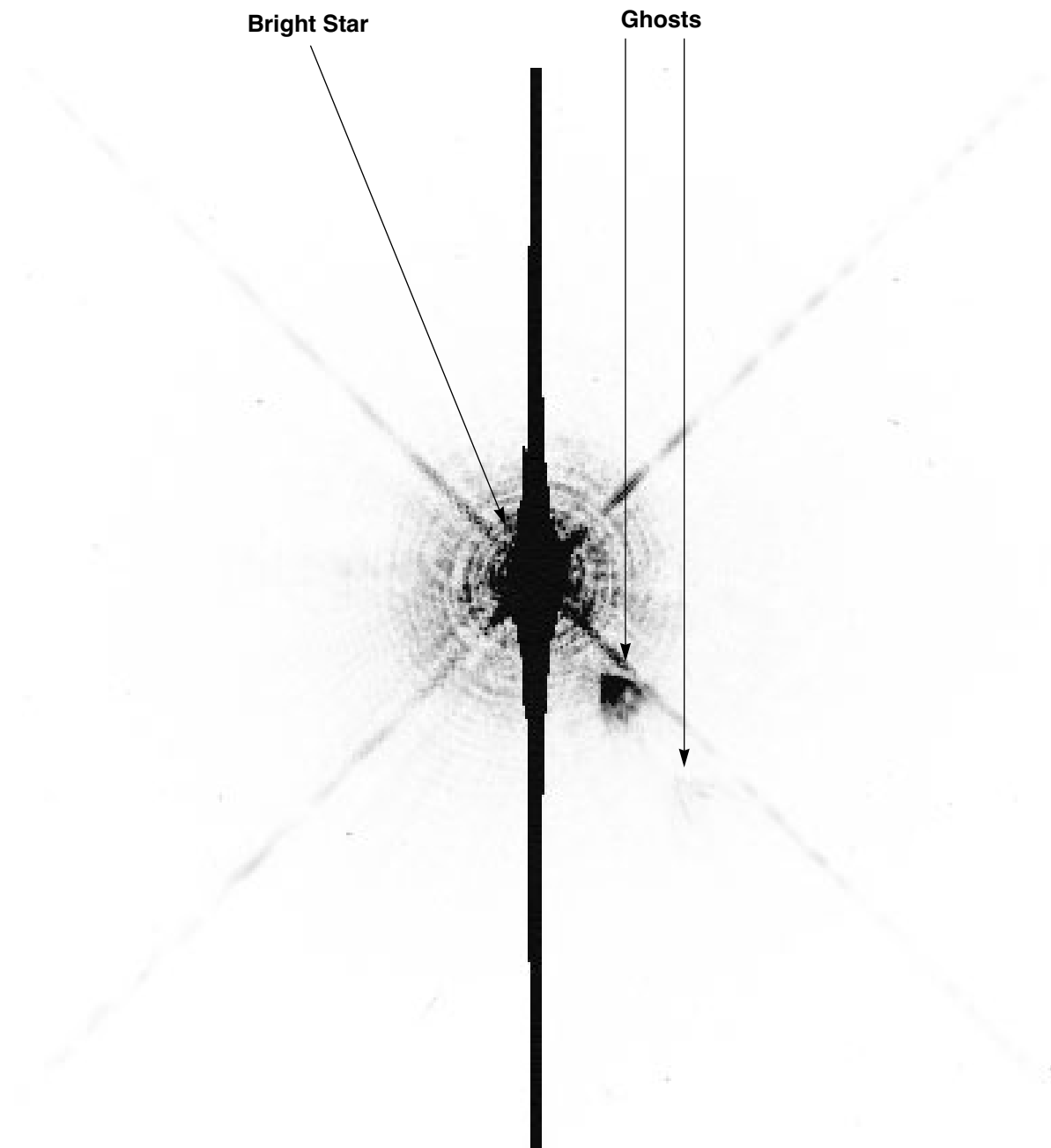
Figure 4.3: Field-Flattener Ghost in WF2—Image Shows Entire CCD



Ghosts may also occur due to reflections on the internal surfaces of a filter. The position of these ghosts will vary from filter to filter and chip to chip. For any given filter and chip combination, the direction of the offset of the ghost from the primary image will be constant, although the size of the offset may vary as a function of the position of the primary image. Filter ghosts can be easily recognized by their comatic (fan-shaped) structure. Particularly bright objects may produce multiple ghosts due to repeated internal reflections. Figure 4.4 shows an example of filter ghosts.



Figure 4.4: Detail of Filter Ghosts on WF4

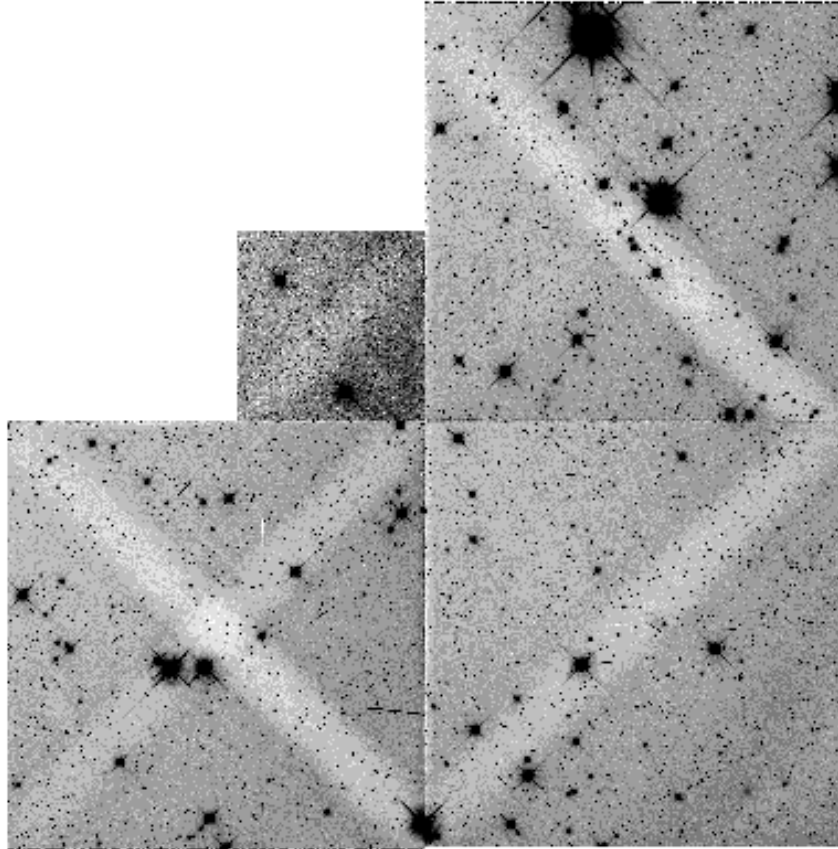


### Earth Reflections

Light from the bright sun-lit Earth is, on rare occasion, reflected off of the Optical Telescope Assembly (OTA) baffles and secondary support and into the WFPC2. These reflections can occur when the bright Earth is less than  $\sim 40$  degrees from the OTA axis. (The default bright Earth limb avoidance is 20 degrees. Science observations are not scheduled at smaller limb angles to the sunlit Earth.) The light raises the overall background

level of the field; however, the WFPC2 camera mirror supports can vignette the scattered light, producing either X-shaped or diagonal depressions in the level of the background. Figure 4.5 shows a typical example of the pattern formed by the scattered light. The scattered light in this image has a level of about 100 electrons. The darkest portion of the X is about 40 electrons below the average background level.

Figure 4.5: Scattered Light Pattern



### 4.4.3 PC1 Stray Light

The WFPC2 was originally intended to contain two separate pyramids—one for four PC cameras and the other for four WF cameras. Budget reductions caused the PC pyramid to be abandoned and the first WF camera to be replaced by a PC camera. However, the pyramid mirror corresponding to the PC camera was not reduced in size. As a result, baffling for the PC chip is not optimal and a bright star falling on the pyramid outside of the PC field of view can produce an obvious artifact, typically shaped like a broad, segmented arc. A star bright enough to produce a total count rate of 1 DN/s on the chip will produce an arc with a count rate of about  $1 \times 10^{-7}$  DN/pixel/s over the affected region. When

scheduling observations, users should avoid placing stars brighter than  $V \sim 14$  in the L-shaped region surrounding the PC.

#### 4.4.4 Other Anomalies

Other image anomalies, such as bright streaks from other spacecraft, scattered light from bright stars near the field of view, and missing image sections due to dropped data occur on rare occasion. For more information, consult *WFPC2 ISR 95-06*, which can be obtained through the WFPC2 Web page or through the STScI Help Desk ([help@stsci.edu](mailto:help@stsci.edu))



# WFPC2 Data Analysis

In this chapter. . .

|                                      |
|--------------------------------------|
| 5.1 Photometric zeropoint / 5-2      |
| 5.2 Photometric Corrections / 5-10   |
| 5.3 Polarimetry / 5-24               |
| 5.4 Astrometry / 5-26                |
| 5.5 Dithering / 5-29                 |
| 5.6 Accuracy of WFPC2 Results / 5-33 |

This chapter deals with several topics pertaining to WFPC2 data analysis. We begin with a practical guide to photometry with WFPC2 where we discuss how to accurately determine the zeropoint, photometric corrections that should be made to WFPC2 data, and common problems and their solutions. We start with the most important aspects of the photometric calibration that affect all observers, largely independently of the final accuracy desired, and in later sections consider subtle effects that can produce relatively small errors. A relatively simple calibration will produce photometric errors of 5 to 10%. With attention to more subtle effects, photometric accuracy between 2 and 5% can be achieved. We then discuss the analysis of polarization data, the astrometric characteristics of WFPC2 images, and the reconstruction of dithered data via the STSDAS **dither** package. Sub-pixel dithering is widely recognized—after the success of the Hubble Deep Field observations—as a valuable way to overcome, in part, the undersampling of WFPC2 images. Finally, we summarize various accuracies to be expected from well-calibrated WFPC2 observations.

## 5.1 Photometric zeropoint

The zeropoint of an instrument, by definition, is the magnitude of an object that produces one count (or data number, DN) per second. The magnitude of an arbitrary object producing DN counts in an observation of length EXPTIME is therefore:

$$m = -2.5 \times \log_{10}(\text{DN} / \text{EXPTIME}) + \text{ZEROPOINT}$$

It is the setting of the zeropoint, then, which determines the connection between observed counts and a standard photometric system (such as Cousins RI), and, in turn, between counts and astrophysically interesting measurements such as the flux incident on the telescope.

### Zeropoints and Apertures

Each zeropoint refers to a count rate (DN/EXPTIME) measured in a specific way. The zeropoints published by Holtzman et al. (1995b) refer to counts measured in a standard aperture of 0.5" radius. The zeropoint derived from the PHOTFLAM header keyword, as well as in other STScI publications, refer—for historical continuity—to counts measured over an “infinite” aperture. Since it is not practical to measure counts in a very large aperture, we use a nominal infinite aperture, defined as having 1.096 times the flux in an aperture with 0.5" radius. This definition is equivalent to setting the aperture correction between a 0.5" radius aperture and an infinite aperture to exactly 0.10 mag.

### 5.1.1 Photometric Systems Used for WFPC2 Data

There are several photometric systems commonly used for WFPC2 data, often causing some confusion about the interpretation of the photometric zeropoint used—and the subsequent photometry results. Before continuing with the discussion, it is worthwhile to define these photometric systems more precisely.

The first fundamental difference between systems has to do with the filter set on which they are based. The WFPC2 filters do not have exact counterparts in the standard filter sets. For example, while F555W and F814W are reasonable approximations of Johnson V and Cousins I respectively, neither match is exact, and the differences can amount to 0.1 mag, clearly significant in precise photometric work. Other commonly used filters, such as F336W and F606W, have much poorer matches in the Johnson-Cousins system. We recommend that, whenever practical, WFPC2 photometric results be referred to a system based on its own filters. It is possible to define “photometric transformations” which convert these results to one of the standard systems; see Holtzman et al. (1995b) for some

examples. However, such transformations have limited precision, and depend on the color range, metallicity, and surface gravity of the stars considered; they easily can have errors of 0.2 mag or more, depending on the filter and on how much the spectral energy distribution differs from that of the objects on which the transformation is defined, which happens frequently for galaxies at high redshift.

Two photometric systems, based on WFPC2 filters, are the WFPC2 flight system, defined by the WFPC2 IDT and detailed in Holtzman et al. (1995b), and the synthetic system, also defined by the IDT and subsequently used in **synphot** as the VEGAMAG system. For more references, see Harris et al. (1993), Holtzman et al. (1995b), *WFPC2 ISR 96-04*, and the *Synphot User's Guide*.

The WFPC2 flight system is defined so that stars of color zero in the Johnson-Cousins UBVRI system have color zero between any pair of WFPC2 filters and have the same magnitude in V and F555W. This system was established by Holtzman et al. (1995b) by observing two globular cluster fields ( $\omega$  Cen and NGC 6752) with HST and from the ground, where the ground-based observations were taken both with WFPC2 flight-spares filters and with standard UBVRI filters. In practice, the system was defined by least-squares optimization of the transformation matrix. The observed stars near color zero were primarily white dwarfs, so the WFPC2 zeropoints defined in this system match the UBVRI zeropoints for stars with high surface gravity; the zeropoints for main sequence stars would differ by 0.02–0.05 mag, depending on the filter.

The zeropoints in the WFPC2 synthetic system, as defined in Holtzman et al. (1995b), are determined so that the magnitude of Vega, when observed through the appropriate WFPC2 filter, would be identical to the magnitude Vega has in the closest equivalent filter in the Johnson-Cousins system. For the filters in the photometric filter set, F336W, F439W, F555W, F675W, and F814W, these magnitudes are 0.02, 0.02, 0.03, 0.039, and 0.035, respectively. The calculations are done via synthetic photometry. In the **synphot** implementation, called the VEGAMAG system, the zeropoints are defined by the magnitude of Vega being *exactly* zero in all filters.

The above systems both tie the zeropoints to observed standards. In recent years, it has become increasingly common to use photometric systems in which the zeropoint is defined directly in terms of a reference flux in physical units. Such systems make the conversion of magnitudes to fluxes much simpler and cleaner, but have the side effect that any new determination of the absolute efficiency of the instrumental setup results in revised magnitudes. The choice between standard-based and flux-based systems is mostly a matter of personal preference.

The prevalent flux-based systems at UV and visible wavelengths are the AB system (Oke 1974) and the STMAG system. Both define an *equivalent flux density* for a source, corresponding to the flux density of a source of predefined spectral shape that would produce the observed count rate, and

convert this equivalent flux to a magnitude. The conversion is chosen so that the magnitude in V corresponds roughly to that in the Johnson system. In the STMAG system, the flux density is expressed per unit *wavelength*, and the reference spectrum is flat in  $f_\lambda$ , while in the AB system, the flux density is expressed per unit *frequency*, and the reference spectrum is flat in  $f_\nu$ . The definitions are:

$$m_{AB} = -48.60 - 2.5 \log f_\nu$$

$$m_{ST} = -21.10 - 2.5 \log f_\lambda$$

where  $f_\nu$  is expressed in  $\text{erg cm}^{-2} \text{s}^{-1} \text{Hz}^{-1}$ , and  $f_\lambda$  in  $\text{erg cm}^{-2} \text{s}^{-1} \text{\AA}^{-1}$ .

Another way to express these zeropoints is to say that an object with  $f_\nu = 3.63 \times 10^{-20} \text{ erg cm}^{-2} \text{s}^{-1} \text{Hz}^{-1}$  will have  $m_{AB}=0$  in every filter, and an object with  $f_\lambda = 3.63 \times 10^{-9} \text{ erg cm}^{-2} \text{s}^{-1} \text{\AA}^{-1}$  will have  $m_{ST}=0$  in every filter. See also the discussion in the *Synphot User's Guide*.

### 5.1.2 Determining the Zeropoint

There are several ways to determine the zeropoint, partly according to which photometric system is desired:

1. ***Do it yourself***: Over the operational life of WFPC2, a substantial amount of effort has gone into obtaining accurate zeropoints for all of the filters used. Nonetheless, if good ground-based photometry is available for objects in your WFPC2 field, it can be used to determine a zeropoint for these observations. This approach may be particularly useful in converting magnitudes to a standard photometric system, provided all targets have similar spectral energy distribution; in this case, the conversions are likely to be more reliable than those determined by Holtzman et al (1995b), which are only valid for stars within a limited range of color, metallicity, and surface gravity.
2. ***Use a summary list***: Lists of zeropoints have been published by Holtzman et al. (1995b), *WFPC2 ISR 96-04*, and *WFPC2 ISR 97-10* (also reported in table 5.1). The Holtzman et al. (1995b) zeropoints essentially *define* the WFPC2 flight photometric system; as discussed above, they are based on observations of  $\omega$  Cen and NGC 6752 for the five main broad band colors (i.e., F336W, F439W, F555W, F675W, F814W), as well as synthetic photometry for most other filters. Transformations from the WFPC2 filter set to UBVRI are included, although these should be used with caution, as stated above. Holtzman et al. (1995b) also includes a cookbook section describing in detail how to do photometry with WFPC2. This paper is available from the STScI WWW or by sending e-mail to



[help@stsci.edu](mailto:help@stsci.edu). The more recent compilations of zeropoints in *WFPC2 ISR 96-04* and *97-10* use new WFPC2 observations, are based on the VEGAMAG system, and do not include new conversions to UBVRI.

3. *Use the PHOTFLAM keyword in the header of your data:* The simplest way to determine the zeropoint of your data is to use the PHOTFLAM keyword in the header of your image. PHOTFLAM is the flux of a source with constant flux per unit wavelength (in  $\text{erg s}^{-1} \text{cm}^{-2} \text{\AA}^{-1}$ ) which produces a count rate of 1 DN per second. This keyword is generated by the synthetic photometry package, **synphot**, which you may also find useful for a wide range of photometric and spectroscopic analyses. Using PHOTFLAM, it is easy to convert instrumental magnitude to flux density, and thus determine a magnitude in a flux-based system such as AB or STMAG (see section 5.1.1); the actual steps required are detailed below.

---

*Note that the zeropoints listed by Holtzman et al. (1995b) differ systematically by 0.85 mag from the synphot zeropoints in table 5.1. Most of the difference, 0.75 mag, is due to the fact that the Holtzman zeropoints are given for gain 14, while the synphot zeropoints are reported for gain 7, which is generally used for science observations. An additional 0.1 mag is due to the aperture correction; the Holtzman zeropoint refers to an aperture of 0.5", while the synphot zeropoint refers to a nominal infinite aperture, defined as 0.10 mag brighter than the 0.5" aperture*

---



The tables used by the **synphot** package were updated in August 1995 and May 1997. With these updates, **synphot** now provides absolute photometric accuracy of 2% rms for broad-band and intermediate-width filters between F300W and F814W, and of about 5% in the UV. Narrow-band filters are calibrated using continuum sources, but checks on line sources indicate that their photometric accuracy is also determined to 5% or better (the limit appears to be in the quality of the ground-based spectrophotometry). Prior to the May 1997 update, some far UV and narrow-band filters were in error by 10% or more; more details are provided in *WFPC2 ISR 97-10*.

Table 5.1 provides lists of the current values for PHOTFLAM. Please note that the headers of images processed before May 1997 contain older values of PHOTFLAM; the up-to-date values can be obtained by reprocessing the image (i.e., re-requesting the data via OTFR), from the table, or more directly by using the **bandpar** task in **synphot** (see “Creation of Photometry Keywords” in section 3.3.2: for an example). Note that to use **bandpar**, the **synphot** version must be up-to-date.<sup>1</sup> Furthermore, when using **bandpar**, it is also possible to directly incorporate the contamination correction (see “Contamination” in section 5.2.1).

The **synphot** package can also be used to determine the transformation between magnitudes in different filters, subject to the uncertainties related to how well the spectrum chosen to do the determination matches the spectrum of the actual source. The transformation is relatively simple using **synphot**, and the actual correction factors are small when converting from the WFPC2 photometric filter set to Johnson-Cousins magnitudes. A variety of [spectral atlases are available on the WWW](#) as well as via **synphot**.

---

1. For instructions on how to retrieve STSDAS **synphot** tables, see appendix section A.3.2.

Table 5.1: Current Values of PHOTFLAM and Zeropoint in the VEGAMAG system.

| Filter <sup>1</sup> | PC           |         | WF2          |         | WF3          |         | WF4          |         |
|---------------------|--------------|---------|--------------|---------|--------------|---------|--------------|---------|
|                     | New photflam | Vega ZP | New photflam | Vega ZP | New photflam | Vega ZP | New photflam | Vega ZP |
| f122m               | 8.088e-15    | 13.768  | 7.381e-15    | 13.868  | 8.204e-15    | 13.752  | 8.003e-15    | 13.778  |
| f160bw              | 5.212e-15    | 14.985  | 4.563e-15    | 15.126  | 5.418e-15    | 14.946  | 5.133e-15    | 15.002  |
| f170w               | 1.551e-15    | 16.335  | 1.398e-15    | 16.454  | 1.578e-15    | 16.313  | 1.531e-15    | 16.350  |
| f185w               | 2.063e-15    | 16.025  | 1.872e-15    | 16.132  | 2.083e-15    | 16.014  | 2.036e-15    | 16.040  |
| f218w               | 1.071e-15    | 16.557  | 9.887e-16    | 16.646  | 1.069e-15    | 16.558  | 1.059e-15    | 16.570  |
| f255w               | 5.736e-16    | 17.019  | 5.414e-16    | 17.082  | 5.640e-16    | 17.037  | 5.681e-16    | 17.029  |
| f300w               | 6.137e-17    | 19.406  | 5.891e-17    | 19.451  | 5.985e-17    | 19.433  | 6.097e-17    | 19.413  |
| f336w               | 5.613e-17    | 19.429  | 5.445e-17    | 19.462  | 5.451e-17    | 19.460  | 5.590e-17    | 19.433  |
| f343n               | 8.285e-15    | 13.990  | 8.052e-15    | 14.021  | 8.040e-15    | 14.023  | 8.255e-15    | 13.994  |
| f375n               | 2.860e-15    | 15.204  | 2.796e-15    | 15.229  | 2.772e-15    | 15.238  | 2.855e-15    | 15.206  |
| f380w               | 2.558e-17    | 20.939  | 2.508e-17    | 20.959  | 2.481e-17    | 20.972  | 2.558e-17    | 20.938  |
| f390n               | 6.764e-16    | 17.503  | 6.630e-16    | 17.524  | 6.553e-16    | 17.537  | 6.759e-16    | 17.504  |
| f410m               | 1.031e-16    | 19.635  | 1.013e-16    | 19.654  | 9.990e-17    | 19.669  | 1.031e-16    | 19.634  |
| f437n               | 7.400e-16    | 17.266  | 7.276e-16    | 17.284  | 7.188e-16    | 17.297  | 7.416e-16    | 17.263  |
| f439w               | 2.945e-17    | 20.884  | 2.895e-17    | 20.903  | 2.860e-17    | 20.916  | 2.951e-17    | 20.882  |
| f450w               | 9.022e-18    | 21.987  | 8.856e-18    | 22.007  | 8.797e-18    | 22.016  | 9.053e-18    | 21.984  |
| f467m               | 5.763e-17    | 19.985  | 5.660e-17    | 20.004  | 5.621e-17    | 20.012  | 5.786e-17    | 19.980  |
| f469n               | 5.340e-16    | 17.547  | 5.244e-16    | 17.566  | 5.211e-16    | 17.573  | 5.362e-16    | 17.542  |
| f487n               | 3.945e-16    | 17.356  | 3.871e-16    | 17.377  | 3.858e-16    | 17.380  | 3.964e-16    | 17.351  |
| f502n               | 3.005e-16    | 17.965  | 2.947e-16    | 17.987  | 2.944e-16    | 17.988  | 3.022e-16    | 17.959  |
| f547m               | 7.691e-18    | 21.662  | 7.502e-18    | 21.689  | 7.595e-18    | 21.676  | 7.747e-18    | 21.654  |
| f555w               | 3.483e-18    | 22.545  | 3.396e-18    | 22.571  | 3.439e-18    | 22.561  | 3.507e-18    | 22.538  |
| f569w               | 4.150e-18    | 22.241  | 4.040e-18    | 22.269  | 4.108e-18    | 22.253  | 4.181e-18    | 22.233  |
| f588n               | 6.125e-17    | 19.172  | 5.949e-17    | 19.204  | 6.083e-17    | 19.179  | 6.175e-17    | 19.163  |
| f606w               | 1.900e-18    | 22.887  | 1.842e-18    | 22.919  | 1.888e-18    | 22.896  | 1.914e-18    | 22.880  |
| f622w               | 2.789e-18    | 22.363  | 2.700e-18    | 22.397  | 2.778e-18    | 22.368  | 2.811e-18    | 22.354  |
| f631n               | 9.148e-17    | 18.514  | 8.848e-17    | 18.550  | 9.129e-17    | 18.516  | 9.223e-17    | 18.505  |
| f656n               | 1.461e-16    | 17.564  | 1.410e-16    | 17.603  | 1.461e-16    | 17.564  | 1.473e-16    | 17.556  |
| f658n               | 1.036e-16    | 18.115  | 9.992e-17    | 18.154  | 1.036e-16    | 18.115  | 1.044e-16    | 18.107  |
| f673n               | 5.999e-17    | 18.753  | 5.785e-17    | 18.793  | 6.003e-17    | 18.753  | 6.043e-17    | 18.745  |
| f675w               | 2.899e-18    | 22.042  | 2.797e-18    | 22.080  | 2.898e-18    | 22.042  | 2.919e-18    | 22.034  |
| f702w               | 1.872e-18    | 22.428  | 1.809e-18    | 22.466  | 1.867e-18    | 22.431  | 1.883e-18    | 22.422  |
| f785lp              | 4.727e-18    | 20.688  | 4.737e-18    | 20.692  | 4.492e-18    | 20.738  | 4.666e-18    | 20.701  |
| f791w               | 2.960e-18    | 21.498  | 2.883e-18    | 21.529  | 2.913e-18    | 21.512  | 2.956e-18    | 21.498  |
| f814w               | 2.508e-18    | 21.639  | 2.458e-18    | 21.665  | 2.449e-18    | 21.659  | 2.498e-18    | 21.641  |
| f850lp              | 8.357e-18    | 19.943  | 8.533e-18    | 19.924  | 7.771e-18    | 20.018  | 8.194e-18    | 19.964  |
| f953n               | 2.333e-16    | 16.076  | 2.448e-16    | 16.024  | 2.107e-16    | 16.186  | 2.268e-16    | 16.107  |
| f1042m              | 1.985e-16    | 16.148  | 2.228e-16    | 16.024  | 1.683e-16    | 16.326  | 1.897e-16    | 16.197  |

1. Values are for the gain 7 setting. The PHOTFLAM values for gain 14 can be obtained by multiplying by the gain ratio: 1.987 (PC1), 2.003 (WF2), 2.006 (WF3), and 1.955 (WF4) (values from Holtzman et al. 1995b). For the zeropoints, add  $-2.5 \log(\text{gain ratio})$ , or -0.745, -0.754, -0.756, and -0.728, respectively. The above values should be applied to the counts referenced to a nominal “infinite aperture”, defined by an aperture correction of 0.10 mag with respect to the standard aperture with 0.5" radius.

For example, the following commands can be used to determine the difference in zeropoint between F814W filter and the Cousins I band for a K0III star on WF3 using the gain=7 setting:

```
sy> calcphot "band(wfpc2,3,a2d7,f814W)" crgridbz77$bz_54
stmag
```

where the Bruzual stellar atlas is being used to provide the spectrum for the K0 III star (file = crgridbz77\$bz\_54). The output is:

```
sy> calcphot "band(wfpc2,3,a2d7,f814W)" crgridbz77$bz_54
stmag
Mode = band(wfpc2,3,a2d7,f814W)
  Pivot      Equiv Gaussian
Wavelength      FWHM
7982.044      1507.155      band(wfpc2,3,a2d7,f814W)
Spectrum: crgridbz77$bz_54
  VZERO      STMAG      Mode: band(wfpc2,3,a2d7,f814W)
  0.          -15.1045
```

Comparing this result with:

```
calcphot "band(cousins,I)" crgridbz77$bz_54 vegamag
Mode = band(cousins,I)
  Pivot      Equiv Gaussian
Wavelength      FWHM
7891.153      898.879      band(cousins,I)
Spectrum: crgridbz77$bz_54
  VZERO      VEGAMAG      Mode: band(cousins,I)
  0.          -16.3327
```

shows that for a star of this color, the correction is 1.2 magnitudes (note that nearly all of this offset is due to the definition of STMAG; the F814W filter is a very close approximation to the Johnson-Cousins I, and color terms between these filters are very small). The Johnson UBVR I throughput data in **synphot** are the U3, B2, and V synthetic passbands given in Buser and Kurucz (1978) and the R,I are from Johnson (1965), Table A1. The Cousins R,I throughputs are from Bessell (1983), Table AII, the Stromgren passbands from Matsushima (1969), and the Walraven bands are from Lub and Pel (1977), Table 6. For more details, please see the *Synphot User's Guide*. The tables below provide representative zeropoint transformations; typical uncertainties are ~5% (worse for U). A larger variety of spectra are available in the [atlases on the WWW](#) as well as in **synphot**.

Table 5.2: Rough Zeropoint Transformations for Johnson UBVRI

| Spectral Type | Atlas File Name | U-F336W | B-F439W | V-F555W | R-F675W | I-F814W |
|---------------|-----------------|---------|---------|---------|---------|---------|
| O5V           | bz_1            | 0.51    | 0.66    | 0.03    | -0.69   | -1.17   |
| B0V           | bz_5            | 0.45    | 0.66    | 0.03    | -0.70   | -1.18   |
| B1V           | bpgs_5          | 0.43    | 0.67    | 0.03    | -0.69   | -1.19   |
| A0V           | bpgs_14         | -0.11   | 0.66    | 0.01    | -0.70   | -1.27   |
| A0V           | bz_13           | -0.08   | 0.66    | -0.00   | -0.70   | -1.27   |
| F2V           | bz_19           | -0.02   | 0.61    | -0.02   | -0.71   | -1.33   |
| F6V           | bpgs_33         | 0.00    | 0.61    | -0.01   | -0.71   | -1.32   |
| G0V           | bpgs_36         | 0.04    | 0.58    | -0.02   | -0.70   | -1.34   |
| G0V           | bz_24           | 0.00    | 0.57    | -0.03   | -0.72   | -1.35   |
| K0V           | bz_28           | -0.06   | 0.52    | -0.03   | -0.72   | -1.36   |
| K7V           | bpgs_64         | -0.00   | 0.42    | -0.01   | -0.79   | -1.47   |
| M0V           | bpgs_66         | -0.05   | 0.38    | -0.02   | -0.89   | -1.56   |
| M0V           | bz_32           | 0.01    | 0.41    | -0.02   | -0.80   | -1.52   |
| M6V           | bz_35           | 0.12    | 0.27    | -0.05   | -1.08   | -1.69   |

Table 5.3: Rough Zeropoint Transformations For Cousins RI

| Spectral Type | Atlas File Name | R-F675W | I-F814W |
|---------------|-----------------|---------|---------|
| O5V           | bz_1            | -0.73   | -1.28   |
| B0V           | bz_5            | -0.72   | -1.28   |
| B1V           | bpgs_5          | -0.72   | -1.28   |
| A0V           | bpgs_14         | -0.70   | -1.26   |
| A0V           | bz_13           | -0.70   | -1.26   |
| F2V           | bz_19           | -0.65   | -1.27   |
| F6V           | bpgs_33         | -0.64   | -1.28   |
| G0V           | bpgs_36         | -0.62   | -1.27   |
| G0V           | bz_24           | -0.62   | -1.27   |
| K0V           | bz_28           | -0.61   | -1.27   |
| K7V           | bpgs_64         | -0.57   | -1.27   |
| M0V           | bpgs_66         | -0.57   | -1.28   |
| M0V           | bz_32           | -0.57   | -1.26   |
| M6V           | bz_35           | -0.59   | -1.23   |

The spectra in the preceding tables were taken from the [Bruzual library \(BZ77\)](#) and the [Bruzual-Persson-Gunn-Stryker atlas \(BPGS\)](#).

---

## 5.2 Photometric Corrections

A number of corrections must be made to WFPC2 data to obtain the best possible photometry. Some of these, such as the corrections for UV throughput variability, are *time dependent*, and others, such as the correction for the geometric distortion of WFPC2 optics, are *position dependent*. Finally, some general corrections, such as the aperture correction, are needed as part of the analysis process. We describe each class in turn.

### 5.2.1 Time-Dependent Corrections

The most important time-dependent correction is that for the contamination of the CCD windows, which primarily affects UV observations. Other time-dependent corrections are due to the change in operating temperature in April 1994 and the variations of the PSF with focus position; the latter is also position-dependent (see “Aperture Correction” for more information).

#### Contamination

Contaminants adhere to the cold CCD windows of the WFPC2. Although these typically have little effect upon the visible and near infrared performance of the cameras, the effect upon the UV is quite dramatic and can reduce throughput for the F160BW filter by about 30% after 30 days. These contaminants are largely removed during periodic warmings (decontaminations) of the camera, and the effect upon photometry is both linear and stable and can be removed using values regularly measured in the WFPC2 calibration program. Table 5.4 shows the monthly contamination rates measured for each detector ([WFPC2 ISR 98-03](#)). Table 5.5 provides decontamination dates up until November 2001; an [updated list of decontamination dates is maintained on the WWW](#).

Contamination is typically measured from the bimonthly observations of the WFPC2 primary standard, the white dwarf GRW+70d5824 (see table 5.4 for rates), and is therefore directly applicable to blue objects. The early observations for the standard photometric filters (F336W, F439W, F555W, F675W, and F814W) have been supplemented by observations of a stellar field in the globular cluster  $\omega$  Cen (mean B–V  $\sim 0.7$  mag); the contamination rates measured (in parentheses in table 5.4) are generally in good agreement with those measured for GRW+70d5824. The  $\omega$  Cen data also indicate a slightly higher contamination rate towards the center of each chip ([WFPC2 ISR 96-04](#)). These results will be verified further with the analysis of UV observations of NGC 2100, a young globular cluster in the LMC.

Based on standard star observations taken 1994 to 1998, the long-term photometric throughput appears to be quite stable: fluctuations are  $\sim 2\%$  or less peak-to-peak in filters longwards of and including F336W (ISR 98-03; and the [WWW monitoring memo](#)). However, the UV throughput has gradually been evolving; specifically, from 1994 to 1998, the clean count rates (measurements immediately after the decons) in some filters, e.g., F160BW by  $\sim 12\%$  in the PC, and F170W by  $\sim 9\%$ , while decreasing slightly in others, e.g., F255W by  $\sim 3\%$ . Furthermore, the monthly contamination rates slowed slightly for the UV filters, e.g., from  $\sim 1\%$  per day to  $0.5\%$  per day in F160BW on the PC (see table 5.4 and [ISR 98-03](#)). Both the monthly and long-term contamination rates reported in the ISR have been incorporated into the WFPC2 contamination tables in `synphot`.

There are three ways observers may correct UV data for the variable decline rates and small zeropoint shifts; note that in general, filters redward of F336W do not require a correction based on day since decon but may benefit from a small zeropoint correction. The first option is to use the `synphot` contamination tables (see example below), which contain both the monthly contamination effects as well as the long term zeropoint changes. Note however, that `synphot` linearly interpolates in both wavelength and date to obtain the final contamination estimate; the only wavelengths currently in the `synphot` contamination tables are the central wavelengths of the monitoring filters. The second option is to use the rates in table 5.4 to correct for contamination based upon the number of days since a decon procedure; the [ISR 98-03](#) provides details on correcting for the small zeropoint offset. The third method is to use the [WWW table of monitoring results](#) to obtain data close in time and wavelength to the science observation and derive an independent model of the contamination effects.

Observers should be aware that the calibration pipeline does *not* automatically correct for contamination. The correction must be applied manually (e.g., using results tabulated in [WFPC2 ISR 98-03](#)) or using `synphot`. The example below illustrates how to use the `calcpHOT` task to determine the effect of contamination in an observation. In this case, the command computes the expected count rate for a WF3, F218W observation taken 20 days (MJD=49835.0) after the April 8, 1995, decontamination, with the gain=7 setup. Removing the `cont#49835.0` from the command will determine the count rate if no contamination was present. *Note that the entire photometric mode must be in double quotes*, otherwise STSDAS treats the `#` as a comment indicator and will ignore the remainder of the command line. An 8000 K black body spectrum was chosen largely as a matter of simplicity—the correction values for contamination depend only on the filter chosen and do not reflect the source spectrum.

```
sy> calcpHOT "wfpc2,3,f218w,a2d15,cont#49835.0" \
>>> spec="bb(8000)" form=counts
```

Table 5.4: Contamination Rates (Percentage Loss per Day)

| Filter | Year <sup>1</sup> | PC                |         | WF2               |         | WF3               |         | WF4               |         |
|--------|-------------------|-------------------|---------|-------------------|---------|-------------------|---------|-------------------|---------|
|        |                   | % decline per day | error   | % decline per day | error   | % decline per day | error   | % decline per day | error   |
| F160BW | 4/94-4/95         | -0.885            | 0.104   | --                | --      | -1.277            | 0.038   | --                | --      |
| F160BW | 4/95-4/96         | -0.840            | 0.137   | -1.281            | 0.089   | -1.227            | 0.057   | -0.930            | 0.102   |
| F160BW | 4/96-4/97         | -0.690            | 0.159   | -1.303            | 0.094   | -1.142            | 0.069   | -1.079            | 0.067   |
| F160BW | 4/97-6/98         | -0.613            | 0.138   | -1.202            | 0.077   | -1.093            | 0.065   | -0.893            | 0.067   |
| F170W  | 4/94-4/95         | -0.564            | 0.009   | -0.949            | 0.011   | -0.988            | 0.009   | -0.801            | 0.012   |
| F170W  | 4/95-4/96         | -0.516            | 0.012   | -0.901            | 0.012   | -0.956            | 0.011   | -0.736            | 0.013   |
| F170W  | 4/96-4/97         | -0.509            | 0.012   | -0.901            | 0.011   | -0.943            | 0.012   | -0.752            | 0.012   |
| F170W  | 4/97-6/98         | -0.452            | 0.013   | -0.804            | 0.011   | -0.772            | 0.012   | -0.643            | 0.012   |
| F218W  | 4/94-4/95         | -0.478            | 0.028   | --                | --      | -0.846            | 0.019   | --                | --      |
| F218W  | 4/95-4/96         | -0.433            | 0.036   | -0.757            | 0.039   | -0.787            | 0.026   | -0.704            | 0.047   |
| F218W  | 4/96-4/97         | -0.442            | 0.044   | --                | --      | -0.845            | 0.033   | --                | --      |
| F218W  | 4/97-6/98         | -0.398            | 0.046   | --                | --      | -0.633            | 0.047   | --                | --      |
| F255W  | 4/94-4/95         | -0.236            | 0.008   | --                | --      | -0.471            | 0.007   | --                | --      |
| F255W  | 4/95-4/96         | -0.235            | 0.007   | -0.445            | 0.013   | -0.490            | 0.007   | -0.385            | 0.013   |
| F255W  | 4/96-4/97         | -0.215            | 0.008   | -0.398            | 0.017   | -0.333            | 0.013   | -0.298            | 0.011   |
| F255W  | 4/97-6/98         | -0.183            | 0.007   | -0.311            | 0.014   | -0.327            | 0.012   | -0.234            | 0.012   |
| F300W  | 4/95-4/96         | --                | --      | -0.260            | 0.015   | --                | --      | --                | --      |
| F336W  | 4/94-4/95         | -0.031            | 0.007   | --                | --      | -0.198            | 0.007   | --                | --      |
| F336W  | 4/95-4/96         | -0.108            | 0.008   | -0.188            | 0.013   | -0.208            | 0.009   | -0.226            | 0.014   |
|        |                   | (-0.127)          | (0.060) | (-0.143)          | (0.030) | (-0.153)          | (0.027) | (-0.157)          | (0.023) |
| F336W  | 4/96-4/97         | -0.068            | 0.009   | -0.286            | 0.014   | -0.285            | 0.010   | -0.153            | 0.010   |
| F336W  | 4/97-6/98         | -0.062            | 0.008   | -0.177            | 0.012   | -0.181            | 0.010   | -0.053            | 0.010   |
| F439W  | 4/94-4/95         | -0.008            | 0.008   | --                | --      | -0.078            | 0.008   | --                | --      |
| F439W  | 4/95-4/96         | -0.037            | 0.007   | -0.121            | 0.013   | -0.080            | 0.009   | -0.127            | 0.014   |
|        |                   | (-0.007)          | (0.047) | (-0.073)          | (0.023) | (-0.077)          | (0.030) | (-0.077)          | (0.023) |
| F439W  | 4/96-4/97         | -0.037            | 0.007   | -0.146            | 0.017   | -0.083            | 0.011   | -0.031            | 0.011   |
| F439W  | 4/97-6/98         | -0.026            | 0.005   | -0.147            | 0.017   | -0.094            | 0.012   | -0.014            | 0.014   |
| F555W  | 4/94-4/95         | -0.018            | 0.007   | --                | --      | -0.067            | 0.007   | --                | --      |
| F555W  | 4/95-4/96         | -0.039            | 0.005   | -0.050            | 0.013   | -0.051            | 0.009   | 0.016             | 0.016   |
|        |                   | (-0.023)          | (0.043) | (-0.023)          | (0.023) | (-0.030)          | (0.030) | (-0.027)          | (0.027) |
| F555W  | 4/96-4/97         | -0.028            | 0.004   | -0.055            | 0.011   | -0.012            | 0.009   | 0.023             | 0.009   |
| F555W  | 4/97-6/98         | -0.010            | 0.004   | -0.048            | 0.012   | -0.031            | 0.011   | -0.020            | 0.011   |
| F675W  | 4/94-4/95         | -0.009            | 0.008   | --                | --      | -0.009            | 0.008   | --                | --      |
| F675W  | 4/95-4/96         | -0.012            | 0.006   | -0.009            | 0.013   | 0.006             | 0.009   | -0.020            | 0.016   |
|        |                   | (-0.067)          | (0.067) | (-0.003)          | (0.037) | (-0.007)          | (0.037) | (-0.013)          | (0.037) |
| F675W  | 4/96-4/97         | -0.034            | 0.007   | --                | --      | 0.000             | 0.000   | --                | --      |
| F675W  | 4/97-6/98         | 0.024             | 0.006   | --                | --      | --                | --      | 0.013             | 0.016   |
| F814W  | 4/94-4/95         | 0.041             | 0.007   | --                | --      | 0.005             | 0.008   | --                | --      |
| F814W  | 4/95-4/96         | -0.014            | 0.006   | -0.001            | 0.012   | -0.038            | 0.009   | 0.045             | 0.015   |
|        |                   | (-0.043)          | (0.063) | (-0.007)          | (0.030) | (-0.000)          | (0.030) | (-0.007)          | (0.033) |
| F814W  | 4/96-4/97         | -0.005            | 0.005   | -0.035            | 0.015   | -0.005            | 0.011   | 0.012             | 0.010   |
| F814W  | 4/97-6/98         | -0.000            | 0.003   | -0.087            | 0.012   | 0.014             | 0.010   | -0.043            | 0.010   |

1. Epoch boundaries are at Apr. 25, 1994 (MJD=49467), Apr. 25, 1995 (MJD=49832), Apr. 25, 1996 (MJD=50198), Apr. 25, 1997 (MJD=50563), and Jun. 29, 1998 (MJD=50993).



Table 5.5: Dates of WFPC2 Decontaminations through November 2001.<sup>2</sup>

| Day-Month-<br>Year | Modified Julian<br>Date | Day-Month-<br>Year | Modified Julian<br>Date | Day-Month-<br>Year | Modified Julian<br>Date |
|--------------------|-------------------------|--------------------|-------------------------|--------------------|-------------------------|
|                    | <b>1994</b>             |                    | <b>1997</b>             | 14 Jul 99          | 51373.1715              |
| 22 Feb 94          | 49405.4840              | 07 Jan 97          | 50455.9875              | 10 Aug 99          | 51400.1667              |
| 24 Mar 94          | 49435.4639              | 09 Feb 97          | 50488.0006              | 09 Sep 99          | 51430.0604              |
| 24 Apr 94          | 49466.0340              | 23 Feb 97          | 50502.7978              | 05 Oct 99          | 51456.6437              |
| 23 May 94          | 49495.6250              | 27 Feb 97          | 50506.2721              | 03 Nov 99          | 51485.2854              |
| 13 Jun 94          | 49516.4597              | 04 Mar 97          | 50511.4278              | 28 Dec 99          | 51540.8215              |
| 10 Jul 94          | 49543.4861              | 21 Mar 97          | 50528.1494              |                    | <b>2000</b>             |
| 28 Jul 94          | 49561.3000              | 05 Apr 97          | 50543.3681              | 03 Jan 00          | 51546.0674              |
| 27 Aug 94          | 49591.4069              | 25 Apr 97          | 50563.9583              | 17 Jan 00          | 51560.6854              |
| 25 Sep 94          | 49620.0319              | 15 May 97          | 50583.8460              | 31 Jan 00          | 51574.6583              |
| 21 Oct 94          | 49646.0285              | 07 Jun 97          | 50606.5461              | 25 Feb 00          | 51599.4465              |
| 19 Nov 94          | 49675.7285              | 24 Jun 97          | 50623.4612              | 23 Mar 00          | 51626.2035              |
| 18 Dec 94          | 49704.2500              | 24 Jul 97          | 50653.7795              | 18 Apr 00          | 51652.8174              |
|                    | <b>1995</b>             | 20 Aug 97          | 50680.0952              | 17 May 00          | 51681.9225              |
| 13 Jan 95          | 49730.6764              | 17 Sep 97          | 50708.7256              | 14 Jun 00          | 51709.4354              |
| 12 Feb 95          | 49760.0792              | 13 Oct 97          | 50734.7506              | 11 Jul 00          | 51736.7583              |
| 11 Mar 95          | 49787.6042              | 14 Nov 97          | 50766.2217              | 06 Aug 00          | 51762.9049              |
| 08 Apr 95          | 49815.4368              | 10 Dec 97          | 50792.4027              | 10 Aug 00          | 51766.9992              |
| 07 May 95          | 49844.0507              |                    | <b>1998</b>             | 07 Sep 00          | 51794.2986              |
| 02 Jun 95          | 49870.7708              | 08 Jan 98          | 50821.0025              | 04 Oct 00          | 51821.0758              |
| 27 Jun 95          | 49895.8333              | 01 Feb 98          | 50845.8021              | 06 Oct 00          | 51823.6767              |
| 30 Jul 95          | 49928.3681              | 06 Mar 98          | 50878.3877              | 02 Nov 00          | 51850.4931              |
| 27 Aug 95          | 49956.2382              | 31 Mar 98          | 50903.5376              | 08 Nov 00          | 51856.0000              |
| 22 Sep 95          | 49982.1528              | 02 May 98          | 50935.5186              | 28 Nov 00          | 51876.7903              |
| 17 Oct 95          | 50007.4053              | 07 Jun 98          | 50971.8757              | 30 Dec 00          | 51908.3093              |
| 15 Nov 95          | 50036.3706              | 09 Jun 98          | 50973.9993              |                    | <b>2001</b>             |
| 14 Dec 95          | 50065.2929              | 12 Jun 98          | 50975.3340              | 23 Jan 01          | 51932.7141              |
|                    | <b>1996</b>             | 25 Jun 98          | 50989.2910              | 20 Feb 01          | 51960.1909              |
| 11 Jan 96          | 50093.9750              | 28 Jun 98          | 50992.5881              | 07 Mar 01          | 51975.2090              |
| 11 Feb 96          | 50124.0208              | 22 Jul 98          | 51016.7889              | 21 Mar 01          | 51989.5163              |
| 10 Mar 96          | 50152.0147              | 21 Aug 98          | 51046.5161              | 17 Apr 01          | 52016.9421              |
| 02 Apr 96          | 50175.0111              | 15 Sep 98          | 51071.0963              | 15 May 01          | 52044.9744              |
| 04 May 96          | 50207.7146              | 14 Oct 98          | 51100.1104              | 17 Jun 01          | 52077.4614              |
| 28 May 96          | 50231.2614              | 10 Nov 98          | 51127.2090              | 11 Jul 01          | 52101.8466              |
| 22 Jun 96          | 50256.9277              | 08 Dec 98          | 51155.5969              | 10 Aug 01          | 52131.5526              |
| 28 Jul 96          | 50292.5653              |                    | <b>1999</b>             | 05 Sep 01          | 52157.2317              |
| 23 Aug 96          | 50318.4242              | 28 Jan 99          | 51206.0458              | 05 Oct 01          | 52187.2807              |
| 18 Sep 96          | 50344.6840              | 23 Feb 99          | 51232.9471              | 02 Nov 01          | 52215.1989              |
| 18 Oct 96          | 50374.3236              | 25 Mar 99          | 51262.8441              |                    |                         |
| 12 Nov 96          | 50399.4031              | 20 Apr 99          | 51288.9910              |                    |                         |
| 15 Dec 96          | 50432.0417              | 19 May 99          | 51317.3528              |                    |                         |
| 19 Dec 96          | 50436.5229              | 16 Jun 99          | 51345.2965              |                    |                         |

<sup>2</sup> A list of decontamination dates is kept updated on the WWW.

### Cool Down on April 23,1994

The temperature of the WFPC2 was lowered from  $-76^{\circ}\text{C}$  to  $-88^{\circ}\text{C}$  on April 23, 1994, in order to minimize the CTE problem. While this change increased the contamination rates, it also improved the photometric throughput, especially in the UV, reduced the CTE losses, and greatly reduced the impact of warm pixels. Table 5.6 provides a partial list of corrections to table 5.1 for the pre-cool down throughput. Including the MJD in a **synphot** calculation (as shown in appendix A of the *Synphot User's Guide*) using up-to-date synphot contamination tables will correct PHOTFLAM for this change.

Table 5.6: Ratio Between Pre- and Post-Cool Down Throughput

| Filter | PC    | PC (mag) | WF    | WF (mag) |
|--------|-------|----------|-------|----------|
| F160BW | 0.865 | -0.157   | 0.895 | -0.120   |
| F170W  | 0.910 | -0.102   | 0.899 | -0.116   |
| F218W  | 0.931 | -0.078   | 0.895 | -0.120   |
| F255W  | 0.920 | -0.091   | 0.915 | -0.096   |
| F336W  | 0.969 | -0.034   | 0.952 | -0.053   |
| F439W  | 0.923 | -0.087   | 0.948 | -0.058   |
| F555W  | 0.943 | -0.064   | 0.959 | -0.045   |
| F675W  | 0.976 | -0.026   | 0.962 | -0.042   |
| F814W  | 0.996 | -0.004   | 0.994 | -0.007   |

### PSF Variations

The point spread function (PSF) of the telescope varies with time, and these variations can affect photometry that relies on very small apertures and PSF fitting. Changes in focus are observed on an orbital timescale due to thermal *breathing* of the telescope and due to desorption, which causes a continual creeping of the focal position. This change had been about  $0.7\ \mu\text{m}$  per month until mid-1996, when it greatly slowed. Currently the focus drift is less than  $0.3\ \mu\text{m}$  per month. The effect of focus position on aperture photometry is described in *WFPC2 ISR 97-01*. About twice a year, the focal position of the telescope is moved by several microns to remove the effect of the desorption; the [focus history](#) is available online.

In addition, *jitter*, or pointing motion, can occasionally alter the effective PSF. The Observatory Monitoring System (OMS) files provide information on telescope jitter during observations (see appendix C). These files are now regularly provided to the observer with the raw data. Observations taken after October 1994 have jitter files in the Archives. Limited requests for OMS files for observations prior to October 1994 can be handled by the STScI Help Desk (E-mail [help@stsci.edu](mailto:help@stsci.edu)).

Remy et al. (1997) have been able to obtain high-quality photometry of well-exposed point sources by modeling the point spread function with TinyTim (Krist, 1995), and taking into account focus and jitter terms via a chi-squared minimization method. Similar results have been obtained using observed PSFs (Surdej et al., 1997), provided that the PSF used is less than 10" from the observed star and corresponds to a spectral energy distribution similar to that of the target. The [WFPC2 PSF library](#) was established to help users find suitable PSFs, if they exist, or carry out experiments with what is available.

## 5.2.2 Position-Dependent Corrections

In this Section we discuss the Charge Transfer Efficiency (CTE) correction and the possibly related long vs. short anomaly, the geometric distortion, the gain differences between different chips, and the effect of pixel centering.

### Charge Transfer Efficiency

The CTE problem (or CTI, charge transfer inefficiency) results in targets losing counts as the WFPC2 chips are read out. The effect is most pronounced for objects near the top (Y~800) of the chip where the more rows the target must be clocked through, the more charge is lost. The problem has been attributed to impurities in the silicon which trap the charge, preventing it from being read out immediately (Holtzman et al., 1995). During on-orbit calibrations early in WFPC2's mission, the Investigation Definition Team (Holtzman et al., 1995) discovered the presence of CTI in the CCDs and at that time, with an operating temperature of -76°C, it was measured at ~10-15%. Lowering the operating temperature reduces the CTI, so the camera temperatures were set as low as possible, -88°C, which reduced the CTE (charge transfer efficiency) losses to ~3-4% in the worst case (top of the chip, in 1994).

After the acquisition of several more years of calibration data, the CTI was found to be increasing over time (Whitmore & Heyer, 1997). Stellar aperture photometry of  $\omega$  Cen showed that the CTE loss for faint stars (20-50 DN in a 2 pixel radius aperture, filter F814W, gain 15) at the top of the chip had gone from 3+/-3% in 1994 to 22+/-3% in 1997, while the CTE loss over time had remained stable for brighter (more than 200 DN) stars. A later study (Whitmore et al., 1999) confirmed that the CTE losses continue to increase for faint stars, up to 40% in February 1999, and the loss for bright targets remains stable. The effect appears to be correctable using the X- and Y-positions of the targets, the count levels in the background, the brightness of the stars, the date of the observation, and the formulae given in Whitmore et al., 1999. The sections below discuss photometric CTE corrections which can be applied during data analysis, including the new

Dolphin (2000) CTE corrections and their relation to the Whitmore et al. (1999) corrections.

### *Effect on Point Sources*

Since the April 1994 cool down, the CTE loss rate has been steadily worsening. Extensive observations made during Cycles 5 through 9 have provided a monitor of the CTE calibration over time; while the effect was about 5% in 1996-1997, the losses are up to 50% or more (peak-to-peak) in 2001 for the faintest targets<sup>3</sup>. Recent publications (PASP, **112**, 1397, PASP **111**, 1559, and *WFPC2 ISRs* 01-09, 97-08) quantify the CTE effect under various observational circumstances and provide empirically-derived correction formulae. After these corrections, the residual CTE effect for well-exposed stars is estimated to be less than 2%.

The correction for CTE depends on a number of variables, including the average background, the average counts over the chip, the counts in the source itself, and the target position on the chip. Assuming a 2 pixel radius aperture, the corrected counts are given by:

$$CTS_{corr} = \left[ 1 + \frac{Y_{CTE}}{100} \times \frac{Y}{800} + \frac{X_{CTE}}{100} \times \frac{X}{800} \right] CTS_{obs}$$

where  $X$  and  $Y$  are the coordinates of the star center in pixels, and  $X_{CTE}$  and  $Y_{CTE}$  are the percentile loss over 800 pixels in the  $x$  and  $y$  direction, respectively. For observed counts less than 4000 DN and backgrounds greater than 0.1 DN, the  $Y$  and  $X$  CTE components are given by:

$$Y_{CTE} = 2.3 \times 10^{-0.256 \times \log BKG} \times [1 + 0.245(0.0313 - 0.0087 \log CTS_{obs}) \times (MJD - 49471)]$$

$$X_{CTE} = 2.5 \times [1 + 0.341(0.00720 - 0.0020 \log CTS_{obs}) \times (MJD - 49471)]$$

For observed counts higher than 4000 DN and blank sky backgrounds greater than 0.1 DN, the  $Y$  and  $X$  CTE contributions are as follows:

$$Y_{CTE} = 2.3 \times 10^{-0.256 \times \log BKG}$$

$$X_{CTE} = 2.5$$

where  $MJD$  is the Modified Julian Date and  $BKG$  is the mean number of counts in DN for a blank region of the background.

For details on the use of these formulae, see Whitmore et al. (PASP **111**, 1559). Note that the equations are for gain = 7, the mode most commonly

---

3. In general, typical WFPC2 exposures are much longer than the short calibration images, resulting in a higher background which significantly reduces the CTE loss and minimizes the CTE problem for most science exposures.

used for science observations. Multiply  $CTS_{obs}$  and  $BKG$  by 2 before using either set of equations for gain=15. Also note that due to small uncertainties in the bias level, negative  $BKG$  can sometimes occur when the background is very low (i.e.,  $\leq 0.05$  DN). For  $BKG < 0.1$  DN, Whitmore et al. (PASP **111**, 1559) recommend linearly scaling the value based on observations using the same filters but with longer exposures of the same field. When longer exposures are not available and the background is blank sky, approximate background levels can be estimated by scaling values provided in Table 1 of the reference given above, though changes in zodiacal light and scattered Earth light may limit their accuracy. Another option is to set  $BKG$  to some threshold value (e.g., 0.1 DN) though this will provide only a rough approximation of  $X_{CTE}$  and  $Y_{CTE}$ .

Other correction formulae for CTE losses in point source photometry have been developed by Dolphin (PASP, **112**, 1397). This new study compared WFPC2 observations with ground based observations of  $\omega$  Cen and NGC 2419, deriving CTE corrections using a baseline through March 2000, a time line roughly a year longer than available for the Whitmore et al. analysis (PASP **111**, 1559). In general, the two studies are in good agreement, except for recent (1998 and later) data at low count levels. A preliminary comparison of the results of the two studies showed that for bright stars ( $>15,000 e^-$ ), the Whitmore et al. formulae tend to overestimate the correction by a few percent while for faint stars (100-500  $e^-$ ), the Whitmore et al. formulae underestimate the corrections. For extremely faint stars (20-50  $e^-$ ), the Dolphin formulae overestimate the corrections by tens of percent, likely due to the lack of faint stars in the sample. *For now, the best compromise is to use the Dolphin corrections for stars brighter than 100  $e^-$  and the Whitmore et al. corrections for fainter stars.*

### *Effect on Extended Sources*

The effect of CTE on the shape and structure of extended sources has also been studied (ISR 00-04). Pairs of images of individual galaxies observed near and far from the read-out amplifier were subtracted. The average profile of such galaxy residuals is distinctly asymmetric and indicates that the charge is primarily lost from the leading (amplifier-side) of the galaxy image. The side of the galaxy away from the amplifier suffers little charge loss because the charge traps encountered during the read-out have already been filled (by the leading edge) and because some trapped charge is being released. Preliminary results of aperture photometry on faint galaxy cores show effects consistent with those predicted for CTE in stellar photometry.

The analysis of how CTE affects galaxies is still at a relatively early stage and it is difficult at this point to provide a quantitative correction which can be employed by WFPC2 observers. Nevertheless, observers may wish to consider that the total CTE loss expected for a galaxy applies only to the half of the galaxy near the amplifier, with the other half experiencing negligible losses.

### Long vs. Short Anomaly (non-linearity)

A comparison of repeated images of the same stellar field can appear to give higher count rates for the faint stars on longer exposures. The effect was first noted by Stetson, as reported in Kelson et al. (1996) and Saha et al. (1996). These authors used a 5 % correction factor for the effect in their papers. A more detailed study was made by Casertano and Mutchler, as reported in [ISR 98-02](#). They found that this apparent non-linearity appears to be strictly a function of total counts in each source. The magnitude errors produced are less than 1% for well-exposed stars (over 30,000 e<sup>-</sup>), but may be much larger for faint stars. However, subsequent studies have not been able to confirm the existence of the so called "long vs. short" anomaly (e.g., Saha, Labhart, & Prosser 2000; and Dolphin 2000).

Based on a recent study by Whitmore and Heyer, it now appears that the effect may only be present for very crowded fields, where accurate sky subtraction becomes difficult or impossible. Hence, it may be largely a function of the photometric parameters and algorithms that are used for a particular study. On typical fields, where the stars are not so crowded that they overlap, the effect appears to be less than a few percent, if it exists at all. Further investigation of this topic is continuing and the reader is referred to a new ISR on the subject that will be out in early 2002.

### Geometric Distortion

Geometric distortion near the edges of the chips results in a change of the surface area covered by each pixel. The flatfielding corrects for this distortion so that surface photometry is unaffected. However, integrated point-source photometry using a fixed aperture *will* be affected by 1 to 2% near the edges, with a maximum of about 4-5% in the corners. A correction image has been produced and is available from the Archive ([f1k1552bu.r9h](#)). The counts measured for a star centered at a given pixel position must be multiplied by the value of these same pixels in the correction image (simply multiplying your image by the correction image and then measuring the counts is easiest). A small residual effect, due to the fact that the aperture radius differs from the nominal size, depends on the aperture used and is generally well below 1%. Please see section 5.4 for additional discussion on geometric distortion and astrometry.

### The 34-th Row Defect

Approximately every 34th row on the WFPC2 detectors possesses a reduced sensitivity (Trauger et al., 1993); these features are likely due to a manufacturing defect that resulted in the affected rows being somewhat narrower than the rest. The pipeline flatfields contain these features and produce calibrated images appropriate for surface brightness measurements. Point source photometry, however, can suffer 1-2% errors; and, the narrow rows have a significant effect on astrometry, causing periodic errors of up to 0.03 pixel. A recent paper by Anderson & King

(1999) provides photometric and astrometric correction formulae for this 34th row effect.

### Gain Variation

The absolute sensitivities of the four chips differ somewhat. Flatfields have been determined using the gain=14 setup, normalized to 1.0 over the region [200:600,200:600]. However, most science observations are taken using the gain=7 setup. Because the gain ratio varies slightly from chip to chip, PHOTFLAM values will be affected. The count ratios for the different chips from Holtzman (1995b) are:

- *PCI*: 1.987
- *WF2*: 2.003
- *WF3*: 2.006
- *WF4*: 1.955

These count ratios should be included in the zeropoint calculation if using values from Holtzman et al. (1995b) on gain=7 data. Conversely, their reciprocals should be applied when using **synphot** zeropoints on gain=14 data. If you use the value of PHOTFLAM from the header to determine your zeropoint, the different gains for the different chips will already be included. Remember to use the new PHOTFLAM values provided in table 5.1 or the post-May 1997 **synphot** tables; those included in the header for data taken before May 1997 will have less accurate values.

### Pixel Centering

Small, sub-pixel variations in the quantum efficiency of the detector could affect the photometry. The position of star relative to the sub-pixel structure of the chip is estimated to have an effect of less than 1% on the photometry. At present there is no way to correct for this effect.

### Possible Variation in Methane Quad Filter Transmission

Based on results from Jupiter and Uranus archival WFPC2 data, the extended wings of the methane filter transmission curve appear to vary across the field of view (Karkoshka, priv. comm.). While this is unimportant for objects with flat spectra, it can have a major impact on photometry of objects with methane bands, where a significant fraction of photons comes from the wings. To provide data to check the methane filter, a set of eight 40-sec Saturn images in a 3x3 grid around the FQCH4W3 methane quad filter aperture (one of the 9 positions falls outside of the filter) is planned as part of the Cycle 10 calibration program (proposal 9256). The magnitude and direction of the effect will be quantified by comparing results from the rings of Saturn (flat spectrum) to results from Saturn itself (deep methane band spectrum).

### Anomalous Rotational Offset in the Linear Ramp Filters

For completeness, this effect is included here though we expect no impact on observations as any photometric effect is estimated to be less than 1%. Analysis of FR533N VISFLAT images has revealed an apparently randomly occurring offset of about 0.5 degrees in the filter wheel rotation for some images, a quantity that corresponds to one filter step. The pivot point of the rotation implicates the filter wheel as the source of the inconsistency. A handful of other filters, on different filter wheels as well, appear to exhibit the same problem; at this time, the source of this anomaly, whether it is mechanical or due to a software error, is unknown. A detailed report is in progress (Nov. 2001); a preliminary report is available in [ISR 01-04](#).

### 5.2.3 Other Photometric Corrections

Miscellaneous corrections that must be taken into account include: aperture corrections, color terms if transforming to non-WFPC2 filters, digitization noise and its impact on the estimate of the sky background, the effect of red leaks and charge traps, and the uncertainty of exposure times on short exposures taken with serial clocks on.

#### Aperture Correction

It is difficult to measure directly the total magnitude of a point source with the WFPC2 because of the extended wings of the PSF, scattered light, and the small pixel size. One would need to use an aperture far larger than is practical. A more accurate method is to measure the light within a smaller aperture and then apply an offset to determine the total magnitude. Typically, magnitudes will be measured in a small aperture well-suited to the data at hand—a radius of 2–4 pixels, with a background annulus of 10–15 pixels, has been found adequate for data without excessive crowding—and the results corrected to the aperture for which the zeropoint is known. The aperture correction can often be determined from the data themselves, by selecting a few well-exposed, isolated stars. If these are not available, encircled energies and aperture corrections have been tabulated by Holtzman et al. (1995a). If PSF fitting is used, then the aperture correction can be evaluated directly on the PSF profile used for the fitting.

For very small apertures (1–2 pixels), the aperture correction can be influenced by the HST focus position at the time of the observation. The secondary mirror of HST is known to drift secularly towards the primary and to move slightly on time scales of order of an orbit. The secular shift is corrected by biannual moves of the secondary mirror, but the net consequence of this motion is that WFPC2 can be out of focus by up to 3–4  $\mu\text{m}$  of secondary mirror displacement at the time of any given observation. This condition affects the encircled energy at very small radii, and thus the aperture corrections, by up to 10% in flux (for 1 pixel aperture in the PC);



see [WFPC2 ISR 97-01](#) for more details. If the use of very small apertures is required—because of crowding, S/N requirements, or other reasons—users are strongly advised to determine the aperture correction from suitable stars in their images. If such are not available, an *approximate* aperture-focus correction can be obtained as described in [WFPC2 ISR 97-01](#).

A standard aperture radius of 0."5 has been adopted by Holtzman et al. (1995b; note that Holtzman et al. 1995a used a radius of 1."0). For historic consistency, the WFPC2 group at STScI and the synphot tasks in STSDAS refer all measurements to the total flux in a hypothetical infinite aperture. In order to avoid uncertain correction to such apertures, both in calibration and in science data, this infinite aperture is defined by an aperture correction of exactly 0.10 mag with respect to the standard 0."5 aperture. This value (0.10 mag) is close to the values tabulated in Holtzman et al. (1995a) as well as consistent with Whitmore (1995); only extended sources larger than  $\sim 1''$  are likely to require a more accurate aperture correction ([ISR 97-01](#)). Equivalently, the total flux is defined as 1.096 times the flux in the standard aperture of 0."5 radius. In practice, this means that observers wishing to use our tables or the synphot zeropoints should:

1. Correct the measured flux to a 0."5 radius aperture.
2. Apply an additional aperture correction of  $-0.10$  mag (equivalently, multiply the flux by 1.096).
3. Determine the magnitude using the zeropoints given.

See also the example in section 5.2.4.

### Color Terms

In some cases it may be necessary to transform from the WFPC2 filter set to more conventional filters (e.g., Johnson UBV or Cousins RI) in order to make comparisons with other datasets. The accuracy of these transformations is determined by how closely the WFPC2 filter matches the conventional filter and by how closely the spectral type (e.g., color, metallicity, surface gravity) of the object matches the spectral type of the calibration observations. Accuracies of 1–2% are typical for many cases, but much larger uncertainties are possible for certain filters (e.g., F336W, see “Red Leaks” section below), and for certain spectral types (e.g., very blue stars). Transformations can be determined by using **synphot**, or by using the transformation coefficients in Holtzman et al. (1995b).

### Digitization Noise

The minimum gain of the WFPC2 CCDs,  $7 e^-/\text{ADU}$ , is larger than the read noise of the chip. As a result, digitization can be a source of noise in WFPC2 images. This effect is particularly pernicious when attempting to determine sky values, because the measured values tend to cluster about a few integral values (dark subtraction and flatfielding cause the values to

differ by slightly non-integral amounts). As a result, using a median filter to remove objects that fall within the background annulus in crowded fields, can cause a substantial systematic error, whose magnitude will depend on the annulus being measured. It is generally safer to use the mean, though care must then be taken to remove objects in the background annulus.

A more subtle effect is that some statistics programs assume Gaussian noise characteristics when computing properties such as the median and mode. Quantized noise can have surprising effects on these programs. Based upon the analysis of a variety of possible strategies for sky determination (WFPC2 ISR 96-03), the centroid and the optimal filter ("ofilter") of the histogram of sky pixel values were found to produce the least biased result for typical WFPC2 data with low background levels.

### Red Leaks

Several of the UV filters have substantial red leaks that can affect the photometry. For example, the U filter (F336W) has a transmission at 7500 Å that is only about a factor of 100 less than at the peak transmission at about 3500 Å. The increased sensitivity of the CCDs in the red, coupled with the fact that most sources are brighter in the red, makes this an important problem in many cases. The **synphot** tasks can be used to estimate this effect for any given source spectrum.

### Charge Traps

There are about 30 macroscopic charge transfer traps, where as little as 20% of the electrons are transferred during each time step during the readout. These defects result in *bad pixels*, or in the worst cases, *bad columns* and should not be confused with microscopic charge traps which are believed to be the cause of the CTE problem. The traps result in dark tails just above the bad pixel, and bright tails for objects farther above the bad pixel that get clocked out through the defect during the readout. The tails can cause large errors in photometric and astrometric measurements. In a random field, about 1 out of 100 stars are likely to be affected. Using a program which interpolates over bad pixels or columns (e.g., **wfixup** or **fixpix**) to make a cosmetically better image can result in very large (e.g., tenths of magnitude) errors in the photometry in these rare cases. See also section 3.5.4.

### Exposure Times: Serial Clocks

The serial clocks option (i.e., the optional parameter **CLOCKS = YES** in the Phase II proposal instructions) is occasionally useful when an extremely bright star is in the field of view, in order to minimize the effects of bleeding. However, the shutter open time can have errors of up to 0.25 second due to the manner in which the shutters are opened when **CLOCKS=YES** is specified. If the keyword **SERIALS = ON** is in the image header, then the serial clocks were employed. Header information can be used to correct this error. The error in the exposure time depends on

the SHUTTER keyword. If the value of this keyword is “A”, then the true exposure time is 0.125 second less than that given in the header. If instead the value is “B”, then the true exposure time is 0.25 second less than the header value.

Users should also note that exposure times of non-integral lengths in seconds cannot be performed with the serial clocks on. Therefore, if a non-integral exposure time is specified in the proposal, it will be rounded to the nearest second. The header keywords will properly reflect this rounding, although the actual exposure time will still be short as discussed above.

### F1042M Extended Halo

Observers using the F1042M filter should be aware that it possesses an anomalous PSF containing additional light in a broad halo component. The defocused halo is likely due to the CCD detector becoming transparent at this wavelength, so that the light is reflected and scattered by the back of the CCD. The scattering will impact photometry in the F1042M filter relative to other filters, since a greater fraction of the counts will lie outside the 1 arcsecond diameter aperture used for photometry on standard stars. The [WFPC2 Instrument Handbook](#) provides a comparison of azimuthal averages for an observed F1042M and F953N PSF; additional PSF examples are in the [WFPC2 PSF Library](#).

## 5.2.4 An Example of Photometry with WFPC2

This example shows the steps involved in measuring the magnitude of the star #1461 (Harris et al., 1993) in the Cousins I passband. The image used for this example can be obtained from the HST Archive, or from the [WWW](#). The WWW directory contains the materials for [WFPC2 ISR 95-04](#), *A Demonstration Analysis Script for Performing Aperture Photometry*. Table 5.7 shows the results from an analysis script similar to [WFPC2 ISR 95-04](#), but including some of the corrections discussed above.

```
Images: u2g40o09t.c0h[1] and u2g40o0at.c0h[1]
Position: (315.37,191.16)
Filter: F814W
Exposure Time: 14 seconds
Date of observation: MJD - 49763.4
```

Table 5.7: Magnitude of Star #1461 in  $\omega$  Cen

| Value                              | Description  |
|------------------------------------|--|
| 2113.49 counts                     | Raw counts in 0.5" radius aperture (11 pixels for PC)  |
| -48.63 = 2064.86 counts            | Background subtraction (0.12779 counts x 380.522 pix obtained from a 40-pixel radius aperture with an annulus of 5 pixels)   |
| x 0.9915 = 2047.31 counts          | Correction for geometric distortion. Not needed if doing surface photometry.   |
| => 15.481 mag                      | Raw magnitude ( $= -2.5 \times \log_{10}(2047.31 / 14 \text{ sec}) + 20.894$ )<br>NOTE: $-2.5 \times \log_{10}(1.987)$ has been added to the zeropoint from section 5.2.2, "Gain Variation" since these calibrations were taken using the gain=14 setup. Most science observations use gain=7. |
| -0.10 = 15.381 mag                 | Aperture correction to total magnitude, estimated from Holtzman (1995a).   |
| -0.028 = 15.353 mag                | CTE correction (using formulas 1, 2d, 3d from <a href="#">WFPC2 ISR 97-08</a> with this data). Note that this example uses relatively old CTE corrections which do not include a time dependence. Please see section 5.2.2 for the most up-to-date corrections.                                |
| -0.000 => $m_{F814W} = 15.353$ mag | Contamination correction ( $0.000 \times [49763.4 - 49760.1]$ ). An additional correction to transform to e.g., Cousin I, could be applied using the method described in "Contamination".  |

## 5.3 Polarimetry

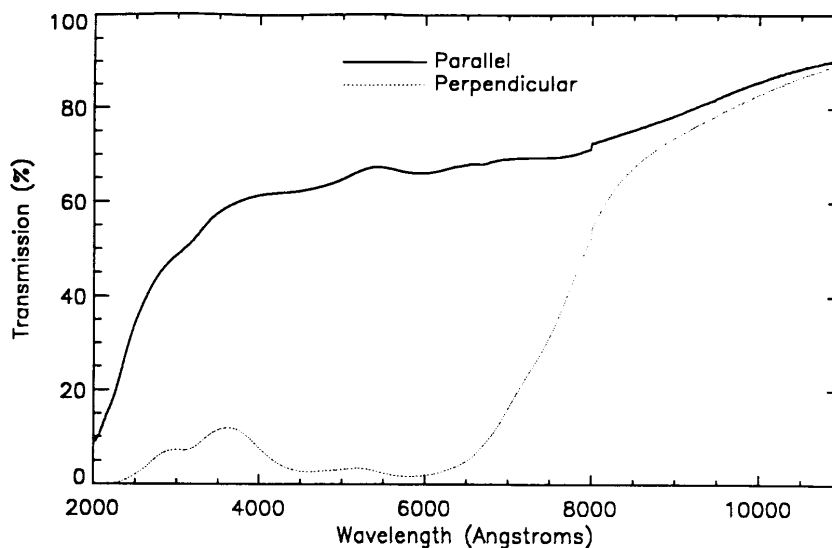
WFPC2 has a polarizer filter which can be used for wide-field polarimetric imaging from about 200 through 700 nm. This filter is a *quad*, meaning that it consists of four panes, each with the polarization angle oriented in a different direction, in steps of  $45^\circ$ . The panes are aligned with the edges of the pyramid, thus each pane corresponds to a chip. However, because the filters are at some distance from the focal plane, there is significant vignetting and cross-talk at the edges of each chip. The area free from vignetting and cross-talk is about 60" square in each WF chip, and 15" square in the PC. It is also possible to use the polarizer in a partially rotated configuration, which gives additional polarization angles at the expense of more severe vignetting.

Each polarimetry observation consists of several images of the same object with different orientations of the polarizer angle. A minimum of three observations is required to obtain full polarimetry information. This can be achieved by observing the target in different chips, by rotating the filter wheel (partial rotation), or by changing the orientation of the HST field of view in the sky, using a different roll angle. In the latter case,

observations must frequently occur at different times, as the solar array constraints on HST allow only a limited range of roll angles at any given time.

Accurate calibration of WFPC2 polarimetric data is rather complex, due to the design of both the polarizer filter and the instrument itself. WFPC2 has an aluminized pick-off mirror with a  $47^\circ$  angle of incidence, which rotates the polarization angle of the incoming light, as well as introducing a spurious polarization of up to 5%. Thus, both the HST roll angle and the polarization angle must be taken into account. In addition, the polarizer coating on the filter has significant transmission of the perpendicular component, with a strong wavelength dependence (see figure 5.1).

Figure 5.1: Parallel and Perpendicular Transmission of the WFPC2 Polarizer



A calibration accuracy of about 2% rms for well-exposed WFPC2 polarimetry data has been achieved (*WFPC2 ISR 97-11*). The method uses a Mueller matrix approach to account for the orientation of both telescope and polarizer, the effect of the pick-off mirror, and the significant perpendicular transmission of the polarizer itself. A full description of the motivation behind this approach, the implementation details, and the necessary caveats are given in the ISR mentioned above. A [web-based tool to aid in the calibration of polarization data has also been developed](#). With the aid of this tool, polarization properties can be derived for point sources and extended sources from an arbitrary combination of polarized images.

The procedure to obtain polarization information begins with the calibrated images, as they come out of the pipeline (plus cosmic ray and warm pixel rejection, if appropriate). The circumstances of the polarized images and the fluxes in each image are entered in the Web tool, and the calculation started. The tool then reports the values of the Stokes parameters  $I$ ,  $Q$ , and  $U$ , as well as fractional polarization and position

angle. The optional **synphot** values in the first part of the tool can be used to fine-tune the results to a specific spectral energy distribution, but are in most cases not necessary.

The tool also reports expressions for  $I$ ,  $Q$ , and  $U$  as a function of fluxes in the three images. These can be used to test the sensitivity of the results to errors in the individual fluxes, or to combine images in order to obtain pixel-by-pixel values of the Stokes parameters for extended objects, resulting in  $I$ ,  $Q$ , and  $U$  images.

More details will be provided in a future ISR, as well as in the extensive help available in the web tool itself.

---

## 5.4 Astrometry

Astrometry with WFPC2 means primarily *relative* astrometry. The high angular resolution and sensitivity of WFPC2 makes it possible, in principle, to measure precise positions of faint features with respect to other reference points in the WFPC2 field of view. On the other hand, the absolute astrometry that can be obtained from WFPC2 images is limited by the positions of the guide stars, usually known to about 0."5 rms in each coordinate, and by the transformation between the FGS and the WFPC2, which introduces errors of order of 0."1 (see *Instrument Science Report OSG-006*).

Because WFPC2 consists of four physically separate detectors, it is necessary to define a coordinate system that includes all four detectors. For convenience, sky coordinates (right ascension and declination) are often used; in this case, they must be computed and carried to a precision of a few mas, in order to maintain the precision with which the relative positions and scales of the WFPC2 detectors are known. It is important to remember that the coordinates are *not* known with this accuracy. The absolute accuracy of the positions obtained from WFPC2 images is typically 0."5 rms in each coordinate and is limited primarily by the accuracy of the guide star positions.




---

***The recommended way to convert pixel coordinates into relative coordinates is to use the task, metric, which can handle both WF/PC-1 and WFPC2 images. The task xy2rd, will provide rough coordinates only and does not take geometric distortion into account.***

---

For WFPC2 images, **metric** corrects the geometric distortion introduced by the camera optics, primarily the field flattening lenses, and brings the four chips into the metachip reference system, defined so as to have the same orientation and plate scale as the WF2 chip at its center. These coordinates are then converted into right ascension and declination by using the position and orientation of the WF2 chip. A related task, **invmetric**, can be used to effect the opposite transformation, from right ascension and declination to chip and pixel position. The final relative positions are accurate to better than 0."005 for targets contained on one chip, and 0."1 for targets on different chips. Note that both **metric** and **invmetric** include specialized information about the geometry of WFPC2 (see [ISR 95-02](#)). They do *not* use the header parameters that describe the world coordinate system (CRVAL1 and 2, CRPIX1 and 2, and the CDMATRIX) to relate positions in different chips. Of these parameters, only the values for WF2 are used to convert the metachip positions to and from right ascension and declination. As a side effect, neither task can work on images that do not contain WF2, for which the **xy2rd** task can be used.

Observers should be aware that the task **xy2rd** provides rough coordinates only. It uses the world coordinate system parameters in each group to determine the coordinates associated with a given pixel position. However, **xy2rd** does *not* use the most recent information on the relative chip positions, and it does *not* apply the geometric correction. Each can result in an error of about 0."3, especially near the edges of the chip; typical errors are closer to 0."1.

Astrometric measurements may be improved in several ways. First, the processing epoch of the images should be evaluated. Early WFPC2 images, particularly non-OTFR data, may contain header parameters with less accurate values of the plate scale and of the chip-to-chip rotations; section 4.3.3 provides detailed recommendations on updating such WFPC2 image headers. Images retrieved via OTFR will contain the most up-to-date parameters available at the time of processing. A significant improvement can be achieved by correcting the systematic errors caused by the 34th row defect, discussed in “The 34-th Row Defect”; this can be accomplished by using the formulae developed by Anderson & King (PASP **111**, 1095). And finally, observers may wish to use the improved geometric distortion solution provided in [ISR 01-10](#) and/or correct for any possible wavelength dependence (Trauger et al. (1995)), as discussed below.

Though the original solution, which is based upon a relatively sparse field, provides an adequate measure of the WFPC2 geometric distortion, it has significant residuals at a level of 5 mas overall and 10-15 mas in the detector corners. The improved solution is based upon multiple observations of a rich star field in  $\omega$  Cen; the new coefficients are tabulated in table 5.8 (see [ISR 01-10](#) for details).

Table 5.8: Parameters of the new astrometric solution (taken from [WFPC2 ISR 01-10](#)). The functional form of the solution and the coefficient nomenclature are the same as those in Holtzman et al. (1995) and Trauger et al. (1995).

| #  | C             |              |               |               |
|----|---------------|--------------|---------------|---------------|
|    | PC            | WF2          | WF3           | WF4           |
| 1  | 3.543560e+2   | -8.096405e+2 | -8.052758e+2  | 7.708965e+2   |
| 2  | 1.000210e+0   | 21.667040e-3 | -2.186307e+0  | 11.503445e-3  |
| 3  | 1.685097e-3   | -2.186781e+0 | -10.318882e-3 | 2.187646e+0   |
| 4  | -0.476421e-6  | -1.081274e-6 | -0.467968e-6  | 1.410633e-6   |
| 5  | -0.128977e-6  | 4.875708e-6  | 2.360098e-6   | -3.662324e-6  |
| 6  | -1.119461e-6  | 1.160592e-6  | -1.881792e-6  | -0.820634e-6  |
| 7  | -38.989762e-9 | -1.068123e-9 | 73.972588e-9  | -0.388185e-9  |
| 8  | 0.495226e-9   | 75.463250e-9 | 0.110498e-9   | -77.222274e-9 |
| 9  | -36.277270e-9 | 0.099408e-9  | 76.882580e-9  | -1.794536e-9  |
| 10 | -0.075298e-9  | 72.628997e-9 | 0.003372e-9   | -76.141940e-9 |

| #  | D             |               |              |              |
|----|---------------|---------------|--------------|--------------|
|    | PC            | WF2           | WF3          | WF4          |
| 1  | 3.436460e+2   | 7.667990e+2   | -7.692243e+2 | -7.708547e+2 |
| 2  | 2.649830e-3   | 2.185899e+0   | 4.282145e-3  | -2.186289e+0 |
| 3  | 0.999790e+0   | 16.771070e-3  | -2.185173e+0 | 16.304679e-3 |
| 4  | -0.915545e-6  | -3.953135e-6  | -1.588401e-6 | 1.692025e-6  |
| 5  | -0.347576e-6  | -2.815106e-6  | 2.574760e-6  | 2.596669e-6  |
| 6  | 0.532097e-6   | 0.309766e-6   | 0.404571e-6  | -1.059466e-6 |
| 7  | -2.592636e-9  | -73.394946e-9 | -0.208263e-9 | 75.750980e-9 |
| 8  | -34.967762e-9 | -1.715681e-9  | 77.114768e-9 | 0.528052e-9  |
| 9  | -1.570711e-9  | -75.104144e-9 | 0.162718e-9  | 75.946626e-9 |
| 10 | -41.901809e-9 | -0.423891e-9  | 74.483675e-9 | -0.237788e-9 |

Systematic residuals in this new solution are very small, about 1.2 mas in WF and less than 4.0 mas in PC. Note, however, that neither solution addresses any possible wavelength dependence - which is predicted to be a change in overall scale rather than higher-order distortions; for this, observers should refer to the ray-tracing solution presented by Trauger et al. (1995) and the PC chip UV scale correction factors in Barstow et al. (2001).

There is also clear evidence for long-term variations in the relative detector positions, based upon an analysis of WFPC2 K-spot images (internal exposures producing eleven fixed artificial stars along the chip quadrant boundaries). The spot positions are found to vary regularly over time, in a systematic fashion. All spot images within each chip move



similar amounts, implying that the changes are due to a lateral motion of the image with respect to the detector rather than a rotation. The shifts were relatively large at first, about 2-4 pixels in the first few months of WFPC2 operation, and later decreased to about 0.1-0.2 pixel/year (*WFPC2 ISR 01-10*). Note that these long-term variations are not accounted for in the pointing information in the headers.

---

## 5.5 Dithering

The pixels of the PC undersample the point spread function (PSF) of the HST by a factor of about two, and the pixels of the WF are a factor of two coarser yet. Thus WFPC2 does not recover a substantial fraction of the spatial information that exists at the focal plane of the instrument. However, this information is not completely lost. Some of it can be recovered by *dithering* or *sub-stepping* the position of the chips by non-integral pixel amounts.

The recovery of high frequency spatial information is fundamentally limited by the pixel response function (PRF). The PRF of an ideal CCD with square pixels is simply a square boxcar function the size of the pixel. In practice, the PRF is a function not only of the physical size of the pixels, but also the degree to which photons and electrons are scattered into adjacent pixels, as well as smearing introduced by telescopic position wandering. The image recorded by the CCD is the “true” image (that which would be captured by an ideal detector at the focal plane) convolved with this PRF. Thus, at best, the image will be no sharper than that allowed by an ideal square pixel. In the case of WFPC2, in which at least 20% of the light falling on a given pixel is detected in adjacent pixels, the image is even less sharp.

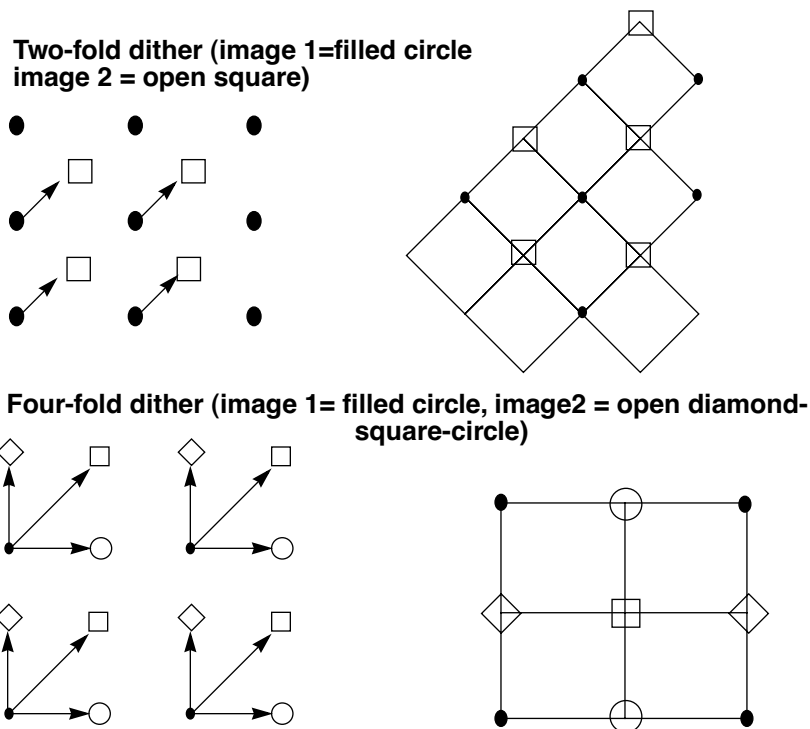
The PRF of an ideal square pixel, that is a boxcar function, severely suppresses power on scales comparable to the size of the pixel. According to the Shannon-Nyquist theorem of information theory the sampling interval required to capture nearly all of the information passed by square pixels is  $1/2$  the size  $l$  of a pixel. This corresponds to dithering the CCD from its starting position of  $(0,0)$  to three other positions,  $(0, 1/2 l)$ ,  $(1/2 l, 0)$  and  $(1/2 l, 1/2 l)$ ; however, in practice, much of the information can be regained by a single dither to  $(1/2 l, 1/2 l)$ .

The process of retrieving high-spatial resolution information from dithered images can be thought of as having two stages. The first, reconstruction, removes the effect of sampling and restores the image to that produced by the convolution of the PSF and PRF of the telescope and detector. The more demanding stage, deconvolution (sometimes called restoration), attempts to remove much of the blurring produced by the optics and detector. In effect, deconvolution boosts the relative strength of

the high-frequency components of the Fourier spectrum to undo the suppression produced by the PSF and PRF.

If your observations were taken with either of the two dither patterns discussed above, and if the positioning of the telescope was accurate to about a tenth of a pixel (this is usually but not always the case), then you can reconstruct the image merely by interlacing the pixels of the offset images. In the case of a two-fold dither—that is images offset by a vector  $(n + 1/2, n + 1/2)$  pixels, where  $n$  is an integer—the interlaced images can be put on a square grid rotated  $45^\circ$  from the original orientation of the CCD (see figure 5.2, top). In the case of a four-fold dither, the images are interlaced on a grid twice as fine as the original CCD and coaligned with it (see figure 5.2, bottom).

Figure 5.2: Interlacing Pixels of Offset Images (filled circles and open squares in the top plots represent pixels in image 1 and 2, respectively; filled circles, open squares, open diamonds, and open circles represent pixels in images 1,2,3,4, respectively, in the lower two plots).



As part of the Hubble Deep Field project, a new method was developed to linearly reconstruct multiple offset images. This method, variable pixel linear reconstruction (also known as *drizzle*), can be thought of as shifting and adding with a variable pixel size. For poorly sampled data, the shifted pixels retain the initial pixel size—the final image combines the shifts correctly, but the gain in resolution is minimal. For a well-sampled field, such as that of the Hubble Deep Field, the size of the shifted pixels can be

made quite small, and the image combination becomes equivalent to interlacing. Drizzling also corrects for the effects of the geometric distortion of WFPC2; correction of geometric distortion is important if shifts between dithered images are of order ten pixels or more.

The drizzle algorithm was implemented as the STSDAS task **drizzle**, as part of the **dither** package, which helps users combine dithered images. The **dither** package is included in STSDAS release v2.0.1 and later, and includes the following tasks:

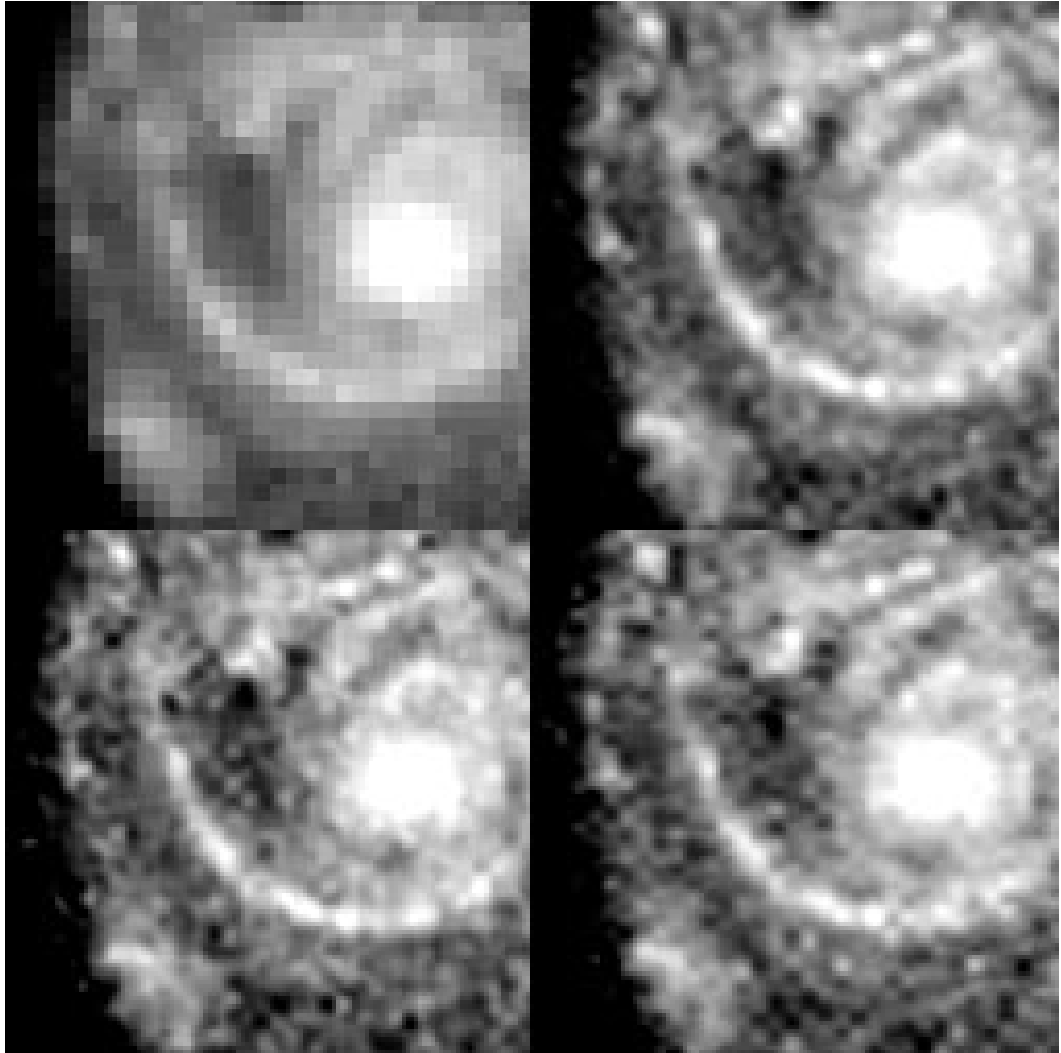
- **precor**: Determines regions of the image containing astrophysical objects and nulls the remainder of the image, substantially reducing the effect of cosmic rays and chip defects on the offset measurement. The output from **precor** is only used for offset determination and not final image creation.
- **offset**: Cross-correlates all four images in a WFPC image, creating output cross-correlation images with names that can be appropriately grouped by later tasks. Uses the task **crossdriz** to perform the cross-correlation.
- **crossdriz**: Cross-correlates two images, after preprocessing which includes trimming, and, if requested, drizzling to remove geometric distortion or rotation. **crossdriz** will also perform a loop over a range of test rotation angles.
- **shiftfind**: Locates the peak in a cross-correlation image and fits for sub-pixel shift information. The search region and details of the fitting can be adjusted by the user.
- **rotfind**: Fits for the rotation angle between two images. **rotfind** is called when **crossdriz** has been used to loop over a range of test rotation angles between two images.
- **avshift**: Determines the shifts between two WFPC2 images by averaging the results obtained on each of the groups after adjusting for the rotation angles between the four groups. **avshift** can also be used to estimate the rotation angle between two different WFPC2 images, when the rotation angle is a small fraction of a degree.
- **blot**: Maps a drizzled image back onto an input image. This is an essential part of the tasks we are developing for removing cosmic rays from singly-dithered images.

Additional information on these tasks is available in Fruchter et al. (1997) and Mutchler and Fruchter (1997), the on-line help files for the task, and the [HST Dither Handbook](#).

Although reconstruction largely removes the effects of sampling on the image, it does not restore the information lost to the smearing of the PSF and PRF. Deconvolution of the images, however, does hold out the possibility of recapturing much of this information. Figure 5.3, supplied by

Richard Hook of the ST-ECF, shows the result of applying the Richardson-Lucy deconvolution scheme to HST data, used extensively in the analysis of WF/PC-1 data. The upper-left image shows one of four input images. The upper-right image shows a deconvolution of all of the data, and the lower two images show deconvolutions of independent subsets of the data. A dramatic gain in resolution is evident.

Figure 5.3: Richardson-Lucy Deconvolution of HST Data



A version of the Richardson-Lucy (RL) deconvolution scheme capable of handling dithered WFPC2 data is already available to STSDAS users. It is the task **acoadd** in the package **stsdas.contrib**. In order to use **acoadd**, users will need to supply the program both with a PSF (which in practice should be the convolution of the PRF with the optical PSF) and with the offsets in position between the various images. The position offset between

the two images can be obtained using the task **crossdriz** in the **dither** package.

In principle, image deconvolution requires an accurate knowledge of both the instrument PSF and PRF. At present, our best models of the WFPC2 PSF come from the publicly available TinyTim software (Krist, 1995). The quality of the TinyTim model can be improved substantially by taking into account the exact position of the source within the pixel. Remy et al. (1997) discuss how this can be accomplished by generating multiple TinyTim images at various focus and jitter values, oversampled with respect to the camera pixels. At present, this is very labor-intensive, and the results cannot be easily integrated into the existing deconvolution software. Another limitation of the existing software is that it cannot incorporate the significant variation of the PSF across the field of view. As a result, the Richardson-Lucy approach can only be applied to limited regions of a chip at a time. Nonetheless, tests done on WFPC2 images suggest that RL deconvolution can give the WFPC2 user a substantial gain in resolution even in the presence of typical PSF and PRF errors. Users interested in more information on dithering, reconstruction, and deconvolution should consult the [HST Dither Handbook](#).

---

## 5.6 Accuracy of WFPC2 Results

Table 5.9 summarizes the accuracy to be expected from WFPC2 observations in several areas. The numbers in the table should be used with care, and only after reading the relevant sections of this handbook and the documents referenced therein; they are presented in tabular form here for easy reference.

Table 5.9: Accuracy Expected in WFPC2 Observations

| Procedure  | Estimated Accuracy  | Notes  |
|--|---|--|
| <b>Calibration (flatfielding, bias subtraction, dark correction)</b> |   |  |
| Bias subtraction   | 0.1 DN rms  | Unless bias jump is present  |
| Dark subtraction   | 0.1 DN/hr rms   | Error larger for warm pixels; absolute error uncertain because of dark glow  |
| Flatfielding   | <1% rms large scale   | Visible, near UV   |
|  | 0.3% rms small scale  |  |
|  | ~10%  | F160BW; however, significant noise reduction achieved with use of correction flats   |
| <b>Relative photometry</b>   |   |  |
| Residuals in CTE correction  | < 3% for the majority (~90%) of cases                       |  |
|  | up to 1-% for extreme cases (e.g., very low backgrounds)    |  |
| Long vs. short anomaly (uncorrected)                                 | < 5%  | Magnitude errors <1% for well-exposed stars but may be larger for fainter stars. Some studies have failed to confirm the effect (see “Long vs. Short Anomaly (non-linearity)”) ) |
| Aperture correction  | 4% rms focus dependence (1 pixel aperture)                  | Can (should) be determined from data   |
|  | <1% focus dependence (> 5 pixel)                            |  |
|  | 1-2% field dependence (1 pixel aperture)                    |  |
| Contamination correction   | 3% rms max (28 days after decon) (F160BW)                   |  |
|  | 1% rms max (28 days after decon) (filters bluer than F555W) |  |
| Background determination   | 0.1 DN/pixel (background > 10 DN/pixel)                     | May be difficult to exceed, regardless of image S/N  |
| Pixel centering  | < 1%  |  |
| <b>Absolute photometry</b>   |   |  |
| Sensitivity  | < 2% rms for standard photometric filters                   | Red leaks are uncertain by ~10%  |
|  | 2% rms for broad and intermediate filters in visible        |  |
|  | < 5% rms for narrow-band filters in visible                 |  |
|  | 2-8% rms for UV filters                                     |  |
| <b>Astrometry</b>  |   |  |
| Relative   | 0.005" rms (after geometric and 34th-row corrections)       | Same chip  |
|  | 0.1" (estimated)  | Across chips   |
| Absolute   | 1" rms (estimated)  |  |

# References

- Anderson, J., and King, I.R. 1999, Astrometric and Photometric Corrections for the 34th Row Error in HST's WFPC2 Camera, *PASP* 111, 1095.
- Baggett, S., et al., 1997, WFPC2 SYNPHOT Update, *ISR* 97-10.
- Baggett, S., and Gonzaga, S., 1998, WFPC2 Long-Term Photometric Stability, *ISR* 98-03.
- Barstow, M.A., et al., 2001, Resolving Sirius-like Binaries with the Hubble Space Telescope, *MNRAS* 322, 891.
- Bernstein, R.A., Freedman, W.L., Madore, B.F., The First Detection of the Extragalactic Background Light at 3000, 5500 and 8000 Å: Results, *ApJ*. 2001 in press (astro-ph 0112153)
- Bessell, M.S., 1983, *PASP* 95, 480.
- Biretta, J., and McMaster, M., 1997, WFPC2 Polarization Calibration, *ISR* 97-11.
- Biretta, J., et al., 1996, A Field Guide to WFPC2 Image Anomalies, *ISR* 95-06.
- Biretta, J., et al. 2001, WFPC2 Instrument Handbook, Version 6.0 (Baltimore: STScI).
- Buser, R. and Kurucz, R.L., 1978, *A&A* 70, 555.
- Casertano, S., and Mutchler, M., 1998, The Long vs. Short Anomaly in WFPC2 Images, *ISR* 98-02.
- Casertano, S., 1998, in *The 1997 HST Calibration Workshop*, eds. S. Casertano et al., (Baltimore: Space Telescope Science Institute), in press.
- Casertano, S., and Wiggs, M., 2001, An Improved Geometric Solution for WFPC2, *ISR* 01-10.
- Dolphin, A., 2000, The Charge-Transfer Efficiency and Calibration of WFPC2, *PASP* 112, 1397.
- Ferguson, H.C., 1996, Background Subtraction in WFPC2 Frames, *ISR* 96-03.

- Fruchter, A.S., et al., in *The 1997 HST Calibration Workshop*, eds. S. Casertano et al., (Baltimore: Space Telescope Science Institute), in press.
- Gonzaga, S., Baggett, S., and Biretta, J., 2001, Preliminary Assessment of the FR533N Filter Anomaly, *ISR* 01-04.
- Harris, H.C., et al., 1993, *AJ*, 105, 1196.
- Heyer, I., 2001, The WFPC2 Photometric CTE Monitor, *ISR* 01-09.
- Holtzman, J.A., et al., 1995a, *PASP*, 107, 156.
- Holtzman, J.A., et al., 1995b, *PASP*, 107, 1065.
- Johnson, H.L., 1965, *ApJ* 141, 923.
- Karkoschka, E., and Biretta, J., WFPC2 Flatfields with Reduced Noise, *ISR* 01-07.
- Kelson, D. D. et al., 1996, *ApJ*, 463, 26.
- Krist, J., 1995, "Simulation of HST PSF Using TinyTim," in *Astronomical Data Analysis, Software, and Systems IV*, Shaw et al., eds. (San Francisco: Astronomical Society of the Pacific), p. 349.
- Lub, J. and Pel, J.W., 1977, *A&A* 54, 137.
- Mack, J., Baggett, S., and Biretta, J., Creating WFPC2 Dark Reference Files: Addendum, *ISR* 01-09.
- Mack, J., and Wiggs, M., Creating WFPC2 Dark Reference Files, *ISR* 01-01.
- Matsushima, S., 1969, *ApJ* 158, 1137.
- Mutchler, M., and A. Fruchter, 1998, in *The 1997 HST Calibration Workshop*, eds. S. Casertano et al., (Baltimore: Space Telescope Science Institute), in press.
- O'Dea, C.P., et al., 1997, Properties of WFPC2 Bias Frames, *ISR* 97-04.
- Oke, J.B., 1974, *ApJS*, 27, 21.
- Ratnatunga, K.U., et al., 1998, in *The 1997 HST Calibration Workshop*, eds. S. Casertano et al., (Baltimore: Space Telescope Science Institute), in press.
- Reiss, A., 2000, How CTE Affects Extended Sources, *ISR* 00-04.
- Remy, M., et al., 1998, in *The 1997 HST Calibration Workshop*, eds. S. Casertano et al., (Baltimore: Space Telescope Science Institute), in press.
- Saha, A. et al., 1996, *ApJ*, 466, 55.



- Saha, A., Labhart, L. & Prosser, C. 2000, *PASP*, 112, 163.
- Suchkov, A., and Casertano, S., 1997, Impact of Focus Drift on Aperture Photometry, *ISR 97-01*.
- Surdej, J., et al., 1998, in *The 1997 HST Calibration Workshop*, eds. S. Casertano et al., (Baltimore: Space Telescope Science Institute), in press.
- Trauger, J.T., et al., 1993, *WFPC2 Science Calibration Prelaunch Report*, by WFPC2 Investigation Definition Team.
- Trauger, J.T., et al., 1994, *ApJ*, 435, L3.
- Trauger, J.T., et al., 1995, in *The 1995 HST Calibration Workshop*, eds. Koratkar, A., and Leitherer, C., (Baltimore: Space Telescope Science Institute).
- Trauger, J.T., 1998, in *The 1997 HST Calibration Workshop*, eds. S. Casertano et al., (Baltimore: Space Telescope Science Institute), in press.
- Whitmore, B., 1995, in *Calibrating Hubble Space Telescope: Post Servicing Mission*, eds. A. Koratkar & C. Leitherer (Baltimore: STScI), 269.
- Whitmore, B., and Heyer, I., 1995, A Demonstration Analysis Script for Performing Aperture Photometry, *ISR 95-04*.
- Whitmore, B., and Heyer, I., 1997, New Results on CTE and Constraints on Flatfield Accuracy, *ISR 97-08*.
- Whitmore, B., Heyer, I., and Baggett, S., 1996, Effects of Contamination on WFPC2 Photometry, *ISR 96-04*.
- Whitmore, B., Heyer, I., and Casertano, S., 1999, Charge-Transfer Efficiency of WFPC2, *PASP* 111, 1559.
- Whitmore, B., and Wiggs, M., Charge Transfer Traps in the WFPC2, *ISR 95-03*.
- Wiggs, M.S., et al., 1998, in *The 1997 HST Calibration Workshop*, eds. S. Casertano et al., (Baltimore: Space Telescope Science Institute), in press.

---

## WWW References

### Space Telescope HST page

<http://hst.stsci.edu>.

## **Space Telescope Astronomy Resources page**

<http://resources.stsci.edu/>

## **Space Telescope Archive page**

<http://archive.stsci.edu/>

## **StarView Page**

<http://starview.stsci.edu/html/>

## **Paper Products Page**

[http://archive.stsci.edu/hst/pdf\\_search.html](http://archive.stsci.edu/hst/pdf_search.html)

## **HST Program Information Page**

<http://www.stsci.edu/public/propinfo.html>

## **Keyword Dictionary**

[http://www.dpt.stsci.edu/cgi-bin/kdct-keyword\\_form?db=Operational](http://www.dpt.stsci.edu/cgi-bin/kdct-keyword_form?db=Operational)

## **Science Instrument Aperture File (SIAF)**

<http://www.stsci.edu/instruments/observatory/siaf.html>

## **Spectral Atlases Page**

[http://www.stsci.edu/instruments/observatory/cdbs/astronomical\\_catalogs\\_alt.html](http://www.stsci.edu/instruments/observatory/cdbs/astronomical_catalogs_alt.html)

## **SYNPHOT Users Guide**

<http://ra.stsci.edu/Files>

Sites below begin with " <http://www.stsci.edu/instruments/wfpc2>" unless otherwise noted.

---

| <b>Site Map of WFPC2 WWW pages</b>                              | <a href="/wfpc2_site.html">/wfpc2_site.html</a>   |
|---|---|
| WFPC2 Advisories  | <a href="/wfpc2_advisory.html">/wfpc2_advisory.html</a>   |
| WFPC2 Documentation   | <a href="/wfpc2_doc.html">/wfpc2_doc.html</a>   |
| WFPC2 Software Tools  | <a href="/wfpc2_tools.html">/wfpc2_tools.html</a>   |
| WFPC2 User Support  | <a href="http://hst.stsci.edu/acs/performance/cte_workgroup/cte_workshop.html">http://hst.stsci.edu/acs/performance/cte_workgroup/cte_workshop.html</a> |
| Frequently Asked Questions                                      | <a href="/wfpc2_top_faq.html">/wfpc2_top_faq.html</a>   |
| WFPC2 Instrument Handbook                                       | <a href="/wfpc2_handbook.html">/wfpc2_handbook.html</a>   |
| WFPC2 Tutorial  | <a href="/wfpc2_doc.html#Hand">/wfpc2_doc.html#Hand</a>   |
| Dither Handbook   | <a href="/Wfpc2_driz/dither_handbook.html">/Wfpc2_driz/dither_handbook.html</a>   |
| WFPC2 Exposure Time Calculators                                 | <a href="/Wfpc2_etc/wfpc2-etc.html">/Wfpc2_etc/wfpc2-etc.html</a>   |
| WFPC2 Reference Files   | <a href="Wfpc2_memos/wfpc2_reffiles.html">Wfpc2_memos/wfpc2_reffiles.html</a>   |
| IDT Reference Files   | <a href="/Wfpc2_memos/wfpc2_idtrefs.html">/Wfpc2_memos/wfpc2_idtrefs.html</a>   |
| WFPC2 PSF page  | <a href="/Wfpc2_psf/wfpc2_psf_page.html">/Wfpc2_psf/wfpc2_psf_page.html</a>   |
| Warmpixel Tables  | <a href="/wfpc2_warmpix.html">/wfpc2_warmpix.html</a>   |
| Instrument Science Reports (ISRs)                               | <a href="/wfpc2_bib.html">/wfpc2_bib.html</a>   |
| Polarizer Calibration Tools                                     | <a href="/wfpc2_pol_top.html">/wfpc2_pol_top.html</a>   |
| Calibrating Linear Ramp Filter data                             | <a href="/Wfpc2_lrf/lrf_calibration.html">/Wfpc2_lrf/lrf_calibration.html</a>   |
| Linear Ramp Filter Calculator                                   | <a href="/Wfpc2_lrf/wfpc2_lrfcalc.html">/Wfpc2_lrf/wfpc2_lrfcalc.html</a>   |
| Photometric Monitoring Memo                                     | <a href="Wfpc2_memos/wfpc2_stdstar_phot3.html">Wfpc2_memos/wfpc2_stdstar_phot3.html</a>   |
| Orientation Memo  | <a href="/orient.html">/orient.html</a>   |
| Decontamination Memo  | <a href="/Wfpc2_memos/wfpc2_history.html">/Wfpc2_memos/wfpc2_history.html</a>   |
| STAN, the Space Telescope Analysis Newsletter                   | <a href="/wfpc2_stan.html">/wfpc2_stan.html</a>   |
| Workshop on Hubble Space Telescope CCD Detector CTE (Jan. 2000) | <a href="http://hst.stsci.edu/acs/performance/cte_workgroup/cte_workshop.html">http://hst.stsci.edu/acs/performance/cte_workgroup/cte_workshop.html</a> |

---

To subscribe to the STAN Newsletter, send a message to [majordomo@stsci.edu](mailto:majordomo@stsci.edu) with the Subject: line blank and the following in the body: subscribe wfpc\_news).



# Index

## A

- absolute sensitivity WFPC2:3—23
- accuracy WFPC2:5—33
- analog-to-digital conversion WFPC2:3—10
- aperture
  - correction WFPC2:5—20
  - zero point WFPC2:5—2
- astrometry WFPC2:5—26
  - improving WFPC2:5—27
  - keywords WFPC2:2—8
  - new solution WFPC2:5—28

## B

- bias
  - jump WFPC2:4—9
- bias correction WFPC2:3—11, WFPC2:4—2
  - errors WFPC2:4—2

## C

- calibration WFPC2:3—1
  - calwp2 WFPC2:3—6
  - editing switches WFPC2:3—21
  - steps WFPC2:3—8
  - switches WFPC2:3—8
- calwp2 WFPC2:3—20
- calwp2 task
  - calibration WFPC2:3—6
  - development WFPC2:3—20
- Camera
  - configurations WFPC2:1—3
- camera
  - WFPC2 WFPC2:1—1

## CCD

- readout modes WFPC2:1—3
- charge transfer efficiency WFPC2:5—15
- charge trap WFPC2:3—34, WFPC2:5—22
- chcalpar WFPC2:3—21
- clock
  - serial WFPC2:5—22
- color
  - transformation WFPC2:5—21
- conversion
  - analog to digital, see "analog-to-digital"  
WFPC2:3—10
- cool down WFPC2:5—14
- cosmic ray
  - co-aligned image WFPC2:3—31
  - cosmicrays task WFPC2:3—27
- counts
  - long vs. short WFPC2:5—18

## D

- daily darks WFPC2:3—29
- dark
  - current subtraction WFPC2:4—5
  - generating custom files WFPC2:3—29
  - glow WFPC2:4—6
  - reference files WFPC2:3—18
  - subtraction WFPC2:3—12
  - warm pixels WFPC2:3—18
- data quality
  - calibration WFPC2:3—16
  - flags WFPC2:3—17
- dataset WFPC2:2—1
- decontamination WFPC2:3—26

deconvolution  
  images WFPC2:5—29  
dithering WFPC2:5—29  
drizzle software WFPC2:5—31

## E

earth reflection WFPC2:4—13  
error sources WFPC2:4—1  
exposure log sheet WFPC2:2—15  
exposures  
  time WFPC2:5—22

## F

field of view WFPC2:1—3  
file  
  trailer WFPC2:3—5  
files  
  calibration WFPC2:3—9  
  dataset WFPC2:2—1  
filters  
  anomalous rotational offset in  
    linear ramp filters WFPC2:5—20  
  possible variation in methane  
    quad transmission WFPC2:5—19

## FITS

  extension WFPC2:2—2  
  waivered WFPC2:2—1  
flatfield WFPC2:3—19  
  1995-1996 epoch WFPC2:4—3  
  correction files WFPC2:3—29  
  effect on point sources WFPC2:4—5  
  errors WFPC2:4—2  
  linear ramp filters WFPC2:3—30  
  post 1996 epoch WFPC2:4—4  
  pre 1995 epoch WFPC2:4—3  
  reference files WFPC2:3—19  
  special purpose filters WFPC2:4—4

## G

gain variation WFPC2:5—19  
GEIS  
  format WFPC2:2—1  
geometric distortion WFPC2:5—18

ghost image WFPC2:4—10  
  bright objects WFPC2:4—11  
group  
  image WFPC2:2—6

## H

header  
  keywords WFPC2:2—7, WFPC2:3—6  
hedit task  
  header WFPC2:2—7  
  set keywords WFPC2:2—15  
histogram WFPC2:3—16  
history record WFPC2:3—10

## I

image  
  deconvolution WFPC2:5—29  
  features WFPC2:3—34, WFPC2:4—9  
  reconstruction,  
    deconvolution WFPC2:5—29  
iminfo task  
  examine header WFPC2:2—14  
invmetric task WFPC2:5—27

## K

keywords  
  calibration switches  
    WFPC2:3—6, WFPC2:3—21  
  header WFPC2:2—7  
  photometry WFPC2:3—13

## L

linear ramp filters  
  flatfielding WFPC2:3—30  
long vs. short anomaly WFPC2:5—18

## M

metric task WFPC2:5—27

**N**

noise  
 digitization WFPC2:5—21

**O**

On-The-Fly Calibration (OTFC) WFPC2:3—2  
 On-The-Fly Reprocessing (OTFR)  
 WFPC2:3—2  
 optical path WFPC2:1—2  
 ORIENT WFPC2:1—2

**P**

PA\_V3 WFPC2:1—2  
 paper products WFPC2:2—16  
 photmode WFPC2:3—14  
 photometry  
 34th-row defect correction WFPC2:5—18  
 aperture correction WFPC2:5—20  
 color terms WFPC2:5—21  
 contamination correction WFPC2:5—10  
 corrections WFPC2:5—10  
 CTE correction WFPC2:5—15  
 example WFPC2:5—23  
 geometric distortion correction  
 WFPC2:5—18  
 keywords WFPC2:3—13  
 long vs. short correction WFPC2:5—18  
 photometric table WFPC2:3—20  
 system WFPC2:5—2  
 zero point, WFPC2:5—2  
 pixel  
 centering WFPC2:5—19  
 pixel response function WFPC2:5—29  
 POD files WFPC2:3—2  
 pointing information  
 small errors prior to Sept. 1997  
 WFPC2:4—8  
 updating WFPC2:4—7  
 polarimetry WFPC2:5—24  
 polarizer WFPC2:5—24  
 pp\_dads WFPC2:2—16

proposal

keywords compared to Phase II  
 WFPC2:2—13

psf

F1042M extended halo WFPC2:5—23  
 variation WFPC2:5—14

**R**

readout

direction WFPC2:1—3  
 modes WFPC2:1—4

recalibration WFPC2:3—17

red leak WFPC2:5—22

reference files WFPC2:3—9, WFPC2:3—21

Richardson-Lucy

deconvolution WFPC2:5—32

**S**

scattered light WFPC2:4—14

sensitivity

absolute WFPC2:3—23

shading WFPC2:3—13

static mask WFPC2:3—10

stray light WFPC2:4—14

streak

pattern WFPC2:3—34

synphot package

absolute sensitivity WFPC2:3—24

zero point WFPC2:5—5

**T**

trailer file WFPC2:3—5

**U**

uchcoord task WFPC2:4—7, WFPC2:5—27

user support

help desk 1:1—ii

**V**

vignetting WFPC2:1—4

**W**

warm pixels WFPC2:3—24, WFPC2:3—27

    repairing WFPC2:3—26

    tables on WWW WFPC2:3—28

wmosaic task

    images WFPC2:1—4

**X**

xy2rd task WFPC2:5—27

    coordinates WFPC2:5—27

**Z**

zero point

    determining WFPC2:5—4

    photometric WFPC2:5—2